ROLES OF GLUTAREDOXIN AND THIOREDOXIN-LIKE NFU PROTEINS IN IRON-SULFUR CLUSTER BIOGENESIS

by

SIBALI BANDYOPADHYAY

(Under the Direction of Michael K. Johnson)

ABSTRACT

Iron-sulfur (Fe-S) clusters are one of the most ancient, ubiquitous and functionally versatile prosthetic groups in nature. Based on the organization of genes in bacterial operons, three highly conserved types of machinery for the biogenesis of Fe-S clusters have emerged, namely the NIF (Nitrogen Fixation), the ISC (Iron-Sulfur Cluster) and the SUF (Sulfur Mobilization) systems. However, recent studies have implicated roles in Fe-S cluster biogenesis for accessory proteins such as glutaredoxins and thioredoxin-like Nfu proteins that are not encoded by genes in *nif*, *isc*, or *suf* operons. This research project was designed to elucidate the role of dithiol and monothiol glutaredoxins and thioredoxin-like Nfu proteins in Fe-S cluster biogenesis. The approach involved structural and/or spectroscopic characterization of clusters assembled on plant dithiol and monothiol glutaredoxins and *Azotobacter vinelandii* NfuA protein coupled with *in vitro* studies of cluster transfer to physiologically relevant acceptor proteins and *in vivo* assessment of function via gene knock out or complementation studies. The *A. vinelandii* NfuA protein was shown to assemble a subunit-bridging $[4Fe\text{-}4S]^{2+}$ cluster which is capable of activating apo aconitase at physiologically relevant rates. Taken together with *in vivo* studies, which indicate impaired maturation of Fe-S proteins in strains inactivated for *nfuA*, the results indicate a role of NfuA as a class of intermediate [Fe-S] cluster carrier proteins in bacteria. Spectroscopic, mutagenesis and crystallographic studies of the cytosolic poplar dithiol glutaredoxin C1 (CGYC active site) have demonstrated that dithiol glutaredoxins can assemble a novel glutathione-ligated $[2Fe\text{-}2S]^{2+}$ cluster at the subunit interface of the homodimer and have established the active-site sequence requirement for Fe-S cluster incorporation. The inability to transfer the $[2Fe\text{-}2S]^{2+}$ clusters to apo forms of acceptor Fe-S proteins suggests that the cluster in dithiol glutaredoxins may play a role in sensing oxidative stress. The chloroplastic poplar monothiol glutaredoxin S14 (CGFS active site) was also shown to assemble a similar glutathione-ligated $[2Fe\text{-}2S]^{2+}$ cluster at the subunit interface of the homodimer. However, in contrast to dithiol glutaredoxins, kinetic studies indicate that the $[2Fe\text{-}2S]^{2+}$ cluster on glutaredoxin S14 is rapidly and stoichiometrically transferred intact to apo *Synechocystis* ferredoxin, a physiologically relevant acceptor protein. Moreover, i*n vivo* studies showed that glutaredoxin S14 can complement the Fe-S cluster assembly deficiency in yeast mitochondrial monothiol glutaredoxin 5 (CGFS active-site) deletion mutants. These results indicate that monothiol glutaredoxins play a role as scaffold proteins involved in the assembly and/or delivery of $[2Fe\text{-}2S]^{2+}$ clusters in mitochondria and chloroplasts.

INDEX WORDS: Iron-sulfur clusters, Cluster transfer, Aconitase assays, Cluster carriers, Scaffold proteins, Glutaredoxins, Glutathione, Dithiol, Monothiol, Poplar, Ferredoxins.

ROLES OF GLUTAREDOXIN AND THIOREDOXIN-LIKE NFU PROTEINS IN IRON-SULFUR CLUSTER BIOGENESIS

by

SIBALI BANDYOPADHYAY

M.Sc. Chemistry, University of Calcutta, Calcutta, India, 1999

B.Sc. Chemistry, Scottish Church College, University of Calcutta, Calcutta, India, 1997

A Dissertation Submitted to the Graduate Faculty of The University of Georgia in Partial Fulfillment of the Requirements for the Degree

DOCTOR OF PHILOSOPHY

ATHENS, GEORGIA

2007

ROLES OF GLUTAREDOXIN AND THIOREDOXIN-LIKE NFU PROTEINS IN IRON-SULFUR CLUSTER BIOGENESIS

by

SIBALI BANDYOPADHYAY

Major Professor:	Michael K. Johnson
Committee:	Michael W. W. Adams Robert A. Scott

Electronic Version Approved:

Maureen Grasso
Dean of the Graduate School
The University of Georgia
December 2007

DEDICATION

To my loving parents

Dr. Monoranjan Banerjee and Mrs. Shanta Banerjee

ACKNOWLEDGEMENTS

My deepest appreciation goes to my advisor and mentor Prof. Michael K. Johnson who introduced me to the field of research in spectroscopy and protein biochemistry and guided me through the course of graduate studies. I also thank my committee members Prof. Michael W.W. Adams, Prof. Robert A. Scott and Dr. Marly Eidsness for their valuable suggestions and guidance during my PhD.

A big thanks goes to our collaborators Prof. Jean-Pierre Jacquot, Prof. Vincent Huynh, Prof. Dennis D. Dean, Dr. Nicolas Rouhier, Dr. Patricia Dos Santos and Dr. Sunil Naik for their tremendous help.

Thanks to all former and present members of the Johnson lab for teaching me the ways of life. I would specially thank Kala for helping me design a lot of experiments and being with me in difficult situations.

It would not be possible for me to complete my PhD without the constant affection and support of my husband Ritesh. I also appreciate the support I received from my friends Nilanjana and Abhijit who helped me settle down in this new country.

I have no words to express my love and gratitude for my parents without whom I would not be where I am today. They have constantly encouraged and supported me in pursuing my dreams and taught me good moral values.

TABLE OF CONTENTS

LIST OF TABLES

Page

LIST OF FIGURES

Page

CHAPTER 1

INTRODUCTION AND LITERATURE REVIEW

Iron-Sulfur Proteins: Background and Importance

Fe-S centers are one of the most ubiquitous and functionally versatile prosthetic groups in nature. There are more than 200 distinct types of enzymes and proteins known to contain Fe-S centers and they collectively referred to as Fe-S proteins (*1-3*). They are broadly defined as proteins containing nonheme Fe with at least partial S coordination. This definition includes a small group of proteins with mononuclear Fe centers coordinated by cysteinate residues and a very large group of proteins containing clusters of Fe bridged by inorganic sulfide that are attached to the protein backbone via predominantly cysteinate ligation.

Research over the past 50 years has shown the structural diversity of Fe-S centers and their involvement in various functions ranging from electron transfer to DNA repair (*3*). There are also highly conserved sets of genes, called Fe-S cluster assembly genes, present in all living organisms that encode proteins designed to direct the biogenesis of Fe-S clusters (*4*). Inability of cells to build Fe-S clusters causes severe phenotypic defects in both prokaryotes and eukaryotes. Clinically relevant mutations in patients with trichothiodystrophy (TTD) and Fanconi anemia disrupt the Fe-S clusters of XPD (xeroderma pigmentosum group D) and FancJ and thus abolish helicase activity (*5*). Dysfunctioning of the Fe-S cluster biosynthetic machinery also leads to neurodegenerative diseases. Deletion of frataxin gene (which encodes for the protein that is responsible for delivering iron to the Fe-S cluster biosynthetic machinery in eukaryotes) is embryonically lethal and reduction of frataxin level by 70% leads to Friedreich's ataxia, a type of

neurodegenerative disease (*6;7*). Friedrich's ataxia is a spino-cerebellar ataxia resulting in speech disorder, muscle weakness, heart disease and progressive damage of the nervous system and symptoms related to X-linked sideroblastic anemia with ataxia (XLSA/A) which includes coordination difficulties and anemia (*8;9*). Recently it was shown that depletion of a specific monothiol glutaredoxin gene (which has been implicated to be involved in Fe-S cluster biogenesis) leads to anemia with excessive iron accumulation and a low number of ringed sideroblasts in humans (*10*). In bacterial pathogens, reductions in virulence are often associated with defects in the Fe-S cluster assembly machinery (*11*). Thus detailed understanding of the Fe-S cluster biosynthetic machinery is medically important because the impairment of genes related to Fe-S cluster biogenesis is responsible for several severe metabolic diseases and because it may offer potential new strategies for fighting bacterial pathogens.

In spite of the vast literature that is available for Fe-S cluster containing proteins and enzymes (*3*), and the recent proliferation of research on Fe-S cluster biogenesis (*4;12;13*), molecular level understanding of the mechanism of the Fe-S cluster biogenesis is still in its infancy. Based on the organization of genes in bacterial operons, three types of Fe-S cluster biosynthetic machinery have emerged (*4*). The NIF (Nitrogen Fixation) is primarily concerned with maturation of Fe-S proteins associated with nitrogen fixation (*14-17*). The ISC (Iron-Sulfur Cluster) system is responsible for general Fe-S cluster biosynthesis in bacteria and mitochondria (*18*). The SUF (Sulfur Mobilization) system is responsible for Fe-S cluster biosynthesis in chloroplasts and many archaea and functions as a back up system under conditions of Fe limitation or oxidative stress in many bacteria (*11;19;20*). However recent studies have indicated that accessory proteins such as glutaredoxin and thioredoxin-like proteins that are not encoded by genes in *nif*, *isc*, or *suf* operons, also play key roles in Fe-S cluster biogenesis (*21-23*).

This research project was designed to elucidate the functions of glutaredoxin and thioredoxin-like Nfu proteins that have been implicated as accessory proteins in Fe-S cluster biogenesis. A range of biophysical techniques, including UV-visible absorption, resonance Raman, Mössbauer, Circular Dichroism (CD), Magnetic Circular Dichroism (MCD) and Electron Paramagnetic Resonance (EPR) spectroscopies, combined with analytical and biochemical assays were used to determine the structure and function of the clusters assembled on the proteins. The results indicate new roles for monothiol glutaredoxins and thioredoxin-like Nfu proteins in the assembly, storage or delivery of Fe-S clusters.

Structure, Spin States and Redox Properties of Simple Fe-S centers

The four fundamental types of biological Fe-S centers involve $Fe(SCys)_4$, $Fe_2(\mu_2\text{-}S)_2(SCys)_4$, $Fe_3(\mu_2\text{-}S)_3(\mu_3\text{-}S)(SCys)_3$ and $Fe_4(\mu_3\text{-}S)_4(SCys)_4$ units, see Figure 1-1. The Fe-S clusters are denoted by the stoichiometry of Fe and inorganic-S in square brackets with the formal charge of the Fe and inorganic-S core indicated as a superscript, i.e. $[2Fe\text{-}2S]^{2+,+}$, $[3Fe\text{-}4S]^{+,0,2-}$ and $[4Fe\text{-}4S]^{3+,2+,+,0}$. The number of unpaired electrons in the electronic ground state is indicated by the spin state, *S* as determined by magnetic and spectroscopic studies at cryogenic temperatures. Depending on the extent of valence localization/delocalization for each type of cluster in each accessible redox state, the formal charge on each Fe can be Fe^{2+}, Fe^{3+} or $Fe^{2.5+}$. Figure 1-2 indicates the extent of valence delocalization and the ground-state spin for each accessible oxidation state of the four simplest types of Fe-S center. It is apparent that $Fe_2(\mu_2\text{-}S)_2$ rhombs are the building block for all higher nuclearity clusters and that valence-delocalized $[2Fe\text{-}2S]^+$ units with $S = 9/2$ ground states are intrinsic to understanding the ground-state electronic and magnetic properties of these clusters. Moreover, valence delocalization facilitates efficient electron

transfer by minimizing reorganization energy (*24;25*), which explains the widespread use of Fe-S clusters in mediating biological electron transfer.

Mononuclear Fe-centers: The mononuclear Fe centers, generally called rubredoxin-type centers, have tetrahedral cysteinyl ligation and are involved in bacterial electron transfer both as mobile electron carriers and intrinsic domains of more complex redox enzymes (*26*). Rubredoxin-type centers undergo redox cycling between high spin Fe(III) to high spin Fe(II) with midpoint potentials between +20 to –87mV in rubredoxins and 2Fe superoxide reductases, while higher potentials are observed for rubredoxin centers in ruberythrin (+281mV) and nigerythrin (+213mV) (*27*).

[2Fe-2S] Clusters: [2Fe-2S] centers generally have complete cysteinyl ligation and undergo redox cycling between 2+ and 1+ core oxidation states. However the Rieske-type [2Fe-2S] clusters have two histidyl ligands at one Fe site (*28*). Redox potentials of the $[2Fe\text{-}2S]^{2+,+}$ centers with all-cysteinyl-ligation range from +100 to –460mV, while Rieske-type centers generally have higher potentials (+380 to –150mV) due to the presence of the more electropositive histidine ligands at the reducible Fe site. There are a few other examples of [2Fe-2S] clusters with one non-cysteinyl ligand. [2Fe-2S] centers with one aspartate ligand are found in some succinate dehydrogenases and a sulfide dehydrogenase, and arginine has been found to ligate the sacrificial [2Fe-2S] cluster in biotin synthase (*29-31*).

The oxidized $[2Fe\text{-}2S]^{2+}$ cluster has two S = 5/2 Fe(III) ions which are antiferromagnetically coupled to give a diamagnetic S = 0 ground state. In the valence-localized reduced $[2Fe\text{-}2S]^{+}$ form, the S = 2 Fe(II) and S = 5/2 Fe(III) sites are antiferromagnetically coupled to give a paramagnetic S = 1/2 ground state with a rhombic or axial g-tensor. Completely reduced $[2Fe\text{-}2S]^{0}$ clusters with two S = 2 Fe(II) sites have diamagnetic S = 0 ground

state as a result of antiferromagnetic coupling. However, the $[2Fe\text{-}2S]^{+,0}$ couple is generally ~1.0V lower than the $[2Fe\text{-}2S]^{2+,+}$ couple which explains why the all ferrous redox state is rarely observed and unlikely to be physiologically relevant. The only known example of a stable $[2Fe\text{-}2S]^{0}$ redox state is for a Rieske-type center where the $[2Fe\text{-}2S]^{0}$ state is stabilized by protonation of one of the μ_2-sulfides (*32*). While the vast majority of the $[2Fe\text{-}2S]^{+}$ clusters are valence-localized systems with $S = 1/2$ ground states, valence-delocalized $[2Fe\text{-}2S]^{+}$ clusters with $S = 9/2$ ground states have been identified in Cys-to-Ser mutants of *Clostridium pasteurianum* ferredoxin (*33-36*). Ferromagnetic coupling facilitates valence-delocalization since the electron with the antiparallel spin can visit both Fe sites without undergoing a spin flip. Valence-delocalized $[2Fe\text{-}2S]^{+}$ units are building blocks for all higher nuclearity clusters and facilitate interpretation of the observed ground and excited-state electronic and magnetic properties. Thus antiferromagnetic interaction between $S = 9/2$ $[2Fe\text{-}2S]^{+}$ fragments and $S = 2$ Fe^{2+}, $S = 5/2$ Fe^{3+}, $S = 5$ $[2Fe\text{-}2S]^{2+}$, $S = 9/2$ $[2Fe\text{-}2S]^{+}$, or $S = 4$ $[2Fe\text{-}2S]^{0}$ fragments can be invoked to rationalize the ground-state electronic properties of $[3Fe\text{-}4S]^{0,-}$ and $[4Fe\text{-}4S]^{3+,2+,+}$ clusters, see Figure 1-2.

Cubane and Linear [3Fe-4S] Clusters: Both cubane and linear [3Fe-4S] clusters have been observed in proteins, but only the cubane-type is currently believed to be physiologically relevant. Cubane-type [3Fe-4S] clusters may be formed by oxidative degradation of [4Fe-4S] clusters resulting in loss of a Fe atom from the corner of cube, as in the case of (de)hydratase enzymes such as aconitase and several ferredoxins, particularly those containing [4Fe-4S] clusters with non-cysteinyl ligation at a unique Fe site (*37*). However, cubane type [3Fe-4S] clusters are also intrinsic components of numerous redox enzymes and proteins based on x-ray structures, primary sequences and *in vivo* detection (*38*). Cubane-type [3Fe-4S] clusters can exist in 1+, 0 and 2- oxidation states. They are involved in mediating electron transport using the [3Fe-

$4S]^{1+,0}$ redox couple with midpoint potentials in the range +90 to –460mV (*38*). The midpoint potential of the two-electron $[3Fe\text{-}4S]^{0,2-}$ redox couple is –700mV at pH 7 and is strongly pH dependent since reduction to the $[3Fe\text{-}4S]^{2-}$ oxidation state requires uptake of three protons (*39*). In contrast linear [3Fe-4S] clusters have been identified in proteins only in 1+ oxidation state. Thus far they have not been identified as a functional component of any Fe-S protein and have been observed only in denatured forms of aconitase and the cytosolic human iron regulatory protein IRP1 (*40-42*).

The ground state properties and valence delocalization schemes for cubane-type [3Fe-4S] clusters is summarized in Figure 1-2. In the cubane-type $[3Fe\text{-}4S]^{+}$ clusters, three $S = 5/2$ Fe(III) ions are antiferromagnetically coupled to give a $S = 1/2$ ground state which gives rise to an isotropic or near-axial EPR signal, while linear $[3Fe\text{-}4S]^{+}$ clusters exhibit a rhombic $S = 5/2$ ground state which results from asymmetric coupling of the three high-spin Fe(III) centers. The one-electron reduced $[3Fe\text{-}4S]^{0}$ state of the cubane-type cluster has a $S = 2$ ground state arising from antiferromagnetic interaction between a valence-delocalized $S = 9/2$ $[2Fe\text{-}2S]^{+}$ fragment and a valence-localized S=5/2 Fe(III) site. The electronic properties of the all ferrous cubane-type $[3Fe\text{-}4S]^{2-}$ center have yet to be established.

[4Fe-4S] Clusters: The cubane [4Fe-4S] clusters can be visualized as two [2Fe-2S] rhombs fused together and they play an ubiquitous role in mediating electron transfer in biology. They usually have all cysteinyl ligations, with the exception of a single aspartate ligand in some ferredoxins and a single histidine ligand in both NiFe and Fe-hydrogenases and nitrate reductases (*43-46*). Biological [4Fe-4S] clusters are known to exist in 3+, 2+, 1+ and 0 core oxidation states. Under physiological conditions, ferredoxin-type [4Fe-4S] clusters utilize the 2+,+ redox couple with midpoint potentials between +80 to –715mV, while the so-called high potential iron-

sulfur proteins (HiPIPs) utilize the 3+,2+ redox couple and higher redox potentials in the range +50 to +500mV. Except for the nitrogenase Fe protein, which has a [4Fe-4S] cluster that is stable in three oxidation states 2+, 1+ and 0 and may have the ability to act as a two-electron donor (*47-49*), all other electron transfer [4Fe-4S] clusters undergo one-electron redox cycles.

The magnetic and electronic properties of the [4Fe-4S] clusters have been rationalized in terms of antiferromagnetic exchange interaction between valence-delocalized, ferromagnetically coupled [2Fe-2S] units. Both $[4Fe\text{-}4S]^{3+}$ and $[4Fe\text{-}4S]^{+}$ centers have $S = 1/2$ ground states, but are distinguishable by EPR spectroscopy. $[4Fe\text{-}4S]^{3+}$ centers generally give rise to axial EPR signals with $g_{ave} > 2.0$, whereas $[4Fe\text{-}4S]^{+}$ centers generally have rhombic EPR signals similar to those of $[2Fe\text{-}2S]^{+}$ centers with $g_{ave} < 2.0$. The $[4Fe\text{-}4S]^{+}$ centers are distinguishable from the $[2Fe\text{-}2S]^{+}$ centers by EPR because the former are faster relaxing and are generally not seen above 30 K. Although the majority of biological $[4Fe\text{-}4S]^{+}$ clusters have a $S = 1/2$ ground state, there are examples of $[4Fe\text{-}4S]^{+}$ clusters with a mixture of species in S=1/2 and 3/2 ground states, pure S=3/2 ground state and quantum mechanically admixed S=1/2 and 3/2 ground states (*50-53*). This implies that the $S = 1/2$ and 3/2 states are close in energy. The $[4Fe\text{-}4S]^{0}$ center in the nitrogenase Fe protein has a $S = 4$ ground state as determined by the combination of EPR and Mössbauer spectroscopies (*47*). Interestingly, the 2.25-Å resolution crystal structure of the $[4Fe\text{-}4S]^{0}$ cluster in the nitrogenase Fe protein shows that the all-ferrous [4Fe-4S] core remains intact without major conformational changes in the protein environment (*48*).

The most complex type of Fe-S cluster that functions in electron transfer is the nitrogenase P cluster which supplies electrons to the MoFe cofactor active-site of nitrogenase. In the reduced state it can be visualized as the fusion of two [4Fe-4S] clusters to form a double

cubane [8Fe-7S] cluster with one μ_6-S^{2-} and two μ_2-bridging Cys-S at the interface of the two clusters (*54*).

Functions of Biological Fe-S Centers

More than 200 distinct types enzymes and proteins are known to contain Fe-S centers. Although the most common function for Fe-S centers is electron transfer, they are also involved in substrate binding and activation, Fe or cluster storage, structural roles, regulation of gene expression and enzymatic activity, disulfide reduction and sulfur donation, see Table 1-1.

Electron Transport: Fe-S proteins with Fe-S centers that perform electron transfer roles can be broadly classified into mobile electron carrier proteins, membrane-bound enzyme complexes and soluble redox enzymes. Many oxidoreductases contain multiple Fe-S clusters in chains connecting the sites of catalysis and interprotein electron transfer. In these cases, structural studies have shown that the Fe-S clusters are closely spaced (edge-to-edge distance of 4-14 Å) to enable efficient tunneling of electrons at rates faster than the substrate redox reactions, thereby obviating the need for specific through-bond electron transfer pathways (*55*).

The mobile electron carriers comprise low potential ferredoxins with one $[2Fe\text{-}2S]^{2+,+}$, $[3Fe\text{-}4S]^{+,0}$ or $[4Fe\text{-}4S]^{2+,+}$ cluster, one $[3Fe\text{-}4S]^{+,0}$ and $[4Fe\text{-}4S]^{2+,+}$ cluster, or two $[4Fe\text{-}4S]^{2+,+}$ clusters, high potential rubredoxins with one $[Fe(SCys)_4]^{2-,-}$ center, and HiPIPs containing one $[4Fe\text{-}4S]^{3+,2+}$ cluster. The $[2Fe\text{-}2S]^{2+,+}$, $[3Fe\text{-}4S]^{+,0}$ and $[4Fe\text{-}4S]^{2+,+}$ clusters that are found in simple Fe-S proteins are also intimately involved in the mitochondrial respiratory and photosynthetic electron transport chains. For example, the mitochondrial respiratory chain involves thirteen Fe-S clusters in four membrane-bound protein complexes while photosystem I of the photosynthetic electron transfer chain contains four Fe-S clusters. In addition, bacterial

respiratory chains get electrons from several multicluster Fe-S enzymes such as hydrogenase, formate dehydrogenase, NADH dehydrogenase and succinate dehydrogenase and use multicluster Fe-S enzymes such as nitrate reductase, fumarate reductase, DMSO reductase and CoB-S-S-CoM heterodisulfide reductase as the terminal electron acceptors. In addition numerous soluble redox enzymes contain one or more $[2Fe\text{-}2S]^{2+,+}$, $[3Fe\text{-}4S]^{+,0}$, or $[4Fe\text{-}4S]^{2+,+}$ clusters which function in electron transport chains to transfer electrons to and from non-heme Fe, Moco/Wco, flavin, thiamin pyrophosphate, corrinoid, Fe-S cluster-containing, or NiFe active sites. The Fe-S centers that function in electron transfer generally have complete cysteinyl ligation. In some cases aspartate, histidine, serine or backbone amide ligation to unique Fe sites has been established and rationalized in terms of facilitating electron transport by modifying redox potential, gating electron transfer, or coupling electron and proton transport (*28;56;57*).

Substrate Binding and Activation: A number of redox and non-redox enzymes have active sites involving Fe-S clusters that bind and activate substrates. Based on the available structural data, three distinct approaches have been utilized for establishing substrate binding and activation sites on Fe-S clusters. The first involves ligating the substrate at a unique, non-cysteinyl-ligated Fe site of a [4Fe-4S] cluster, aconitase being the best characterized example (*58*). The substrate binds at unique iron site of a [4Fe-4S] cluster which activates the enzyme for a dehydration/hydration reaction as in the case of the wide range of dehydratases and hydratases (*59*). A similar mechanism is used for binding *S*-adenosylmethionine (SAM) via the amino and carboxyl groups of the methionine fragment to facilitate the reductive cleavage of the S-C bond and generation of 5'-deoxyadenosyl radical (*60;61*). Based on bioinformatic analyses, there are likely to be more than 600 different enzymes in radical-SAM superfamily that catalyze radical reactions involved in the formation of numerous DNA precursors, vitamins, cofactors, and

antibiotics, and in herbicide biosynthesis and degradation pathways (*60;62;63*). The second method involves incorporation of a heteroatom into the Fe-S cluster to facilitate substrate binding or activation. This approach is used in the [Ni-4Fe-5S] cluster active site of CO dehydrogenase which uses Ni as the CO binding site (*64*). The third approach involves attaching a substrate-binding metal site to a unique Fe site of a [4Fe-4S] cluster via a bridging cysteinyl residue. Examples include sulfite and nitrite reductases, which uses a siroheme as the substrate-binding site, acetyl coenzyme A synthase which uses a dinickel center as the substrate-binding site, and FeFe-hydrogenase which uses an organometallic diiron center as the substrate-binding site. (*44;65-69*)

Structure: Fe-S clusters are known to play important structural roles as in the case of the DNA repair enzymes endonuclease III and MutY where the [4Fe-4S] cluster controls the structure of the protein loop essential for recognition and repair of damaged DNA (*70-73*).

Iron and Cluster Storage: The 8Fe (2 x [4Fe-4S]) ferredoxins in *Clostridia* and many anaerobic bacteria and archaea have been proposed to be involved in iron storage (*74*). This is supported by the presence of polyferredoxins in methanogenic archaea, containing up to 12 [4Fe-4S] clusters in tandem repeats of 8Fe ferredoxin-like domain (*75;76*). Alternatively they may function either as scaffolds for assembly or storage for [4Fe-4S] clusters in anaerobic organisms.

Transcriptional and Translational Regulators of Gene Expression: [Fe-S] cluster-containing regulatory proteins have a cluster binding domain and a DNA binding domain. Each of these regulatory proteins use a distinct sensing mechanism involving cluster assembly, cluster conversion or cluster redox chemistry to sense a different type of environmental stimuli and thereby trigger changes in DNA binding ability. A sensing mechanism involving cluster redox chemistry is utilized by SoxR, which functions as a redox responsive protein for monitoring

cellular oxidative stress in bacteria via the oxidation of its $[2Fe\text{-}2S]^{2+,+}$ cluster (*77*). Under oxidative stress, SoxR mediates transcriptional regulation of the *soxRS* regulon, which in turn activates the genes that facilitate repair of oxidative damage. In presence or absence of oxidative stress SoxR remains tightly bound to the target *soxS* promoter (*78*). Cluster conversion is used as the oxygen-sensing mechanism in the *E. coli* fumarate-nitrate reduction (FNR) protein, the regulatory protein that controls the switch between aerobic and anaerobic respiration by controlling the expression of >100 genes. The DNA-binding homodimeric form of FNR contains one $[4Fe\text{-}4S]^{2+}$ cluster in each monomer, but is converted to a monomeric $[2Fe\text{-}2S]^{2+}$ cluster-containing form with lower affinity for DNA on exposure to oxygen (*79*). Cluster assembly is used as the sensing mechanism for intracellular Fe levels by the iron-regulatory protein (IRP) (*58*). The translational regulation of ferritin and transferrin receptors is controlled by the presence or absence of the [4Fe-4S] cluster on IRP. Under conditions of iron starvation in eukaryotic cells, apo IRP stabilizes the transferrin receptor and inhibits the translation of ferritin mRNAs by binding to the iron-responsive elements (IREs) within their untranslated region. Under iron replete conditions, IRP assembles a [4Fe-4S] cluster with three cysteine ligands and prevents IRE binding (*58;79*)

Regulation of Enzymatic Activity: Fe-S clusters are involved in the regulation of enzymatic activity in response to external stimuli. The best-characterized example of an enzyme containing a regulatory [Fe-S] cluster is *Bacillus subtilis* glutamine phosphoribosyl-pyrophosphate amidotransferase, which acts as an oxygen sensor to regulate the first step in purine nucleotide biosynthesis. Biochemical and crystallographic evidence suggest that the [4Fe-4S] cluster is selectively degraded by O_2 with concomitant proteolysis (*80;81*) Another example is the [2Fe-2S] cluster in the mammalian ferrochelatases, the terminal enzyme involved in heme

biosynthesis (*82*). The [2Fe-2S] cluster is required for the activity of mammalian ferrochelatates and is rapidly degraded by NO, but is not generally present in bacterial ferrochelatatases. Hence it has been suggested that the cluster acts a sensor to locally shut off heme biosynthesis in the region of a bacterial infection, thereby preventing the bacterial pathogen from utilizing heme synthesized by the host (*83*).

Disulfide Reduction: There are two classes of Fe-S cluster-containing disulfide reductases known – ferredoxin:thioredoxin reductase in chloroplasts and heterodisulfide reductase in the methanogenic archaea (*84-86*). These proteins use an active-site [4Fe-4S] cluster to cleave disulfide bonds in two sequential one-electron steps via an intermediate involving two thiolate ligands at a unique Fe site.

Sulfur Donor: Recent studies have suggested that Fe-S clusters can play a role as sacrificial S donors in radical-SAM enzymes that catalyze S-insertion reactions. The best example is biotin synthase, which has a [2Fe-2S] cluster in addition to the [4Fe-4S] cluster that is involved in the reductive cleavage of SAM. Spectroscopic and isotopic labeling studies indicate that the [2Fe-2S] cluster degrades and provides the sulfur for the conversion of dethiobiotin to biotin in the single catalytic turnover (*29;87;88*).

Three Fe-S Cluster Assembly Systems

It has been known for many years that anaerobic addition of S^{2-} and $Fe^{2+/3+}$ can lead to reconstitution of both [2Fe-2S] and [4Fe-4S] clusters in apo forms of simple Fe-S proteins. However spontaneous self-assembly of Fe-S clusters is unlikely to occur *in vivo* because of the insolubility of ferric salts at neutral pH and the physiological toxicity of ferrous and sulfide ions at the levels required for *in vitro* maturation. Moreover, research over the past decade has

identified specific proteins which sequester Fe and S in nontoxic forms for assembly of transient Fe-S clusters on scaffold proteins (*4*). The Fe-S clusters assembled on scaffold proteins are subsequently transferred intact into apo Fe-S proteins (*4*). On the basis of organization of genes in bacterial operons three distinct types of biological machinery for Fe-S cluster biogenesis have emerged termed the NIF, ISC and SUF systems, see Figure 1-3 (*4*). Each involves a common theme of cysteine desulfurase-mediated assembly of transient Fe-S clusters on scaffold proteins, followed by direct cluster transfer to apo Fe-S proteins. The properties and functions of the individual components in each system are summarized below.

NIF system: The NIF system is primarily associated with nitrogen fixing organisms and is responsible for the assembly of Fe-S clusters in nitrogenase and the enzymes and proteins involved in nitrogenase maturation (*14;16;17;89*). However the NIF system is also present in some non-nitrogen fixing bacteria like *Helicobacter pylori* (*90*). The Fe-S cluster assembly genes in the *nif* operon of the nitrogen-fixing bacteria, *A. vinelandii* are shown in Figure 1-3. Deletion of the *nifU* and *nifS* genes, individually or together resulted in a dramatic loss in the activity of the nitrogenase Fe and MoFe proteins suggesting that both NifU and NifS are involved in the production of Fe-S clusters for nitrogenase maturation (*15*). Subsequently NifS was shown to be a homodimeric pyridoxal phosphate (PLP) containing cysteine desulfurase that catalyses the elimination of S from L-cysteine to yield L-alanine and a cysteine persulfide on a flexible arm (*91*). The cysteine persulfide is then transferred to an active-site cysteine residue on the NifU scaffold protein to facilitate the assembly of clusters destined for the maturation of Fe-S proteins involved with nitrogen fixation. NifU is a modular homodimeric protein with three distinct domains – an IscU-like N-terminal domain, a C-terminal domain containing a thioredoxin-like CXXC motif, and a central ferredoxin-like domain which houses a permanent redox-active [2Fe-

2S]$^{2+,+}$ cluster (*92-94*). NifS mediates sequential assembly of transient [2Fe-2S]$^{2+}$ and [4Fe-4S]$^{2+}$ clusters on the N- terminal domain of NifU and transient [4Fe-4S]$^{2+}$ clusters on the C-terminal domain of NifU, and the [4Fe-4S]$^{2+}$ clusters assembled on both domains are capable of activating the apo-form of the nitrogenase Fe protein via intact cluster transfer (*94;95*). The *nif* operon also has an A-type scaffold protein designated as ^{nif}IscA, which is capable of binding Fe^{2+} as well as assembling transient [2Fe-2S] and [4Fe-4S] clusters (*96*). The *cysE* gene which cotranscribes with the *nifS* gene in the *nif* operon encodes for o-acetyl serine synthase which catalyzes the rate-limiting step in cysteine biosynthesis and therefore promotes Fe-S cluster biosynthesis by increasing the production of cysteine for use as a substrate by NifS (*97*).

ISC system: The nine linked genes designated as *cysE2, iscR, iscS, iscU, iscA, hscB, hscA, fdx* and *orf3* form the *isc* operon (Figure 1-3) and are primarily involved in maturation of Fe-S proteins not involved with nitrogen fixation (*4;89*). The *isc* operon is often referred to as the housekeeping system for Fe-S cluster assembly in nitrogen fixing organisms such as *A vinelandii*. It is the most common type of assembly machinery found in mesophilic bacteria and also constitutes the Fe-S cluster assembly machinery found in mitochondria. Deletion of *iscS*, *iscU*, *hscA* and *fdx* are all lethal and their depletion causes deficiency in the maturation of aconitase implying that these genes play pivotal roles in Fe-S cluster assembly in this organism (*18;89*).

IscS is similar to NifS i.e. a homodimeric, pyridoxal phosphate (PLP) containing cysteine desulfurase that converts L-cysteine into L-alanine and sulfane sulfur (S^0) in the form of an active-site cysteine persulfide. The crystal structures of *E. coli* IscS (*98*) and *Thermotoga maritima* SufS (the SUF member of the NifS family of cysteine desulfurases) (*99*) have confirmed the proposed mechanism of cysteine desulfuration (*91*). Hence, sulfur is trafficked

through the cell in the nontoxic form of L-cysteine and transferred from cysteine desulfurases to scaffold proteins for the assembly of Fe-S clusters as S^0 rather than S^{2-}.

IscU is homologous to the N-terminal domain of NifU protein and functions as a cluster scaffold. It is capable of assembling and later transferring intact clusters to target acceptor proteins. IscU has three rigorously conserved cysteine residues Cys^{37}, Cys^{63} and Cys^{106} (numbering for *A. vinelandii*) and has been shown to sequentially assemble redox-labile [2Fe-2S] and [4Fe-4S] clusters in an IscS-mediated process (*100;101*). The fourth ligand to the clusters assembled on IscU is not definitively known. Due to the lability Fe-S clusters assembled on IscU in presence of oxygen and reducing agents and the highly fluxional protein backbone, structures of cluster-bound forms of IscU are not currently available. However a 2.3 Å resolution crystal structure of the closely related SufU from *Streptococcus pyrogenes* and a NMR solution structure of *Heamophilis influenzae* IscU have recently been solved, both with Zn bound to the active site. The structures indicate a globular core and flexible N- and C-termini with Zn bound in a solvent exposed site and tetrahedrally coordinated by the three active-site cysteines and either a histidine or aspartate residue (*102;103*). *H. influenzae* IscU has a histidine that is conserved in all IscU and NifU proteins, but not in SufU proteins, as the fourth ligand, whereas *S. pyrogenes* SufU has an aspartate that is rigorously conserved in all IscU, NifU and SufU proteins, as the fourth ligand. Mutagenesis studies indicate the conserved aspartate is responsible for labilizing the Fe-S clusters assembled on the U-type scaffolds in cluster transfer reactions (*95;104;105*) and resonance Raman studies indicate that the vibrational properties of clusters assembled on U-type scaffolds are sensitive to mutation of the conserved aspartate (*106*) .

Recent studies have demonstrated that $[4Fe\text{-}4S]^{2+}$ cluster assembly on IscU occurs at the homodimer subunit interface via the reductive coupling of two adjacent $[2Fe\text{-}2S]^{2+}$ clusters

(*138*). However, the mechanism of the initial $[2Fe\text{-}2S]^{2+}$ cluster assembly on U-type scaffolds and the nature of the Fe-donor are still the subject of much debate and controversy. For example, it is unclear if the initial event in assembly of the $[2Fe\text{-}2S]^{2+}$ cluster involves S or Fe transfer. Mass spectrometry studies have shown that sulfur is transferred as S^0 from the cysteine persulfide on IscS to a cysteine on IscU (*107*) and that any of the three conserved cysteines on IscU can accept the sulfane sulfur from IscU (*108*). However, the conditions required to assemble cluster starting with a persulfide- or polysulfide-bound form of IscU have yet to be elucidated. Calorimetry and surface plasmon resonance studies of a SufU have been interpreted in terms of an Fe-bound form that is competent for cluster assembly (*109*) but spectroscopic and analytical studies of IscU proteins from a wide variety of organisms has failed to confirm significant Fe^{2+} and Fe^{3+} binding to IscU (*4*). In contrast IscA has been shown to tightly bind ferric ions in a mononuclear site that are released by cysteine and can be used to assemble clusters on U-type scaffolds (*110-113*). However in eukaryotes, frataxin has been implicated to be the Fe donor to IscU based on evidence for IscU/frataxin complex formation and *in vitro* evidence for Fe-loaded frataxin being a competent Fe donor to apo IscU (*114;115*). CyaY, the bacterial homolog of frataxin has also been shown to donate Fe for [2Fe-2S] cluster assembly on IscU (*116;117*) Recent studies have suggested that IscA and CyaY donate Fe for Fe-S cluster assembly on U-type scaffolds under different conditions (*118*). While IscA is capable of recruiting intracellular iron under normal physiological conditions, CyaY may serve as an iron chaperone to sequester redox-active free iron under oxidative stress conditions.

In addition to a putative role as a specific Fe donor to IscU, the A-type proteins that are found in *nif, isc,* and *suf* operons (^{Nif}IscA, IscA, and SufA, respectively) have also been shown to have the potential to act as scaffold proteins for the assembly and transfer of [2Fe-2S] and [4Fe-

4S] clusters (*96;119;120*). Moreover the structure of a [2Fe-2S] cluster-bound form of IscA has recently been crystallographically defined (*121*). The [2Fe-2S] cluster is ligated asymmetrically at the subunit interface of a homodimer using the three conserved cysteines from one monomer and only one of the conserved cysteines from the other monomer. Interestingly, [2Fe-2S] clusters assembled on IscU can be transferred to IscA while the reverse reaction is not possible (*120*), implying that IscU is the primary scaffold protein while IscA is an alternate scaffold protein or an intermediate carrier protein for delivering clusters assembled on U-type scaffolds.

The *isc* operon also contains the molecular chaperones HscA and HscB, which are closely related to the DnaK and DnaJ class of molecular chaperones that mediate general protein folding and unfolding. However, in contrast to DnaK/DnaJ which interact with a wide variety of proteins, HscA and HscB, and their eukaryotic homologs, Ssq1 and Jac1, respectively, are specifically involved in the maturation of Fe-S clusters (*122-126*). HscA and Ssq1 bind to both the apo and holo cluster-loaded forms of IscU through the highly conserved LPPVK motif located adjacent to the cluster-binding site of IscU (*127-133*). HscA has intrinsic ATPase activity, which is tremendously enhanced when HscA binds IscU in the presence of HscB. There have been conflicting reports on the role of the chaperones in Fe-S cluster biogenesis. Studies in *T. maritima* and human showed that the nonspecific DnaK/DnaJ chaperone system inhibited the transfer of a [2Fe-2S] cluster from IscU to apo Fdx (*134*), while immunoprecipitation studies in yeast showed that depletion of the chaperones resulted in accumulation of Fe on Isu suggesting a function for the chaperones in transferring clusters from IscU to acceptor proteins (*21*). This has recently been confirmed by *in vitro* studies which demonstrated a dramatic (20-fold) enhancement in the rate of cluster transfer from [2Fe-2S] IscU to apo Isc ferredoxin in the

presence of HscA/HscB and excess MgATP (*135*). Hence [2Fe-2S] cluster transfer from IscU to acceptor proteins is mediated by HscA/HscB in an ATP-dependent reaction.

IscFdx is a $[2Fe\text{-}2S]^{2+,+}$ ferredoxin that plays an important role in Fe-S cluster maturation. *In vivo* studies in yeast have shown that deletion of this ferredoxin is lethal to the organism and depletion of this gene results in decreased activity of other mitochondrial Fe-S proteins and accumulation of Fe in the mitochondria of higher organisms (*136;137*). *In vitro* studies have demonstrated that IscFdx has the potential to mediate formation of $[4Fe\text{-}4S]^{2+}$ clusters on IscU via reductive coupling of two $[2Fe\text{-}2S]^{2+}$ clusters (*138*). Whether or not IscFdx has a redox role in Fe-S cluster biogenesis remains to be established.

The *isc* operon is regulated by *iscR* which encodes for a regulatory protein IscR comprising both a DNA binding domain and an Fe-S cluster binding domain that can accommodate both [2Fe-2S] and [4Fe-4S] clusters (*139*) (Chandramouli and Johnson, unpublished results). Proteins containing Fe-S clusters compete with IscR for the available clusters produced by the cluster assembly genes. When the supply of clusters exceeds the demand, apo IscR acquires [2Fe-2S] clusters and the [2Fe-2S] cluster-bound form acts as a transcriptional repressor of the entire *isc* operon (*139*). More recently *in vivo* studies in *E. coli* have demonstrated a more general role for IscR as a global regulator of numerous Fe-S proteins and an activator of both the *isc* and *suf* operons in response to oxidative stress (*140;141*). Global transcriptional profiling studies revealed that 40 genes in 20 predicted operons are regulated by IscR and DNase footprinting studies indicate at least two different classes of IscR binding sites. Of particular interest is the observation that although the Fe-S cluster-bound form of IscR acts as a repressor of the *isc* operon, it is the apo-form of IscR that is responsible for binding an oxidant-responsive element and thereby activating transcription of the *suf* operon. Since the [4Fe-4S]

cluster-bound form of IscR is rapidly degraded by oxygen and reactive oxygen species, it is tempting to speculate that the [4Fe-4S] cluster-bound form of IscR is responsible for sensing oxidative stress.

SUF system: The third system involved in the biogenesis of Fe-S proteins is the SUF system, see Figure 1-3. In many bacteria such as *E. coli* and *Yersinia pestis*, the SUF system is used as an alternate pathway for assembly of Fe-S clusters that function during adverse stress conditions such as oxidative stress or iron limitation (*11;19;20*). It also constitutes the sole type of Fe-S cluster assembly machinery in plant chloroplasts (*13*) and in many hyperthermophilic archaea and bacteria e.g. *Pyrococcus furiosis, T. maritima* and *Mycobacterium tuberculosis (142).*

The *sufABCDSE* operon in *E. coli* encodes for six proteins. SufA, which is homologous to IscA probably, plays the role of an Fe-S cluster scaffold protein. It has been shown to be capable of assembling [2Fe-2S] and [4Fe-4S] clusters and transferring the clusters to ferredoxin and biotin synthase (*143*). However, the absence of strong phenotype for *sufA, iscA,* and *iscA/sufA* deletion in cyanobacteria has raised the possibility of a regulatory role rather than scaffolding role for A-type scaffold proteins (*144*). SufC is a soluble ATPase protein and shares a number of properties with ATP-binding cassette (ABC) transporter superfamily (*11*). This includes the presence of three motifs (Walker sites A and B and motif C typical for a ATP-hydrolyzing domain) and ATPase activity requiring Mn or Mg as seen in the crystal structure of SufC from *Thermus thermophilus* (*145*). However, SufC is at best an atypical ABC transporter since it is not membrane-spanning like other ABC transporters. SufB and SufD are homologous to each other and they interact with SufC to form the SufBCD complex (*146-149*). Recently it has been shown that *E. coli* SufB can accommodate an Fe-S cluster, most likely a $[4Fe\text{-}4S]^{2+}$

cluster that degrades to a $[2Fe\text{-}2S]^{2+}$ cluster on exposure to air, suggesting a role as a scaffold protein for the SUF machinery. However, unlike other scaffold poteins, EPR studies indicate that the cluster is stable in both $S = 0$ $[4Fe\text{-}4S]^{2+}$ and $S=1/2$ $[4Fe\text{-}4S]^{+}$ oxidation states, which raises the possibility that the cluster may have a redox role related to the hitherto uncharacterized function of the SufBCD complex (*150*). SufS is a cysteine desulfurase similar to IscS and NifS (*151*). However in contrast to IscS and NifS cysteine desulfurases, SufS often has a partner(*150*) SufE protein which forms a complex with SufS and functions as a sulfur transferase to transfer the cysteine persulfide formed on SufS to more accessible cysteine on SufE, thereby enhancing the cysteine desulfurase activity of SufS (*152;153*). Interestingly SufE shows structural homology to SufU and IscU implying a similar sulfur transfer mechanism for SufS to SufE and for IscS to IscU (*153;154*). The SufBCD complex has been shown to further enhance the SufE-dependent stimulation of SufS activity and SufB accepts sulfur transferred from SufE for Fe-S cluster assembly (*148;150*).

The SUF machinery in cyanobacteria has a *sufR* gene located directly upstream of the conserved sufBCDS operon. It encodes for the SufR protein which harbors two [4Fe-4S] clusters and functions as a transcriptional repressor of the *sufBCDS* operon and as an autoregulator for *sufR* (*155*). As indicated in Figure 1-3, some *suf* operons such as the one in *T. maritima* encode for a SufU rather than a SufA scaffold protein. SufU has the same three conserved cysteine residues as IscU but does not have the LPPVK motif and does not involve the molecular chaperones for the maturation of Fe-S proteins.

Accessory Proteins Involved in Fe-S Cluster Biogenesis

The above discussion of the NIF, ISC and SUF Fe-S cluster assembly machineries indicates two major types of scaffold proteins, the U-type (IscU, SufU, N-terminal domain of NifU) and A-type (IscA, SufA, ^{nif}IscA), with the possibility of a third type corresponding to the C-terminal domain of NifU (Nfu type) and a fourth type corresponding to SufB. However, considering the large number of Fe-S proteins, it seems likely that there are scaffold proteins for the assembly or delivery of Fe-S clusters that are not part of the *nif*, *isc,* or *suf* operons and that have specific rather than general roles in Fe-S cluster maturation. The recently discovered ErpA protein, which has sequence similar to A-type scaffold proteins, provides a good example of scaffold protein that functions in a specific metabolic pathway (*156*). Recently ErpA was shown to be essential for growth of *E. coli* in the presence of oxygen and to be involved with maturation of IspG, an Fe-S protein involved in one of the key steps in the isoprenoid biosynthetic pathway. The cluster assembled on ErpA is transferred to apo IspG, which catalyzes isopentyl diphosphate biosynthesis in *E. coli* (*156*).

My research program has focused on addressing the role of two ubiquitous classes of proteins, Nfu-type proteins and glutaredoxins, in Fe-S cluster biosynthesis. The potential for each class of protein to be involved with Fe-S biosynthesis is summarized below.

Nfu proteins: Nfu-type proteins, with sequence homology to the C-terminus of NifU including a conserved CXXC motif, are present in both prokaryotes and eukaryotes and *in vivo* studies in yeast, cyanobacteria and plants indicate they play an important role in Fe-S cluster biogenesis (*144;157;158*). *In vitro* evidence for a role of Fe-S cluster scaffolding proteins has come from the presence of Fe-S clusters in as purified recombinant proteins and/or the ability to reconstitute clusters in cysteine desulfurase-mediated reactions, coupled with the ability to

transfer clusters to physiologically relevant acceptor proteins. For example, analytical and spectroscopic studies showed that a subunit-bridging and labile $[4Fe\text{-}4S]^{2+}$ cluster can be reconstituted on human Nfu under anaerobic conditions. (*159*). Likewise $[4Fe\text{-}4S]^{2+}$ clusters can be reconstituted on the C-terminal Nfu domain of *A. vinelandii* NifU and subsequently used for the maturation of the nitrogenase Fe-protein (*94*). Finally. the NifU-like or Nfu protein from *Synechocystis* was purified in a form containing a $[2Fe\text{-}2S]^{2+}$ cluster per dimer and found to be competent for maturation of apo ferredoxin (*22*).

In plants two different Fe-S cluster assembly machineries exist – an ISC system in the mitochondria involving IscU, IscA and Nfu as potential scaffold proteins and a SUF system in chloroplasts involving SufA, SufB and Nfu as potential scaffold proteins (*13;150;160*). There are five genes encoding for Nfu proteins present in *Arabidopsis thaliana,* which are separated into two classes – AtNfu1-3 which are located in the chloroplast and are unique to the plants and AtNfu4 and AtNfu5 which are localized in the mitochondria (*23*). *In vitro* studies have shown that AtNfu2 is capable of binding a labile [2Fe-2S] cluster at the subunit interface of the homodimer (*23*) and *in vivo* studies indicate that *nfu2* gene disruption leads to an impaired assembly of Fe-S proteins containing both [4Fe-4S] and [2Fe-2S] clusters (*161*). Although the plant growth is strongly reduced by *nfu2* gene disruption, it is not lethal to the plant implying that another protein, possibly Nfu1 or Nfu3, may partially complement the defect in the Nfu2 protein. Interestingly mitochondrial Nfu proteins house [4Fe-4S] clusters while the plastid Nfu proteins usually assemble [2Fe-2S] clusters. A possible explanation for this could be that the mitochondria is more oxygen-depleted and thereby allows Nfu proteins to assemble oxygen-labile [4Fe-4S] clusters, whereas the chloroplast environment is more oxygen-rich resulting in the assembly of more oxygen-tolerant [2Fe-2S] clusters.

Glutaredoxins: Glutaredoxins are small ubiquitous oxidoreductases of the thioredoxin family, which are involved in the reduction of disulfide bonds and glutathionylated proteins. Plants contain more than 30 glutaredoxins which can be grouped into three subclasses based on active-site sequence and phylogenetic considerations, see Figure 1-4 (*162*). The first class is characterized by a CXX[C/S] or more precisely [Y/W]C[G/P/S]Y[C/S] active site and is dominated by the classical dithiol glutaredoxins with CGYC and CPYC active sites that are common in other organisms. The second class with a rigorously conserved CGFS active site, commonly referred to as monothiol glutaredoxins, is also widespread in other organisms. The third class is the largest and is generally unique to plants. It comprises a CCX[C/S/G] or more precisely a [S/T/G]CC[M/L][C/S/G] active site and includes all other plant glutaredoxin isoforms.

The dithiol glutaredoxins play a number of biological roles under oxidative stress conditions as seen for Grx1 and Grx2 *in Schizosaccharomyces pombe (163)*. These include the activation of ribonucleotide reductase and 3'-phosphoadenylylsulfate reductase, reduction of ascorbate, glutathione-mediated reduction of dihydrolipoamide, regulation of the DNA binding activity of nuclear factors, neuronal protection against dopamine-induced apoptosis and excitotoxic mitochondrial damage and regulation of signal cascades that protect against oxidative stress (*164-172*). They play a major role in protecting the cell against protein oxidative damage by regulating the glutathionylated state of essential sulfhydryl groups (*173*). Three dithiol glutaredoxins from *E. coli* stimulate insertion of Fe-S cluster in the bacterial fumarate nitrate reductase regulator (FNR) apoprotein (*174*). In humans, one of the two dithiol glutaredoxins Grx2 has been shown to accommodate a [2Fe-2S] cluster bridged by two Grx2 monomers that is proposed to act as a sensor to activate the glutaredoxin under conditions of oxidative stress (*175*).

In the work presented in this dissertation (see Appendix), *Populus trichocarpa* Grx C1 was shown to coordinate a [2Fe-2S] cluster ligated by two cysteines from the two glutaredoxins and two cysteines from glutathione molecules. Subsequent crystallographic studies of human Grx2 revealed analogous [2Fe-2S] cluster ligation to that found in *P. trichocarpa* Grx C1, as shown in Figure 1-5 (*176*). To summarize, dithiol glutaredoxins are primarily involved in redox regulation and some are able to assemble subunit-bridging [2Fe-2S] cluster that may function as a regulatory protein and /or in Fe-S cluster assembly.

The monothiol glutaredoxins containing CGFS active-sites are ubiquitous in biology and recent *in vivo* studies in the yeast *Saccharomyces cerevisiae* implicate roles in Fe regulation and Fe-S cluster biogenesis. *S. cerevisiae* contains three monothiol glutaredoxins, Grx3 and Grx4 which have cytosolic or nuclear locations and Grx5 which is located in the mitochondria. Grx3 and Grx4 were found to interact with and modulate the activity of the iron regulatory transcription factor Aft1p (*177*). Deletion of Grx5 in yeast cells resulted in greater sensitivity to oxidative stress, iron overload and impaired mitochondrial Fe-S cluster biogenesis as evidenced by decreased activity of mitochondrial Fe-S enzymes like aconitase and succinate dehydrogenase (*178;179*). Moreover, immunoprecipitation studies of ^{55}Fe radiolabelled Grx5 deletion mutations revealed build up of Fe on the Isu1p scaffold protein, implicating a role for Grx5 in mediating transfer of Fe-S clusters preassembled on Isu1p to target apo proteins (*21*). Perhaps most intriguing is the observation that deletion of Grx5 in *shiraz* zebrafish results in a deficiency in vertebrate heme synthesis which indicates a role for Grx5 in channeling Fe into Fe-S cluster biosynthesis and heme biosynthesis in mammals (*180*). A recent report has also demonstrated that Grx5 deficiency in human results in sideroblastic-like microcytic anemia and iron overload (*10*).

Summary of Presented Work

(i) Chapter 2 reports the genetic, biochemical and spectroscopic characterization of the *A. vinelandii nfuA* gene product. The combination of UV-visible absorption, resonance Raman and Mössbauer spectroscopic studies and analytical data revealed that the NfuA protein could assemble a $[4Fe\text{-}4S]^{2+}$ cluster at the subunit interface of the homodimer. This cluster can be reduced to an S=1/2 $[4Fe\text{-}4S]^{1+}$ state as indicated by UV-visible absorption, EPR and VTMCD spectroscopies. *In vitro* experiments show that the oxidized [4Fe-4S] cluster assembled on Nfu can activate apo aconitase at physiologically relevant rates.

(iii) Chapter 3 reports the function of chloroplast monothiol glutaredoxins as scaffold proteins involved in the assembly and delivery of $[2Fe\text{-}2S]^{2+}$ clusters. *In vivo* studies show that poplar GrxS14 is a monothiol glutaredoxin that can complement the Fe-S cluster assembly deficiency in yeast Grx5 deletion mutants. Recombinant GrxS14 contains a subunit-bridging $[2Fe\text{-}2S]^{2+}$ cluster as purified and reconstitution of apo GrxS14 in presence of glutathione yields the same cluster-bound species. *In vitro* kinetic studies monitored by CD spectroscopy indicate that the $[2Fe\text{-}2S]^{2+}$ cluster on GrxS14 can be rapidly and stoichiometrically transferred intact to apo *Synechocystis* ferredoxin, a physiologically relevant acceptor protein.

(ii) The appendix reports the functional, structural, and spectroscopic characterization of a $[2Fe\text{-}2S]^{2+}$ cluster in a plant dithiol glutaredoxin. UV-visible absorption, CD and resonance Raman spectroscopies revealed that the cluster has all cysteinyl ligation and the combination of spectroscopic and mutagenesis studies were used to define the cluster ligation and the active-site sequence determinants for cluster assembly. The 2.2 Å crystal structure shows that the $[2Fe\text{-}2S]^{2+}$ cluster is ligated by two cysteines from two monomers and two cysteines from two glutathione molecules.

References

1. Beinert, H., Holm, R. H., and Münck, E. (1997) Iron-sulfur clusters; Nature's modular, multipurpose structures, *Science 277*, 653-659.

2. Beinert, H. (2000) Iron-sulfur proteins: ancient structures, still full of surprises, *J. Biol. Inorg. Chem. 5*, 2-15.

3. Johnson, M. K. and Smith, A. D. (2005) Iron-sulfur proteins, in *Encyclopedia of Inorganic Chemistry, Second Edition* (King, R. B., Ed.) pp 2589-2619, John Wiley & Sons, Chichester.

4. Johnson, D. C., Dean, D. R., Smith, A. D., and Johnson, M. K. (2005) Structure, function and formation of biological iron-sulfur clusters, *Annu. Rev. Biochem. 74*, 247-281.

5. Rudolf, J., Makrantoni, V., Ingledew, W. J., Stark, M. J. R., and White, M. F. (2006) The DNA repair helicases XPD and FancJ have essential iron-sulfur domains, *Molecular Cell 23*, 801-808.

6. Campuzano, V., Montermini, L., Molto, M. D., Pianese, L., Cossee, M., Cavalcanti, F., Monros, E., Rodius, F., Duclos, F., and Monticelli, A. (1996) Friedreich's ataxia:autosomal recessive disease caused by an intronic GAA triplet repeat expansion, *Science 271*, 1423-1427.

7. Cossee, M., Puccio, H., Gansmuller, A., Koutnikova, H., and Dierich, A. (2000) Inactivation of the Friedreich ataxia mouse gene leads to early embryonic lethality without iron accumulation, *Hum. Mol. Genet. 9*, 1219-1226.

8. Karthikeyan, G., Santos, J. H., Graziewicz, M. A., Copeland, W. C., Isaya, G., Houten, B., and Resnick, M. A. (2003) Reduction in fraxatin causes progressive accumulation of mitochondrial damage, *Hum. Mol. Genet. 12*, 3331-3342.

9. Mandavalli, B. S., Santos, J. H., and Houten, B. (2002) Mitochondrial DNA repair and aging, (Glickman, B. W., Ed.) 509 ed., pp 127-151, Elsevier Science.

10. Camaschella, C., Campanelle, A. F. L., Boschetto, L., Merlini, R., Silvestri, L., Levi, S., and Iolascon, A. (2007) The human counterpart of zebrafish *shiraz* shows sideroblastic-like microcytic anemia and iron overload., *Blood 110*, 1353-1358.

11. Nachin, L., El Hassouni, M., Loiseau, L., Expert, D., and Barras, F. (2001) SoxR-dependent response to oxidative stress and virulence of *Erwinia chrysanthemi*: the key role of SufC, an orphan ABC ATPase, *Mol. Microbiol. 39*, 960-972.

12. Lill, R. and Mühlenhoff, U. (2005) Iron-sulfur-protein biogenesis in eukaryotes, *Trends Biochem. Sci. 30*, 133-141.

13. Balk, J. and Lobréaux, S. (2005) Biogenesis of iron-sulfur proteins in plants, *Trends Plant Sci 10*, 324-331.

14. Dean, D. R., Bolin, J. T., and Zheng, L. (1993) Nitrogenase metalloclusters: Structures, organization, and synthesis, *J. Bacteriol. 175*, 6737-6744.

15. Jacobson, M. R., Cash, V. L., Weiss, M. C., Laird, N. F., Newton, W. E., and Dean, D. R. (1989) Biochemical and genetic analysis of the *nifUSVWZM* cluster from *Azotobacter vinelandii*, *Mol. Gen. Genet. 219*, 49-57.

16. Rees, D. C. and Howard, J. B. (2000) Nitrogenase: standing at the crossroads, *Curr. Opin. Chem. Biol. 4*, 260-266.

17. Seefeldt, L. C. and Dean, D. R. (1997) Role of nucleotides in nitrogenase catalysis, *Acc. Chem. Res. 30*, 260-266.

18. Zheng, L., Cash, V. L., Flint, D. H., and Dean, D. R. (1998) Assembly of iron-sulfur clusters. Identification of an *iscSUA-hscBA-fdx* gene cluster from *Azotobacter vinelandii*, *J. Biol. Chem. 273*, 13264-13272.

19. Outten, F. W., Djaman, O., and Storz, G. (2004) A *suf* operon requirement for Fe-S cluster assembly during iron starvation in *Escherichia coli*, *Mol. Microbiol. 52*, 861-872.

20. Takahashi, Y. and Tokumoto, U. (2002) A third bacterial system for the assembly of iron-sulfur clusters with homologs in archaea and plastids, *J. Biol. Chem. 277*, 28380-28383.

21. Mühlenhoff, U., Gerber, J., Richhardt, N., and Lill, R. (2003) Components involved in assembly and dislocation of iron-sulfur clusters on the scaffold protein Iscu1p, *EMBO J. 22*, 4815-4825.

22. Nishio, K. and Nakai, M. (2000) Transfer of iron-sulfur cluster from NifU to apoferredoxin, *J. Biol. Chem. 275*, 22615-22618.

23. Léon, S., Touraine, B., Ribot, C., Briat, J.-F., and Lobréaux, S. (2003) Iron-sulfur cluster assembly in plants: Distinct NFU proteins in mitochondria and plastids from *Arabidopsis thaliana*, *Biochem. J. 371*, 823-830.

24. Bominaar, E. L., Hu, Z., Münck, E., Girerd, J.-J., and Borshch, S. A. (1995) Double exchange and vibronic coupling in mixed-valence systems. Electronic structure of exchange-coupled siroheme-$[Fe_4S_4]^{2+}$ chromophore in oxidized *E. coli* sulfite reductase, *J. Am. Chem. Soc. 117*, 6976-6989.

25. Noodleman, L., Lovell, T., Liu, T., Himo, F., and Torres, R. A. (2002) Insights into properties and energetics of iron-sulfur proteins from simple clusters to nitrogenase, *Curr. Opin. Chem. Biol. 6*, 259-273.

26. Romao, M. J. and Archer, M. (1999) Structural versatility of proteins containing rubredoxin-type centers, in *Iron Metabolism* (Ferreira, G. C., Moura, J. J. G., and Franco, R., Eds.) pp 341-358, Wiley-VCH Verlag, Weinheim.

27. Kurtz, D. M., Jr. and Coulter, E. D. (2001) Bacterial nonheme iron proteins and oxidative stress, *Chemtracts, Inorg. Chem. 14*, 407-435.

28. Link, T. A. (1999) The structures of Rieske and Rieske-type proteins, *Adv. Inorg. Chem. 47*, 83-157.

29. Berkovitch, F., Nicolet, Y., Wan, J. T., Jarrett, J. T., and Drennan, C. L. (2004) Crystal structure of biotin synthase, an *S*-adenosylmethionine-dependent radical enzyme, *Science 303*, 76-79.

30. Hagen, W. R., Silva, P. J., Amorim, M. A., Hagedoorn, P. L., Wassink, H., Haaker, H., and Robb, F. T. (2000) Novel structure and redox chemistry of the prosthetic groups of the iron-sulfur flavoprotein sulfide dehydrogenase from *Pyrococcus furiosus*; evidence for a [2Fe-2S] cluster with Asp(Cys)3 ligands., *J. Biol. Inorg. Chem. 5*, 527-534.

31. Yankovskaya, V., Horsefield, R., Törnroth, S., Luna-Chavez, C., Miyoshi, H., Léger, C., Byrne, B., Cecchini, G., and Iwata, S. (2003) Architecture of succinate dehydrogenase and reactive oxygen species generation, *Science 299*, 700-704.

32. Leggate, E. J., Bill, E., Essigke, T., Ullmann, G. M., and Hirst, J. (2004) Formation and characterization of an all-ferrous Rieske cluster and stabilization of the $[2Fe\text{-}2S]^0$ core by protonation, *Proc. Natl. Acad. Sci. USA 101*, 10913-10918.

33. Achim, C., Golinelli, M.-P., Bominaar, E. L., Meyer, J., and Münck, E. (1996) Mossbauer study of Cys56Ser mutant 2Fe ferredoxin from *Clostridium pasteurianum*: Evidence for double exchange in an $[Fe_2S_2]^+$ cluster, *J. Am. Chem. Soc. 118*, 8168-8169.

34. Achim, C., Bominaar, E. L., Meyer, J., Peterson, J., and Münck, E. (1999) Observation and interpretation of temperature-dependent valence delocalization in the $[2Fe\text{-}2S]^+$ cluster in ferredoxin from *Clostridium pasteurianum*, *J. Am. Chem. Soc. 121*, 3704-3714.

35. Crouse, B. R., Meyer, J., and Johnson, M. K. (1995) Spectroscopic evidence for a reduced Fe_2S_2 cluster with a $S = 9/2$ ground state in mutant forms of *Clostridium pasteurianum* 2Fe ferredoxin, *J. Am. Chem. Soc. 117*, 9612-9613.

36. Johnson, M. K., Duin, E. C., Crouse, B. R., Golinelli, M.-P., and Meyer, J. (1998) Valence-delocalized $[Fe_2S_2]^+$ clusters, in *Spectroscopic methods in bioinorganic chemistry* (Solomon, E. I. and Hodgson, K. O., Eds.) pp 286-301, American Chemical Society, Washington, D.C.

37. Beinert, H. and Thomson, A. J. (1983) Three-iron clusters in iron-sulfur proteins, *Arch. Biochem. Biophys. 222*, 333-361.

38. Johnson, M. K., Duderstadt, R. E., and Duin, E. C. (1999) Biological and synthetic $[Fe_3S_4]$ clusters, *Adv. Inorg. Chem. 47*, 1-82.

39. Duff, J. L. C., Breton, J. L., Butt, J. N., Armstrong, F. A., and Thomson, A. J. (1996) Novel redox chemistry of the [3Fe-4S] clusters: Electrochemical characterization of the

all-Fe(II) form of the [3Fe-4S] cluster generated reversibly in various proteins and its spectroscopic investigation in *Sulfolobus acidocaldarius* ferredoxin, *J. Am. Chem. Soc. 118*, 8593-8603.

40. Kennedy, M. C., Kent, T. A., Emptage, M. H., Merkle, H., Beinert, H., and Münck, E. (1984) Evidence for the formation of a linear [3Fe-4S] cluster in partially unfolded aconitase, *J. Biol. Chem. 259*, 14463-14471.

41. Richards, A. J. M., Thomson, A. J., Holm, R. H., and Hagen, K. S. (1990) The magnetic circular dichroism spectra of the linear trinuclear clusters $[Fe_3S_4(SR)_4]^{3-}$ in purple aconitase and in a synthetic model, *Spectrochim. Acta 46A*, 987-993.

42. Gailer, J., George, G. N., Pickering, I. J., Prince, R. C., Kohlhepp, P., Zhang, D., Walker, F. A., and Winzerling, J. J. (2001) Human cytosolic iron regulatory protein 1 contains a linear iron-sulfur cluster, *J. Am. Chem. Soc. 123*, 10121-10122.

43. Calzolai, L., Gorst, C. M., Zhou, Z.-H., Teng, Q., Adams, M. W. W., and La Mar, G. N. (1995) ^{1}H-NMR investigation of the electronic and molecular structure of the 4-iron cluster ferredoxin from the hyperthermophile *Pyrococcus furiosus* - identification of Asp-14 as a cluster ligand in each of the 4 redox states., *Biochemistry 34*, 11373-11384.

44. Peters, J. W., Lanzilotta, W. N., Lemon, B. J., and Seefeldt, L. C. (1998) X-ray crystal structure of the Fe-only hydrogenase (Cp1) from *Clostridium pasteurianum* to 1.8 Angstrom resolution, *Science 282*, 1853-1858.

45. Volbeda, A., Charon, M.-H., Piras, C., Hatchikian, E. C., Frey, M., and Fontecilla-Camps, J. C. (1995) Crystal structure of the nickel-iron hydrogenase from *Desulfovibrio gigas*, *Nature 373*, 580-587.

46. Bertero, M. G., Rothery, R. A., Palak, M., Hou, C., Lim, D., Blasco, F., Weiner, J. H., and Strynadka, N. C. (2003) Insights into the respiratory electron transfer pathway from the structure of nitrate reductase A, *Nat. Struct. Biol. 10*, 681-687.

47. Angove, H. C., Yoo, S. J., Burgess, B. K., and Münck, E. (1997) Mössbauer and EPR evidence for an all-ferrous Fe_4S_4 cluster with $S = 4$ in the Fe protein of nitrogenase, *J. Am. Chem. Soc. 119*, 8730-8731.

48. Strop, P., Takahara, P. M., Chiu, H.-J., Angove, H. C., Burgess, B. K., and Rees, D. C. (2001) Crystal structure of the all-ferrous $[4Fe\text{-}4S]^0$ form of the nitrogenase iron protein from *Azotobacter vinelandii*, *Biochemistry 40*, 651-656.

49. Watt, G. D. and Reddy, K. R. N. (1994) Formation of an all ferrous Fe_4S_4 cluster in the iron-protein-component of *Azotobacter vinelandii* nitrogenase, *J. Inorg. Biochem. 53*, 281-294.

50. Arendsen, A. F., Hadden, J., Card, G., McAlpine, A. S., Bailey, S., Zaitsev, V., Duke, E. H. M., Lindley, P. F., Kröckel, M., Trautwein, A. X., Feiters, M. C., Charnock, J. M., Garner, C. D., Marritt, S. J., Thomson, A. J., Kooter, I. M., Johnson, M. K., van den

Berg, W. A. M., van Dongen, W. M. A. M., and Hagen, W. R. (1998) The "prismane" protein resolved: X-ray structure at 1.7 Å and multiple spectroscopy of two novel 4Fe clusters, *J. Biol. Inorg. Chem. 3*, 81-95.

51. Duderstadt, R. E., Brereton, P. S., Adams, M. W. W., and Johnson, M. K. (1999) A pure $S = 3/2$ $[Fe_4S_4]^+$ cluster in the A33Y variant of *Pyrococcus furiosus* ferredoxin, *FEBS Lett. 454*, 21-26.

52. Johnson, M. K. (1994) Iron-sulfur proteins, in *Encyclopedia of inorganic chemistry* (King, R. B., Ed.) 1st ed., pp 1896-1915, John Wiley & Sons, Chichester.

53. Koehler, B. P., Mukund, S., Conover, R. C., Dhawan, I. K., Roy, R., Adams, M. W. W., and Johnson, M. K. (1996) Spectroscopic characterization of the tungsten and iron centers in aldehyde ferredoxin oxidoreductases from two hyperthermophilic archaea, *J. Am. Chem. Soc. 118*, 12391-12405.

54. Peters, J. W., Stowell, M. H. B., Soltis, S. M., Finnegan, M. G., Johnson, M. K., and Rees, D. C. (1997) Redox-dependent structural-changes in the nitrogenase P-cluster, *Biochemistry 36*, 1181-1187.

55. Page, C. C., Moser, C. C., Chen, X., and Dutton, P. L. (1999) Natural engineering principles of electron tunnelling in biological oxidation-reduction, *Nature 402*, 47-52.

56. Calzolai, L., Zhou, Z.-H., Adams, M. W. W., and La Mar, G. N. (1996) The role of cluster-ligated aspartate in gating electron transfer in the four-iron ferredoxin from the hyperthermophilic archaeon *Pyrococcus furiosus*, *J. Am. Chem. Soc. 118*, 2513-2514.

57. Hunsicker-Wang, L. M., Heine, A., Chen, Y., Luna, E. P., Todaro, T., Zhang, Y. M., Williams, P. A., McRee, D. E., Hirst, J., Stout, C. D., and Fee, J. A. (2003) High-resolution structure of the soluble, respiratory-type Rieske protein from *Thermus thermophilus*: Analysis and comparison, *Biochemistry 42*, 7303-7217.

58. Beinert, H., Kennedy, M. C., and Stout, C. D. (1996) Aconitase as iron-sulfur protein, enzyme, and iron-regulatory protein, *Chem. Rev. 96*, 2335-2373.

59. Flint, D. H. and Allen, R. M. (1996) Iron-sulfur proteins with non-redox functions, *Chem. Rev. 96*, 2315-2334.

60. Jarrett, J. T. (2003) The generation of 5'-deoxyadenosyl radicals by adenosylmethioine-dependent radical enzymes, *Curr. Opin. Chem. Biol. 7*, 174-182.

61. Marsh, E. N. G., Patwardhan, A., and Huhta, M. S. (2004) *S*-adenosylmethionine radical enzymes, *Bioorg. Chem. 32*, 326-340.

62. Layer, G., Heinz, D. W., Jahn, D., and Schubert, W.-D. (2004) Structure and function of radical SAM enzymes, *Curr. Opin. Chem. Biol. 8*, 468-476.

63. Sofia, H. J., Chen, G., Hetzler, B. G., Reyes-Spindola, J. F., and Miller, N. E. (2001) Radical SAM, a novel protein superfamily linking unresolved steps in familiar biosynthetic pathways with radical mechanisms: Functional characterization using new analysis and information visualization methods, *Nucleic Acids Res. 29*, 1097-1106.

64. Dobbek, H., Svetlitchnyi, V., Gremer, L., Huber, R., and Meyer, O. (2001) Crystal structure of carbon monoxide dehydrogenase reveals a [Ni-4Fe-5S] cluster, *Science 293*, 1281-1285.

65. Crane, B. R., Siegel, L. M., and Getzoff, E. D. (1995) Sulfite reductase structure at 1.6 Å - Evolution and catalysis for reduction of inorganic anions, *Science 270*, 59-67.

66. Darnault, C., Volbeda, A., Kim, E. J., Legrand, P., Vernède, X., Lindahl, P. A., and Fontecilla-Camps, J. C. (2003) Ni-Zn-[Fe4-S4] and Ni-Ni-[Fe4-S4] clusters in closed and open subunits of acetyl-CoA synthase/carbon monoxide dehydrogenase., *Nat. Struct. Biol. 10*, 271-279.

67. Doukov, T. I., Iverson, T. M., Seravalli, J., Ragsdale, S. W., and Drennan, C. L. (2002) A Ni-Fe-Cu center in a bifunctional carbon monoxide dehydrogenase/acetyl-CoA synthase, *Science 298*, 567-572.

68. Nicolet, Y., Cavazza, C., and Fontecilla-Camps, J. C. (2002) Fe-only hydrogenases: structure, function and evolution, *J. Inorg. Biochem. 91*, 1-8.

69. Svetlitchnyi, V., Dobbek, H., Meyer-Klaucke, W., Meins, T., Thiele, T., Rõmer, P., Huber, R., and Meyer, O. (2004) A functional Ni-Ni-[4Fe-4S] cluster in the monomeric acetyl-CoA synthase from *Carboxydothermus hydrogenoformans*, *Proc. Natl. Acad. Sci. USA 101*, 446-451.

70. Cunningham, R. P., Asahara, H., Bank, J. F., Scholes, C. P., Salerno, J. C., Surerus, K. K., Münck, E., McCracken, J., Peisach, J., and Emptage, M. H. (1989) Endonuclease III is an iron-sulfur protein, *Biochemistry 28*, 4450-4455.

71. Guan, Y., Manuel, R. C., Arvai, A. S., Parikh, S. S., Mol, C. D., Miller, J. H., Lloyd, R. S., and Tainer, J. A. (1998) MutY catalytic core, mutant and bound adenine structures define specificity for DNA repair enzyme superfamily, *Nat. Struct. Biol. 5*, 1058-1064.

72. Kuo, C.-F., McRee, D. E., Fisher, C. L., O'Handley, S. F., Cunningham, R. P., and Tainer, J. A. (1992) Atomic structure of the DNA repair [4Fe-4S] enzyme endonuclease III, *Science 258*, 434-440.

73. Porello, S. L., Cannon, M. J., and David, S. S. (1998) A substrate recognition role for the [4Fe-4S]$^{2+}$ cluster of the DNA repair glycosylase MutY, *Biochemistry 37*, 6465-6475.

74. Thauer, R. K. and Schönheit, P. (1982) Iron-sulfur complexes of ferredoxin as a storage form of iron in *Clostridium pasteurianum*, in *Iron-Sulfur Proteins* (Spiro, T. G., Ed.) pp 329-341, Wiley, New York.

75. Hedderich, R., Albracht, S. P. J., Linder, D., Koch, J., and Thauer, R. K. (1992) Isolation and characterization of polyferredoxin from *Methanobacterium thermoautotrophicum*. The *mvhB* gene product of the methylviologen-reducing hydrogenase operon, *FEBS Lett. 298*, 65-68.

76. Reeve, J. N., Beckler, G. S., Cram, D. S., Hamilton, P. T., Brown, J. W., Krzycki, J. A., Kolodziej, A. F., Alex, L. A., Orme-Johnson, W. H., and Walsh, C. T. (1989) A hydrogenase-linked gene in *Methanobacterium thermoautotrophicum* strain ΔH encodes a polyferredoxin, *Proc. Natl. Acad. Sci. USA 86*, 3031-3035.

77. Demple, B., Ding, H., and Jorgensen, M. (2002) *Escherichia coli* SoxR protein:sensor/transducer of oxidative stress and nitric oxide, *Meth. Enzymol. 348*, 355-364.

78. Gaudu, P. and Weiss, B. (1996) SoxR, a [2Fe-2S] transcription factor, is active only in its oxidized form, *Proc. Natl. Acad. Sci. USA 93*, 10094-10098.

79. Kiley, P. J. and Beinert, H. (2003) The role of Fe-S proteins in sensing and regulation in bacteria, *Curr. Opin. Microbiol. 6*, 181-185.

80. Grandoni, J. A., Switzer, R. L., Marakoff, C. A., and Zalkin, H. (1989) Evidence that the iron-sulfur cluster of Bacillus subtilis glutamine phosphoribosylpyrophosphate amidotransferase determines stability of the enzyme to degradation in vivo, *J. Biol. Chem. 264*, 6058-6064.

81. Smith, J. L., Zaluzec, E. J., Wery, J.-P., Niu, L., Switzer, R. L., Zalkin, H., and Satow, Y. (1994) Structure of the allosteric regulatory enzyme of purine biosynthesis, *Science 264*, 1427-1433.

82. Wu, C.-K., Dailey, H. A., Rose, J. P., Burden, A., Sellers, V. M., and Wang, B.-C. (2001) The 2.0 Å structure of human ferrochelatase, the terminal enzyme of heme biosynthesis, *Nature Struct. Biol. 8*, 156-160.

83. Sellers, V. M., Johnson, M. K., and Dailey, H. A. (1996) Function of the [2Fe-2S] cluster in mammalian ferrochelatase: A possible role as a nitric oxide sensor, *Biochemsitry 35*, 2699-2704.

84. Dai, S., Schwendtmayer, C., Schürmann, P., Ramaswamy, S., and Eklund, H. (2000) Redox signaling in chloroplasts: Cleavage of disulfides by an iron-sulfur cluster, *Science 287*, 655-658.

85. Duin, E. C., Madadi-Kahkesh, S., Hedderich, R., Clay, M. D., and Johnson, M. K. (2002) Heterodisulfide reductase from *Methanothermobacter marburgensis* contains an active-site [4Fe-4S] cluster that is directly involved in mediating heterodisulfide reduction, *FEBS Lett. 512*, 263-268.

86. Walters, E. M. and Johnson, M. K. (2004) Ferredoxin:thioredoxin reductase: disulfide reduction catalyzed via novel site-specific [4Fe-4S] cluster chemistry, *Photosynth. Res. 79*, 249-264.

87. Jameson, G. N. L., Cosper, M. M., Hernández, H. L., Johnson, M. K., and Huynh, B. H. (2004) Role of the [2Fe-2S] cluster in recombinant *Escherichia coli* biotin synthase, *Biochemistry 43*, 2022-2031.

88. Ugulava, N. B., Gibney, B. R., and Jarrett, J. T. (2001) Biotin synthase contains two distinct iron-sulfur cluster binding sites: chemical and spectroelectrochemical analysis of iron-sulfur cluster interconversions, *Biochemistry 40*, 8343-8351.

89. Johnson, D. C., Unciuleac, M.-C., and Dean, D. R. (2006) Controlled expression and functional analysis of iron-sulfur cluster biosynthetic components within *Azotobacter vinelandii*, *J. Bacteriol. 188*, 7551-7561.

90. Olson, J. W., Agar, J. N., Johnson, M. K., and Maier, R. J. (2000) Characterization of the NifU and NifS Fe-S cluster formation proteins essential for the viability of *Helicobacter pylori*, *Biochemistry 39*, 16213-16219.

91. Zheng, L., White, R. H., Cash, V. L., Jack, R. F., and Dean, D. R. (1993) Cysteine desulfurase activity indicates a role for NIFS in metallocluster biosynthesis, *Proc. Natl. Acad. Sci. USA 90*, 2754-2758.

92. Agar, J. N., Yuvaniyama, P., Jack, R. F., Cash, V. L., Smith, A. D., Dean, D. R., and Johnson, M. K. (2000) Modular organization and identification of a mononuclear iron-binding site within the NifU protein, *JBIC,J. Biol. Inorg. Chem. 5*, 167-177.

93. Fu, W., Jack, R. F., Morgan, T. V., Dean, D. R., and Johnson, M. K. (1994) *nifU* gene product from *Azotobacter vinelandii* is a homodimer that contains two identical [2Fe-2S] clusters., *Biochemistry 33*, 13455-13463.

94. Smith, A. D., Jameson, G. N. L., Dos Santos, P. C., Agar, J. N., Naik, S., Krebs, C., Frazzon, J., Dean, D. R., Huynh, B. H., and Johnson, M. K. (2005) NifS-mediated assembly of [4Fe-4S] clusters in the N- and C-terminal domains of the NifU scaffold protein, *Biochemistry 44*, 12955-12969.

95. Yuvaniyama, P., Agar, J. N., Cash, V. L., Johnson, M. K., and Dean, D. R. (2000) NifS-directed assembly of a transient [2Fe-2S] cluster within the NifU protein, *Proc. Natl. Acad. Sci. USA 97*, 599-604.

96. Krebs, C., Agar, J. N., Smith, A. D., Frazzon, J., Dean, D. R., Huynh, B. H., and Johnson, M. K. (2001) IscA, an alternative scaffold for Fe-S cluster biosynthesis, *Biochemistry 40*, 14069-14080.

97. Evan, D. J., Jones, R., Woodley, P. R., Wilborn, J. R., and Robson, R. L. (1991) Nucleotide sequence and genetic analysis of the *Azotobacter chroococcum nifUSVWZM*

gene cluster, including a new gene (*nifP*) which encodes a serine acetyltransferase, *J. Bacteriol. 173*, 5457-5469.

98. Cupp-Vickery, J. R., Urbina, H. D., and Vickery, L. E. (2003) Crystal structure of IscS, a cysteine desulfurase from *Escherichia coli*, *J. Mol. Biol. 330*, 1049-1059.

99. Kaiser, J. T., Clausen, T., Bourenkow, G. P., Bartunik, H.-D., Steinbacher, S., and Huber, R. (2000) Crystal structure of a NifS-like protein from *Thermotoga maritima*: Implications for iron-sulfur cluster assembly, *J. Mol. Biol. 297*, 451-464.

100. Agar, J. N., Zheng, L., Cash, V. L., Dean, D. R., and Johnson, M. K. (2000) Role of the IscU protein in iron-sulfur cluster biosynthesis: IscS-mediated assembly of a $[Fe_2S_2]$ cluster in IscU, *J. Am. Chem. Soc. 122*, 2136-2137.

101. Agar, J. N., Krebs, B., Frazzon, J., Huynh, B. H., Dean, D. R., and Johnson, M. K. (2000) IscU as a scaffold for iron-sulfur cluster biosynthesis: Sequential assembly of [2Fe-2S] and [4Fe-4S] clusters in IscU, *Biochemistry 39*, 7856-7862.

102. Liu, J., Oganesyan, N., Shin, D. H., Jancarik, J., Yokota, H., Kim, R., and Kim, S.-H. (2005) Structural characterization of an iron-sulfur cluster assembly protein IscU in a zinc-bound form, *Proteins:Struct. Func. Bioinform. 59*, 875-881.

103. Ramelot, T. A., Cort, J. R., Goldsmith-Fischman, S., Kornhaber, G. J., Xiao, R., Shastry, R., Acton, T. B., Honig, B., Montelione, G. T., and Kennedy, M. A. (2004) Solution NMR structure of the iron-sulfur cluster assembly protein U (IscU) with zinc bound at the active site, *J. Mol. Biol. 344*, 567-583.

104. Unciuleac, M.-C., Chandramouli, K., Naik, S., Mayer, S., Huynh, B. H., Johnson, M. K., and Dean, D. R. (2007) *In vitro* activation of apo-aconitase using a [4Fe-4S] cluster-loaded form of the IscU [Fe-S] cluster scaffolding protein, *Biochemistry 46*, 6812-6821.

105. Wu, S.-P., Wu, G., Surerus, K. K., and Cowan, J. A. (2002) Iron-sulfur cluster biosynthesis: Kinetic analysis of [2Fe-2S] cluster transfer from holo ISU to apo Fd: Role of redox chemistry and a conserved aspartate, *Biochemistry 41*, 8876-8885.

106. Agar, J. N., Dean, D. R., and Johnson, M. K. (2003) Iron-sulfur cluster biosynthesis, in *Biochemistry and Physiology of Anaerobic Bacteria* (Ljungdahl, L. G., Adams, M. W. W., Barton, L. L., Ferry, J. G., and Johnson, M. K., Eds.) pp 46-66, Springer-Verlag, New York.

107. Smith, A. D., Agar, J. N., Johnson, K. A., Frazzon, J., Amster, I. J., Dean, D. R., and Johnson, M. K. (2001) Sulfur transfer from IscS to IscU: The first step in iron-sulfur cluster biosynthesis, *J. Am. Chem. Soc. 123*, 11103-11104.

108. Smith, A. D., Frazzon, J., Dean, D. R., and Johnson, M. K. (2005) Role of conserved cysteines in mediating sulfur transfer from IscS to IscU, *FEBS Lett. 579*, 5236-5240.

109. Nuth, M., Yoon, T., and Cowan, J. A. (2002) Iron-sulfur cluster biosynthesis: Characterization of iron nucleation sites for the assembly of the $[2Fe\text{-}2S]^{2+}$ cluster core in IscU proteins, *J. Am. Chem. Soc. 124*, 8774-8775.

110. Ding, H. and Clark, R. J. (2004) Characterization of iron-binding in IscA, an ancient iron-sulfur cluster assembly protein, *Biochem. J. 379*, 433-440.

111. Ding, H., Clark, R. J., and Ding, B. (2004) IscA mediates iron delivery for assembly of iron-sulfur clusters in IscU under limited "free" iron conditions, *J. Biol. Chem. 279*, 37499-37504.

112. Ding, H., Harrison, K., and Lu, J. (2005) Thioredoxin reductase system mediates iron binding in IscA and iron-delivery for the iron-sulfur cluster assembly in IscU, *J. Biol. Chem. 280*, 30432-30437.

113. Yang, J., Bitoun, J. P., and Ding, H. (2006) Interplay of IscA and IscU in biogenesis of iron-sulfur clusters, *J. Biol. Chem. 281*, 27956-27963.

114. Shan, Y., Napoli, E., and Cortopassi, G. (2007) Mitochondrial frataxin interacts with ISD11 of the NFS1/ISCU complex and multiple mitochondrial chaperones, *Hum. Mol. Genet. 16*, 929-941.

115. Yoon, T. and Cowan, J. A. (2003) Iron-sulfur cluster biosynthesis. Characterization of frataxin as an iron donor for assembly of [2Fe-2S] clusters in ISU-type proteins, *J. Am. Chem. Soc. 125*, 6078-6084.

116. Cho, S.-J., Lee, M. G., Yang, J. K., Lee, J. Y., Song, H. K., and Suh, S. W. (2000) Crystal structure of *Escherichia coli* CyaY protein reveals a previously unidentified fold for the evolutionarily conserved frataxin family, *Proc. Natl. Acad. Sci. USA 97*, 8932-8937.

117. Layer, G., Ollagnier-de-Choudens, S., Sanakis, Y., and Fontecave, M. (2006) Iron-sulfur cluster biosynthesis. Characterization of *Eschericia coli* CyaY as an iron donor for the assembly of [2Fe-2S] clusters in the scaffold IscU, *J. Biol. Chem. 281*, 16256-16263.

118. Ding, H., Yang, J., Coleman, L. C., and Yeung, S. (2007) Distinct iron binding property of two putative iron donors for the iron-sulfur cluster assembly: IscA and the bacterial frataxin ortholog CyaY under physiological and oxidative stress conditions, *J. Biol. Chem. 282*, 7997-8004.

119. Ollagnier-de-Choudens, S., Mattioli, T., Takahashi, Y., and Fontecave, M. (2001) Iron-sulfur cluster assembly. Characterization of IscA and evidence for a specific functional complex with ferredoxin, *J. Biol. Chem. 276*, 22604-22607.

120. Ollagnier-de-Choudens, S., Sanakis, Y., and Fontecave, M. (2004) SufA/IscA: reactivity studies of a class of scaffold proteins involved with [Fe-S] cluster assembly, *J. Biol. Inorg. Chem. 9*, 828-838.

121. Morimoto, K., Yamashita, E., Kondou, Y., Lee, S. J., Arisaka, F., Tsukihara, T., and Nakai, M. (2006) The asymmetric IscA homodimer with an exposed [2Fe-2S] cluster suggests the structural basis of the Fe-S cluster biosynthetic scaffold, *J. Mol. Biol. 360*, 117-132.

122. Kim, R., Saxena, S., Gordon, D. M., Pain, D., and Dancis, A. (2001) J-domain protein, Jac1p, of yeast mitochondria required for iron homeostasis and activity of Fe-S cluster proteins, *J. Biol. Chem. 276*, 17524-17532.

123. Lutz, T., Westermann, B., Neupert, W., and Herrmann, J. M. (2001) The mitochondrial proteins Ssq1 and Jac1 are required for the assembly of iron-sulfur clusters in mitochondria, *J. Mol. Biol. 307*, 815-825.

124. Takahashi, Y. and Nakamura, M. (1999) Functional assignment of the ORF2-*iscS-iscA-hscB-hscA-fdx*-ORF3 gene cluster involved in the assembly of Fe-S clusters in *Escherichia coli*, *J. Biochem. 126*, 917-926.

125. Tokumoto, U. and Takahashi, Y. (2001) Genetic analysis of the *isc* operon in *Escherichia coli* involved with the biogenesis of cellular iron-sulfur proteins, *J. Biochem. 130*, 63-71.

126. Voisine, C., Cheng, Y. C., Ohlson, M., Schilke, B., Hoff, K., Beinert, H., Marszalek, J., and Craig, E. A. (2001) Jac1, a mitochondrial J-type chaperone, is involved in the biogenesis of Fe/S clusters in *Saccharomyces cerevisiae*, *Proc. Natl. Acad. Sci. USA 98*, 1483-1488.

127. Cupp-Vickery, J. R., Peterson, J. C., Ta, D. T., and Vickery, L. E. (2004) Crystal structure of the molecular chaperone HscA substrate binding domain complexed with the IscU recognition peptide ELPPVKIHC, *J. Mol. Biol. 342*, 1265-1278.

128. Hoff, K. G., Silberg, J. J., and Vickery, L. E. (2000) Interaction of the iron-sulfur cluster assembly protein IscU with the Hsc66/Hsc20 molecular chaperone system of *Escherichia coli*, *Proc. Natl. Acad. Sci. USA 97*, 7790-7795.

129. Hoff, K. G., Ta, D. T., Tapley, T. L., Silberg, J. J., and Vickery, L. E. (2002) Hsc66 substrate specificity is directed toward a discrete region of the iron-sulfur cluster template protein IscU, *J. Biol. Chem. 277*, 27353-27359.

130. Hoff, K. G., Cupp-Vickery, J. R., and Vickery, L. E. (2003) Contributions of the LPPVK motif of the iron-sulfur template protein IscU to interactions with the Hsc66-Hsc20 chaperone system, *J. Biol. Chem. 278*, 37582-37589.

131. Mayer, M. P., Brehmer, D., Gassler, C. S., and Bukau, B. (2001) Hsp70 chaperone machines, *Adv. Protein Chem. 59*, 1-44.

132. Silberg, J. J. and Vickery, L. E. (2000) Kinetic characterization of the ATPase cycle of the molecular chaperone Hsc66 from *Escherichia coli*, *J. Biol. Chem. 275*, 7779-7786.

133. Silberg, J. J., Tapley, T. L., Hoff, K. G., and Vickery, L. E. (2004) Regulation of the HscA ATPase reaction cycle by the co-chaperone HscB and the iron-sulfur cluster assembly protein IscU, *J. Biol. Chem. 279*, 53924-53931.

134. Wu, S.-P., Mansy, S. S., and Cowan, J. A. (2005) Iron-sulfur cluster biosynthesis. Molecular chaperone DnaK promotes IscU-bound [2Fe-2S] cluster stability amd inhibits cluster transfer activity, *Biochemistry 44*, 4284-4293.

135. Chandramouli, K. and Johnson, M. K. (2006) HscA and HscB stimulate [2Fe-2S] cluster transfer from IscU to apoferredoxin in an ATP-dependent reaction, *Biochemistry 45*, 11087-11095.

136. Jung, Y.-S., Gao-Sheridan, H. S., Christiansen, J., Dean, D. R., and Burgess, B. K. (1999) Purification and biophysical characterization of a new [2Fe-2S] ferredoxin from *Azotobacter vinelandii*, a putative [Fe-S] cluster assembly/repair protein, *J. Biol. Chem. 274*, 32402-32410.

137. Lange, H., Kaut, A., Kispal, G., and Lill, R. (2000) A mitochondrial ferredoxin is essential for biogenesis of cellular iron-sulfur proteins, *Proc. Natl. Acad. Sci. USA 97*, 1050-1055.

138. Chandramouli, K., Unciuleac, M.-C., Naik, S., Dean, D. R., Huynh, B. H., and Johnson, M. K. (2007) Formation and properties of [4Fe-4S] clusters on the IscU scaffold protein, *Biochemistry 46*, 6804-6811.

139. Schwartz, C. J., Giel, J. L., Patschkowski, T., Luther, C., Ruzicka, F. J., Beinert, H., and Kiley, P. J. (2001) IscR, an Fe-S cluster-containing transcription factor, represses expression of *Escherichia coli* genes encoding Fe-S cluster assembly proteins, *Proc. Natl. Acad. Sci. USA 98*, 14895-14900.

140. Giel, J. L., Rodionov, D., Liu, M., Blattner, F. R., and Kiley, P. J. (2006) IscR-dependent gene expression links iron-sulphur cluster assembly to the control of O_2-regulated genes in *Escherichia coli*, *Mol. Microbiol. 60*, 1058-1075.

141. Yeo, W.-S., Lee, J.-H., Lee, K.-C., and Roe, J.-H. (2006) IscR acs as an activator in response to oxidative stress for the *suf* operon encoding Fe-S assembly proteins, *Mol. Microbiol. 61*, 206-218.

142. Huet, G., Daffe, M., and Saves, I. (2005) Identification of the *Mycobacterium tuberculosis* SUF machinery as the exclusive mycobacterial system of [Fe-S] cluster assembly: evidence for its implication in the pathogen's survival, *J. Bacteriol. 187*, 6137-6146.

143. Ollagnier-de-Choudens, S., Nachin, L., Sanakis, Y., Loiseau, L., Barras, F., and Fontecave, M. (2003) SufA from *Erwinia chrysanthemi*. Characterization of a scaffold protein required for iron-sulfur cluster assembly, *J. Biol. Chem. 278*, 17993-18001.

144. Balasubramanian, R., Shen, G., Bryant, D. A., and Golbeck, J. H. (2006) Regulatory roles for IscA and SufA in iron homeostasis and redox stress responses in the cyanobacterium *Synechococcus* sp. strain PCC 7002, *J. Bacteriol. 188*, 3182-3191.

145. Watanabe, S., Kita, A., and Miki, K. (2005) Crystal structure of atypical cytoplasmic ABC-ATPase SufC from *Thermus thermophilus*, *J. Mol. Biol. 353*, 1043-1054.

146. Eccleston, J. F., Petrovic, A., Davis, C. T., Rangachari, K., and Wilson, R. J. (2006) The kinetic mechanism of the SufC ATPase: The cleavage step is accelerated by SufB, *J. Biol. Chem. 281*, 8371-8378.

147. Nachin, L., Loiseau, L., Expert, D., and Barras, F. (2003) SufC: an unorthodox cytoplasmic ABC/ATPase required for [Fe-S] biogenesis under oxidative stress, *EMBO J. 22*, 427-437.

148. Outten, F. W., Wood, M. J., Muñoz, F. M., and Storz, G. (2003) The SufE protein and the SufBCD complex enhance SufS cysteine desulfurase activity as part of a sulfur transfer pathway for Fe-S cluster assembly in *E. coli*, *J. Biol. Chem. 278*, 45713-45719.

149. Rangachari, K., Davis, C. T., Eccleston, J. F., Hirst, E. M. A., Saldanha, J. W., Strath, M., and Wilson, R. J. M. (2002) SufC hydrolyzes ATP and interacts with SufB from *Thermotoga maritima*, *FEBS Lett. 514*, 225-228.

150. Layer, G., Gaddam, S. A., Ayala-Castro, C. N., Ollagnier-de-Choudens, S., Lascoux, D., Fontecave, M., and Outten, F. W. (2007) SufE transfers sulfur from SufS to SufB for iron-sulfur cluster assembly, *J. Biol. Chem. 282*, 13342-13350.

151. Mihara, H. and Esaki, N. (2002) Bacterial cysteine desulfurases: their function and mechanisms, *Appl. Microbiol. Biotechnol. 60*, 12-23.

152. Loiseau, L., Ollagnier-de-Choudens, S., Nachin, L., Fontecave, M., and Barras, F. (2003) Biogenesis of Fe-S cluster by the bacterial Suf system. SufS and SufE form a new type of cysteine desulfurase, *J. Biol. Chem. 278*, 38352-38359.

153. Ollagnier-de-Choudens, S., Lascoux, D., Loiseau, L., Barras, F., Forest, E., and Fontecave, M. (2003) Mechanistic studies of the SufS-SufE cysteine desulfurase: evidence for S transfer from SufS to SufE, *FEBS Lett. 555*, 263-267.

154. Goldsmith-Fischman, S., Kuzin, A., Edstrom, W. C., Benach, J., Shastry, R., Xiao, R., Acton, T. B., Honig, B., Montelione, G. T., and Hunt, J. F. (2004) The SufE sulfur-acceptor protein contains a conserved core structure that mediates interdomain interactions in a variety of redox protein complexes, *J. Mol. Biol. 344*, 549-565.

155. Shen, G., Balasubramanian, R., Wang, T., Wu, Y., Hoffart, L. M., Krebs, C., Bryant, D. A., and Golbeck, J. H. (2007) SufR coordinates two $[4Fe\text{-}4S]^{2+,1+}$ clusters and functions as a transcriptional repressor of the *sufBCDS* operon and an autoregulator of *sufR* in cyanobacteria, *J. Biol. Chem. 282*, 31909-31919.

156. Loiseau, L., Gerez, C., Bekker, M., Ollagnier-de-Choudens, S., Py, B., Sanakis, Y., Teixeira, M., Fontecave, M., and Barras, F. (2007) ErpA, an iron-sulfur (Fe-S) protein of the A-type essential for respiratory metabolism in *Escherichia coli*, *Proc. Natl. Acad. Sci. USA 104*, 13626-13631.

157. Schilke, B., Voisine, C., Beinert, H., and Craig, E. (1999) Evidence for a conserved system for iron metabolism in the mitochondria of *Saccharomyces cerevisiae*, *Proc. Natl. Acad. Sci. USA 96*, 10206-10211.

158. Yabe, T., Morimoto, K., Kikuchi, S., Nishio, K., Terashima, I., and Nakai, M. (2004) The arabidopsis chloroplast NifU-like protein CnfU, which can act as an iron-sulfur cluster scaffold protein, is required for the biogenesis of ferredoxin and photosystem I, *Plant Cell 16*, 993-1007.

159. Tong, W.-H., Jameson, G. N. L., Huynh, B. H., and Rouault, T. A. (2003) Subcellular compartmentalization of human Nfu, an iron-sulfur cluster scaffold protein and its ability to assemble a [4Fe-4S] cluster, *Proc. Natl. Acad. Sci. USA 100*, 9762-9767.

160. Ye, H., Pilon, M., and Pilon-Smits, E. A. (2007) CpNifS-dependent iron-sulfur biogenesis in chloroplasts, *New Phytol 171*, 285-292.

161. Touraine, B., Boutin, J. P., Marion-Poll, A., Briat, J. F., Peltier, G., and Lobréaux, S. (2004) Nfu2: a scaffold protein required for [4Fe-4S] and ferredoxin iron-sulfur cluster assembly in *Arabidopsis* chloroplasts, *Plant J. 40*, 101-111.

162. Rouhier, N., Gelhaye, E., and Jacquot, J.-P. (2004) Plant glutaredoxins: still mysterious reducing systems, *Cell. Mol. Life Sci. 61*, 1266-1277.

163. Chung, W.-H., Kim, K.-D., Cho, Y.-J., and Roe, J.-H. (2004) Differential expression and role of two dithiol glutaredoxins Grx1 and Grx2 in *Schizosaccharomyces pombe*, *Biochem. Biophys. Res. Commun. 321*, 922-929.

164. Aslund, F., Ehn, B., Miranda-Vizuete, A., Pueyo, C., and Homgren, A. (1994) Two Additional Glutaredoxins Exist in Escherichia coli: Glutaredoxin 3 is a Hydrogen Donor for Ribonucleotide Reductase in a Thioredoxin/Glutaredoxin 1 Double Mutant, *Proc. Natl. Acad. Sci. USA 91*, 9813-9817.

165. Bandyopadhyay, B., Starke, D. W., Mieyal, J. J., and Gronostajski, R. M. (1998) Thioltransferase (Glutaredoxin) Reactivates the DNA-binding Activity of Oxidation-inactivated Nuclear Factor I, *J. Biol. Chem. 273*, 392-397.

166. Daily, D., Vlamis-Gardikas, A., Offen, D., Mittelman, L., Melamed, E., Holmgren, A., and Barzilai, A. (2001) Glutaredoxin Protects Cerebellar Granule Neurons from Dopamine-induced Apoptosis by Activating NF-B via Ref-1, *J. Biol. Chem. 276*, 1335-1344.

167. Kenchappa, R. S., Diwakar, L., Boyd, M. R., and Ravindranath V. (2002) Thioltransferase (glutaredoxin) mediates recovery of motor neurons from excitotoxic mitochondrial injury, *J Neurosci. 22*, 8402-8410.

168. Lillig, C. H., Prior, A., Schwenn, J. D., Åslund, F., Ritz, D., Vlamis-Gardikas, A., and Holmgren, A. (1999) New Thioredoxins and Glutaredoxins as Electron Donors of 3'-Phosphoadenylylsulfate Reductase, *J. Biol. Chem. 274*, 7695-7698.

169. Murata, H., Ihara, Y., Nakamura, H., Yodoi, J., Sumikawa, K., and Kondo, T. (2003) Glutaredoxin Exerts an Antiapoptotic Effect by Regulating the Redox State of Akt, *J. Biol. Chem. 278*, 50266-50233.

170. Porras, P., Pedrajas, J. R., Martinez-Galisteo, E., Padilla, C. A., Johansson, C., Holmgren, A., and Barcena, J. A. (2002) Glutaredoxins catalyze the reduction of glutathione by dihydrolipoamide with high efficiency, *Biochem. Biophys. Res. Commun. 295*, 1046-1051.

171. Song, J. J., Rhee, J. G., Suntharalingam, M., Walsh, S. A., Spitz, D. R., and Lee, Y. J. (2002) Role of Glutaredoxin in Metabolic Oxidative Stress. Glutaredoxin as a sensor of oxidative stress mediated by H_2O_2, *J. Biol. Chem. 277*, 46566-46575.

172. Wells, W. W., Xu, D. P., Yang, Y. F., and Rocque, P. A. (1990) Mammalian thioltransferase (glutaredoxin) and protein disulfide isomerase have dehydroascorbate reductase activity, *J. Biol. Chem. 265*, 15361-15364.

173. Cotgreave, I. A. and Gerdes, R. G. (1998) Recent Trends in Glutathione Biochemistry—Glutathione–Protein Interactions: A Molecular Link between Oxidative Stress and Cell Proliferation?, *Biochem. Biophys. Res. Commun. 242*, 1-9.

174. Achebach, S., Tran, Q. H., Vlamis-Gardikas, A., Mullner, M., Holmgren, A., and Unden G. (2004) Stimulation of Fe-S cluster insertion into apoFNR by Escherichia coli glutaredoxins 1, 2 and 3 in vitro, *FEBS Lett. 565*, 203-206.

175. Lillig, C. H., Berndt, C., Vergnolle, O., Lönn, M. E., Hudemann, C., Bill, E., and Holmgren, A. (2005) Characterization of human glutaredoxin 2 as an iron-sulfur protein: A possible role as a redox sensor, *Proc. Natl. Acad. Sci. USA 102*, 8168-8173.

176. Johansson, C., Kavanagh, K. L., Gileadi, O., and Oppermann U. (2007) Reversible Sequestration of Active Site Cysteines in a 2Fe-2S-bridged Dimer Provides a Mechanism for Glutaredoxin 2 Regulation in Human Mitochondria, *J. Biol. Chem. 282*, 3077-3082.

177. Ojeda, L., Keller, G., Mühlenhoff, U., Rutherford, J. C., Lill, R., and Winge, D. R. (2006) Role of Glutaredoxin-3 and Glutaredoxin-4 in the Iron Regulation of the Aft1 Transcriptional Activator in *Saccharomyces cerevisiae*, *J. Biol. Chem. 281*, 17661-17669.

178. Rodríguez-Manzaneque, M. T., Ros, J., Cabrito, I., Sorribas, A., and Herrero, E. (1999) Grx5 glutaredoxin plays a central role in protection against protein oxidative damage in *Saccharomyces cerevisiae*, *Mol. Cell. Biol. 19*, 8180-8190.

179. Rodríguez-Manzaneque, M. T., Tamarit, J., Bellí, G., Ros, J., and Herrero, E. (2002) Grx5 is a mitochondrial glutaredoxin required for the activity of iron/sulfur enzymes, *Mol. Biol. Cell 13*, 1109-1121.

180. Wingert, R. A., Galloway, J. L., Barut, B., Foott, H., Fraenkel, P., Axe, J. L., Weber, G. J., Dooley, K., Davidson, A. J., Schmidt, B., Paw, B. H., and Shaw, G. C. (2005) Deficiency of glutaredoxin 5 reveals Fe-S clusters are required for vertebrate haem synthesis, *Nature 436*, 1035-1039.

Table 1-1: Functions of biological Fe-S clusters (adapted from (*4*))

Function	Type of cluster/center	Examples
Electron Transfer	[2Fe-2S], $[2Fe-2S]_R$	Ferredoxins, soluble and membrane –
	[3Fe-3S], [4Fe-4S]	bound redox enzymes
Coupled electron and	$[2Fe-2S]_R$	Rieske protein
proton transfer	[8Fe-7S]	Nitrogenase Fe protein
Substrate binding and	[4Fe-4S]	Radical SAM enzymes
activation	Fe SOR	Superoxide reductase
	Ni-Fe-H_2ase	NiFe-hydrogenase
	[Mo-7Fe-9S-X]	Nitrogenase Mo-Fe protein
	[Ni-4Fe-5S]	CO dehydrogenase
Structural	[4Fe-4S]	Endonuclease III
	[4Fe-4S]	MutY
Iron and cluster storage	[4Fe-4S]	Ferredoxins
	[4Fe-4S]	Polyferredoxins
Regulation of gene	[2Fe-2S]	IscR
expression	[2Fe-2S]	SoxR
	[4Fe-4S]/[2Fe-2S]	FNR
	[4Fe-4S]	IRP
Regulation of enzymatic	[2Fe-2S]	Ferrochelatase
activity	[4Fe-4S]	Glutamine PRPP amidotransferase
Disulfide reduction	[4Fe-4S]	Ferredoxin:thioredoxin reductase
	[4Fe-4S]	Heterodisulfide reductase
Sulfur donor	[2Fe-2S]	Biotin synthase

Figure 1-1: Crystallographically defined structures for Fe-S centers that function in biological electron transfer. Structures are taken from coordinates deposited in the Protein Data bank: A. Fe Rd, PDB ID# 8RXN, rubredoxin from *Desulfovibrio vulgaris*; B. [2Fe-2S], PDB ID# 1FRD, *Anabaena* pcc7120 Fd; C. [3Fe-4S], PDB ID# 6FDR, *Azotobacter vinelandii* FdI; D. [4Fe-4S], PDB ID# 6FDR, *Azotobacter vinelandii* FdI; E. [8Fe-7S], PBD ID# 1M1N, dithionite-reduced *Azotobacter vinelandii* MoFe protein. Color code: red, Fe; yellow, S. Unlabelled S atoms correspond to bridging sulfides (*4*).

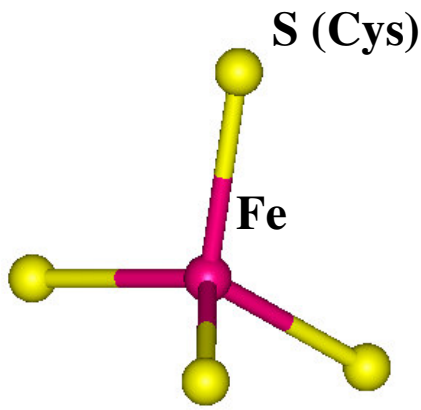

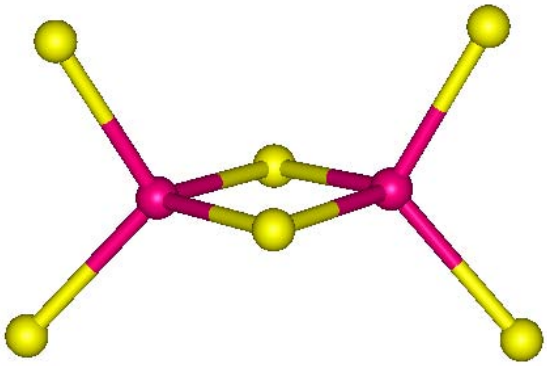

[2Fe-2S]

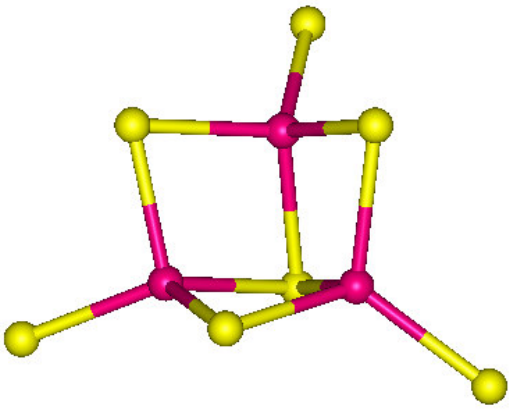

[3Fe-4S]

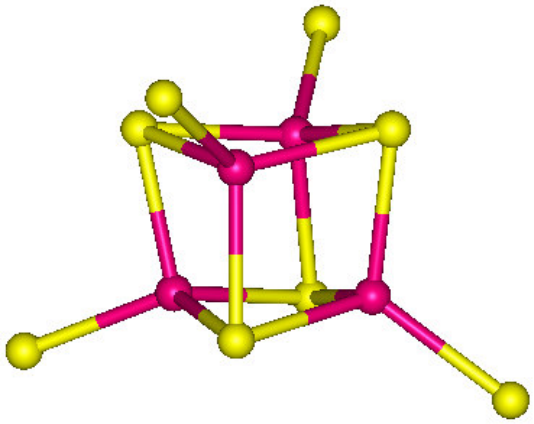

[4Fe-4S]

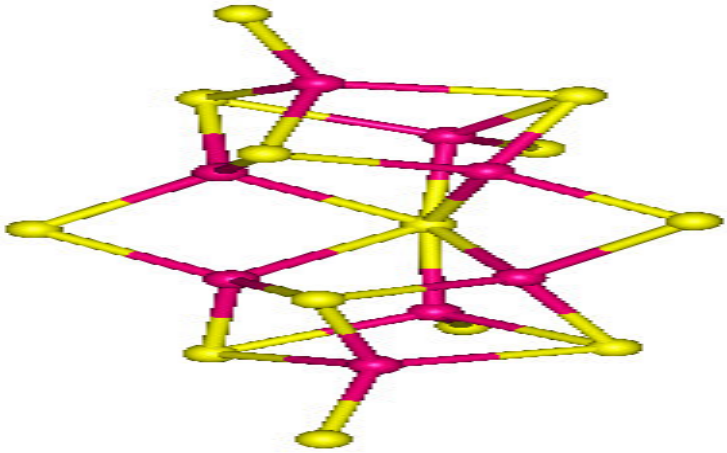

[8Fe-7S]

Figure 1-2: Ground state spin (*S*) and valence delocalization schemes for fundamental types of Fe-S clusters. Color code:Fe^{3+}, red; Fe^{2+}, blue; $Fe^{2.5+}$, green; S, yellow; O, white (*3*).

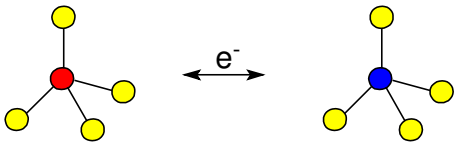

Fe^{3+} (S = 5/2) Fe^{2+} (S = 2)

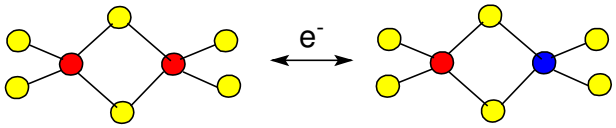

$[2Fe\text{-}2S]^{2+}$ (S = 0) $[2Fe\text{-}2S]^{+}$ (S = 1/2)

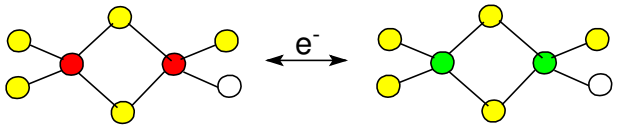

$[2Fe\text{-}2S]^{2+}$ (S = 0) $[2Fe\text{-}2S]^{+}$ (S = 9/2)

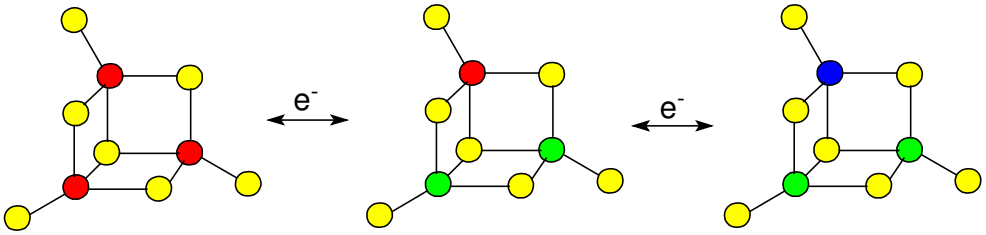

$[3Fe\text{-}4S]^{+}$ (S = 1/2) $[3Fe\text{-}4S]^{0}$ (S = 2) $[3Fe\text{-}4S]^{-}$ (S = 5/2)

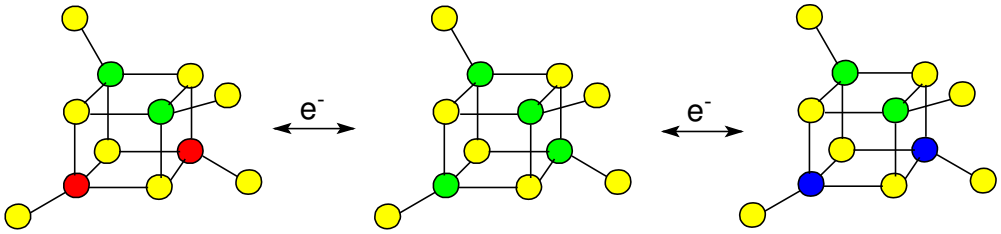

$[4Fe\text{-}4S]^{3+}$ (S = 1/2) $[4Fe\text{-}4S]^{2+}$ (S = 0) $[4Fe\text{-}4S]^{+}$ (S = 1/2)

Figure 1-3: Organization of genes from various organisms whose products are known or suspected to be involved in [Fe-S] protein maturation. (*4*).

Azotobacter vinelandii (Av)

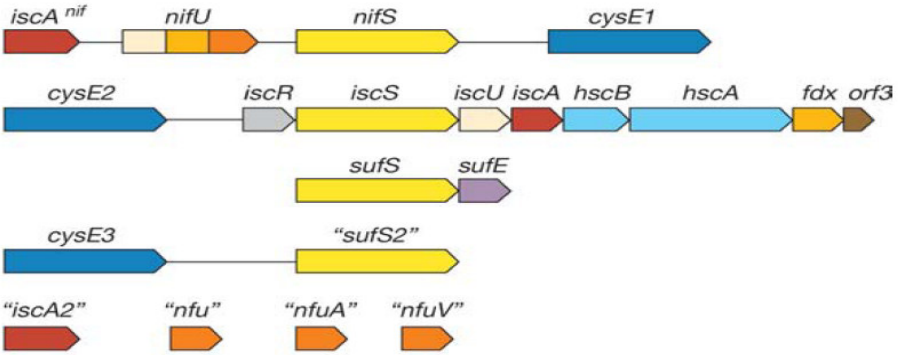

Escherichia coli (Ec)

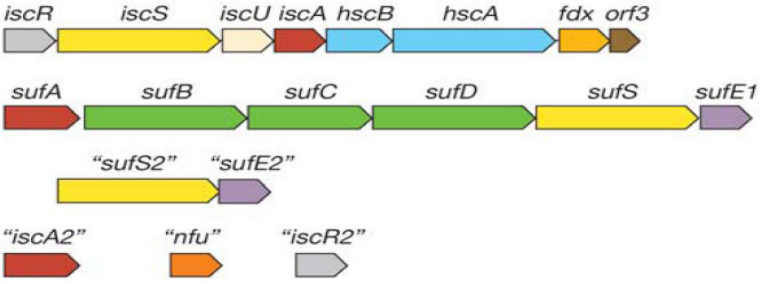

Thermatoga maritima (Tm)

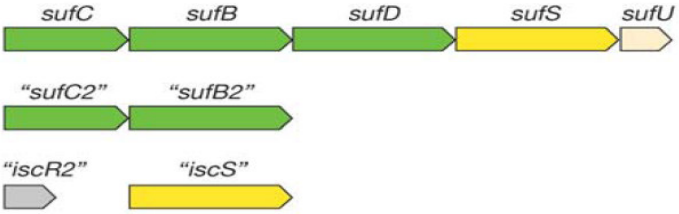

Helicobacter pylori (Hp)

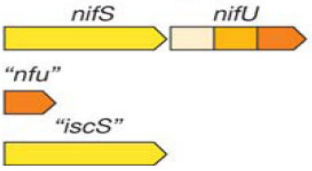

Figure 1-4: Classification of glutaredoxins in plants *(162).*

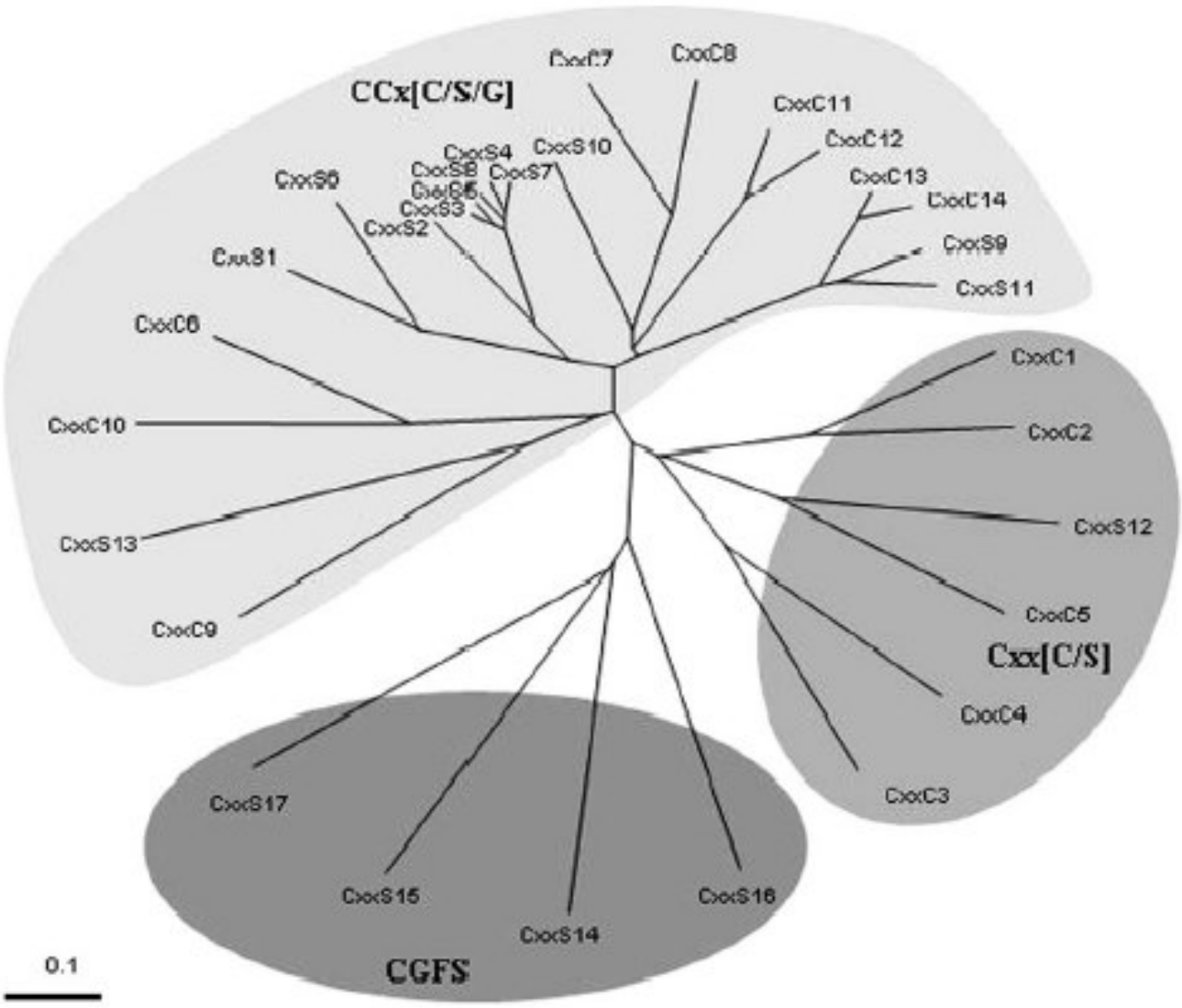
CCx[C/S/G]
CxxC8
CxxC11
CxxC12
CxxS10
CxxS4
CxxS7
CxxC13
CxxC14
CxxS9
CxxS11
CxxS1
CxxC6
CxxC10
CxxS13
CxxC9
CxxC1
CxxC2
CxxS12
CxxC5
Cxx[C/S]
CxxC4
CxxC3
CxxS17
CxxS15
CxxS16
CxxS14
CGFS
0.1

Figure 1-5: Glutathione binding to monomeric and dimeric human Grx2. *A*, detail of glutathione binding in the active site of monomeric GLRX2. *B*, α-carbon trace of the GLRX2 dimer. The dimer is bridged by a 2Fe-2S cluster. *C,* stereo view of the GLRX2 iron-sulfur cluster and coordinating ligands. The monomeric structure is shown semitransparently superimposed upon the individual dimer subunits to highlight the differences in the side-chain conformations of Ser-38 and Tyr-39 (*176*).

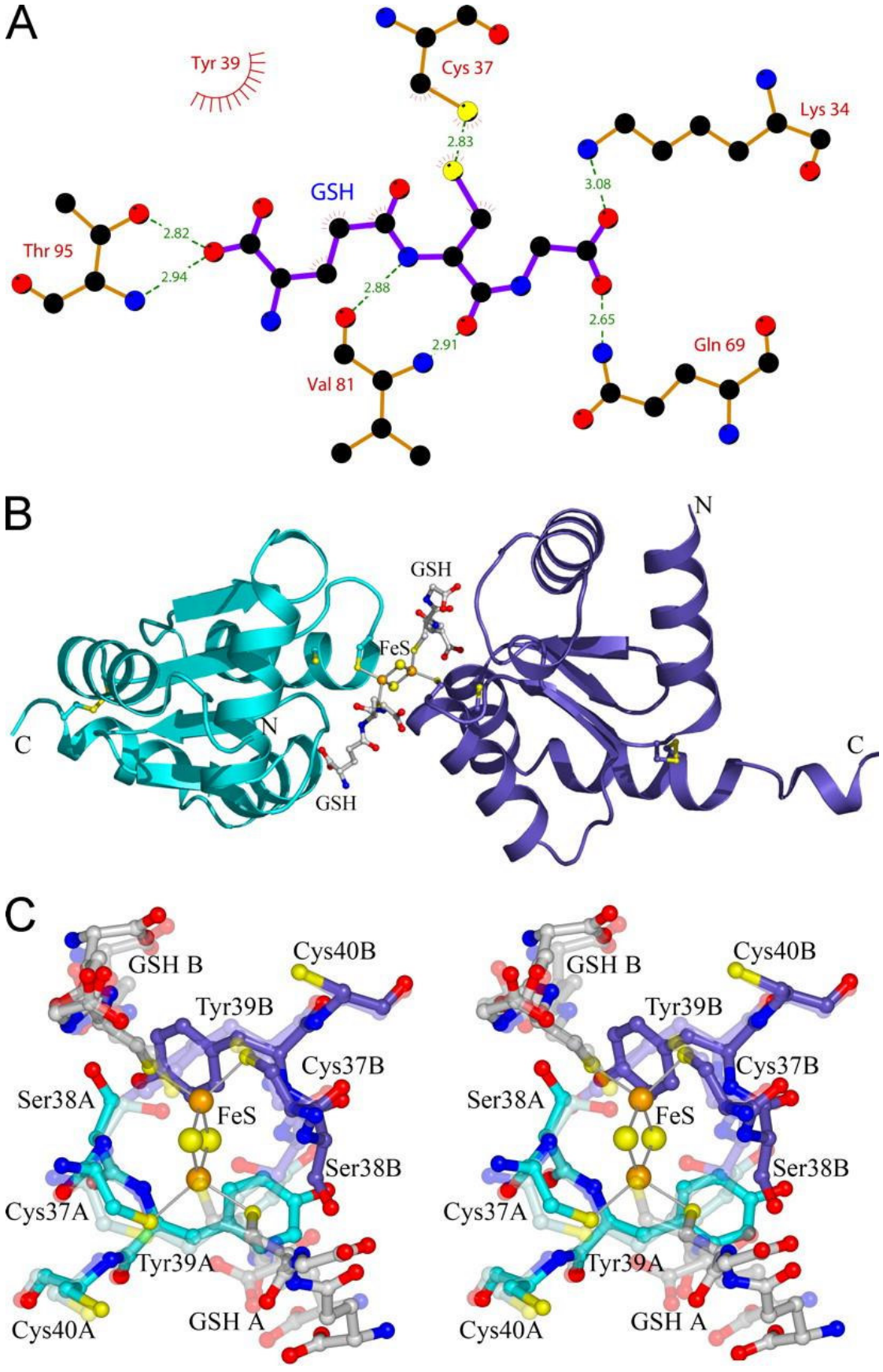
A
Tyr 39
Cys 37
Lys 34
2.83
3.08
GSH
Thr 95
2.82
2.94
2.88
2.65
2.91
Gln 69
Val 81
B
N
GSH
FeS
C
N
C
GSH
C
GSH B
Cys40B
Tyr39B
Cys37B
Ser38A
FeS
Ser38B
Cys37A
Tyr39A
Cys40A
GSH A
GSH B
Cys40B
Tyr39B
Cys37B
Ser38A
FeS
Ser38B
Cys37A
Tyr39A
Cys40A
GSH A

CHAPTER 2

GENETIC, BIOCHEMICAL AND SPECTROSCOPIC ANALYSIS OF THE *AZOTOBACTER VINELANDII NFUA* GENE PRODUCT

Bandyopadhyay, S., Naik, S. G., O'Carroll, I. P., Huynh, B. H., Dean, D. R., Johnson, M. K. and Dos Santos, P. C.
Submitted to *J. Biol. Chem*.

Abstract

Iron-sulfur clusters ([Fe-S] clusters) are assembled on molecular scaffolds and then used for the maturation of proteins that require [Fe-S] clusters for their corresponding functions. Previous studies have shown that *Azotobacter vinelandii* produces at least two [Fe-S] cluster assembly scaffolds: NifU, upon which [Fe-S] clusters are assembled for maturation of nitrogenase, and IscU, upon which [Fe-S] clusters destined for general maturation of [Fe-S] proteins are assembled. *A. vinelandii* also encodes a protein designated NfuA, which bears primary sequence similarity to the C-terminal region of NifU. A strain inactivated for *nfuA* exhibits a substantially lower level in activity for aconitase, a [4Fe-4S] cluster-containing enzyme, and also results in a null growth phenotype when cultivated under elevated oxygen concentrations. NifU is able to rescue the *nfuA* phenotype, but only when it is produced at abundant levels, indicating that a low level of functional replacement of NfuA by NifU can occur. Spectroscopic and analytical studies indicate that one [4Fe-4S] cluster can be assembled *in vitro* within a dimeric form of NfuA. The resultant [4Fe-4S] cluster-loaded form of NfuA is competent for rapid *in vitro* activation of apo-aconitase. Based on these results a model is proposed where NfuA represents a class of intermediate [Fe-S] cluster carriers.

Introduction

The *in vivo* maturation of simple [Fe-S] proteins is proposed to require preassembly of [Fe-S] species on molecular scaffolds. The first [Fe-S] cluster assembly system to be described is the NIF system from *Azotobacter vinelandii*, which consists of a cysteine desulfurase, encoded by *nifS* and a proposed scaffold protein, encoded by *nifU* (1). The NIF system is specialized for the maturation of [Fe-S] proteins involved in nitrogen fixation. *In vitro* and *in vivo* experiments have established that NifS and NifU are necessary and sufficient for the maturation of the nitrogenase Fe-protein, which requires a [4Fe-4S] cluster for its activity (2, 3). NifS and NifU therefore appear to comprise a minimum unit for [Fe-S] protein maturation where NifS mobilizes the S necessary for [Fe-S] cluster formation and NifU provides the assembly scaffold.

A. vinelandii also contains a second [Fe-S] protein maturation system, designated ISC, which is required for the general maturation of cellular [Fe-S] proteins involved in intermediary metabolism, such as aconitase (4). The ISC system is more complicated than the NIF system as it includes the products of eight contiguous genes, five of which (*iscS*, *iscU*, *hscB*, *hscA* and *fdx*) are necessary to sustain cellular metabolism in *A. vinelandii* (5). It has recently been shown that both the NIF and ISC systems exhibit physiological target specificity with respect to [Fe-S] protein maturation. Nevertheless, the ISC and NIF systems can partially replace the function of each other, but only when the complementary system is expressed at levels that exceed the normal physiological amounts (6, 7).

Although the NIF and ISC systems are differentiated by their apparent target specificities, they share a number of common structural and functional features. For example, NifS and IscS both exhibit cysteine desulfurase activity and they also bear a significant level of primary sequence identity when compared to each other (4). IscU also shares considerable primary

sequence identity when compared to the N-terminal domain of NifU, including conservation of three cysteine residues that are likely to provide the nucleation site(s) for [Fe-S] cluster assembly (4, 8). Another feature shared by both the NIF and ISC systems is that they respectively include similar proteins designated $IscA^{Nif}$ and IscA (4). Although neither protein is essential for maturation of [Fe-S] proteins in their corresponding systems, they have both been shown by *in vitro* experiments to have the capacity to bind [Fe-S] clusters and could therefore have functions related to the *in vivo* formation or trafficking of [Fe-S] clusters (9). IscA has also been proposed to be an agent of Fe delivery to the IscU scaffold (10). Both $IscA^{Nif}$ and IscA share primary sequence identity, including three conserved cysteines (9). In the case of *Escherichia coli* there are two other proteins, designated SufA (11) and ErpA (12), which also bear primary sequence similarity when compared to *A. vinelandii* $IscA^{Nif}$ and IscA. SufA is encoded within a cluster of genes whose products are required for maturation of [Fe-S] proteins under conditions of oxygen stress or iron limitation (13, 14). Other studies have shown that ErpA is necessary to sustain a capacity for cellular respiration, which is apparently linked to the involvement of ErpA in the maturation of IspG. IspG contains a [4Fe-4S] cluster and is involved in catalyzing isopentenyl phosphate formation (12). *A. vinelandii* does not encode an intact SUF system but does encode a protein homologous to ErpA, and this gene is also essential in *A. vinelandii* (our unpublished results).

NifU is a modular protein that contains three distinct domains. The central domain contains a stable [2Fe-2S] cluster, which has redox properties similar to the [2Fe-2S] cluster of the Fdx protein encoded by the ISC system (15). Neither the function of the central domain within NifU, nor the function of Fdx is known, although *in vitro* studies have shown that Fdx is competent to mediate [4Fe-4S] cluster formation on IscU via reductive coupling of two [2Fe-2S]

clusters (16). *In vitro* and *in vivo* experiments have established that labile [Fe-S] clusters can be assembled on both the N-terminal and C-terminal domains of NifU and such cluster-loaded forms of NifU can be used for activation of the nitrogenase Fe-protein (2, 3). Thus, NifU contains two different sites upon which [Fe-S] clusters can be assembled *in vitro* but the functional relationship between these sites with regard to nitrogenase maturation is not yet known.

There are no genes encoded within the ISC transcriptional unit that bear primary sequence similarity to the C-terminal domain of NifU. However, the *A. vinelandii* genome encodes a gene, designated *nfuA*, whose C-terminal primary sequence is similar to the C-terminal domain of NifU. Such primary sequence conservation between NifU and NfuA includes two cysteine residues that are required for the *in vitro* assembly of [Fe-S] clusters within the NifU C-terminal domain. Like NifU, NfuA also appears to be a modular protein because the primary sequence within its N-terminal region exhibits some similarity when compared to the IscA/IscA^{Nif}/SufA/ErpA family of proteins. However, this primary sequence conservation does not include the three cysteine residues conserved among this family. Primary sequence conservation between the N-terminal region of NfuA and the IscA family of proteins, as well as the conservation between the respective C-terminal domains of NfuA and NifU suggests that NfuA could play a role in [Fe-S] protein maturation. This possibility is supported by evidence that [Fe-S] clusters can be assembled on NfuA-like proteins (termed Nfu or NifU-like proteins) from other organisms (17-20) and that, in some cases, loss of NfuA-like function impairs [Fe-S] protein maturation (20-23). In the present work we have performed a genetic, biochemical and spectroscopic analysis of NfuA from *A. vinelandii* in order to gain insight into its cellular function.

Experimental Procedures

Materials: Materials used in this work were purchased from Sigma, Fisher Scientific, New England Biolabs, Invitrogen, or from other sources as indicated throughout the text. *Bioinformatics and DNA analysis*—Sequence alignments were performed using the SDSC Biology Workbench program. The Lasergene 7 software was used to analyze DNA and protein sequences. When necessary, *A. vinelandii* genomic DNA was extracted, amplified, and sequenced as described previously (7).

Plasmid and Strain Construction: Construction of *A. vinelandii* strains via transformation with appropriate plasmids has been described previously (24). In this work, DJ1707 was obtained by transformation of our wild type laboratory strain designated DJ (ATCC BAA-1303) with pDB1598, a plasmid that includes a kanamycin resistance cartridge inserted into the *Xho*I sites of *nfuA*. This construct results in deletion of a 290 bp fragment from the *nfuA* gene. DJ1759 and DJ1769 respectively produce the $NfuA^{C152A}$- and $NfuA^{C155A}$-substituted forms of NfuA and were constructed by using plasmids pDB1610 and pDB1614, which contain site-directed cysteine to alanine substitutions (codon change of UGC to GCC) at residue positions 152 and 155, respectively. Site-directed mutagenesis procedures were conducted using the GeneEditor™ system by Promega. The parent plasmid used for deletion, insertion or amino acid substitutions was pDB1577, which contains the intact *nfuA* gene, as well as 570 bp downstream of the gene, in the pUC-7 vector.

Abundant production and controlled expression of NifUS and their variants was achieved by placing the desired genes under the control of the inducible arabinose regulatory elements as described previously (7). Plasmid pDB1598 was used to inactivate *nfuA* in DJ1626, a strain where *nifUS* are placed under the control of the *araBAD* promoter with concomitant in-frame

deletion of the *nif*-regulated *nifUS* (7). This inactivation yielded strain DJ1772. Similarly, strains DJ1773 and DJ1791 were constructed, which contain *nifU* variants with cysteine to alanine substitutions at residues 35 and 275 respectively and are otherwise isogenic to DJ1772.

Plasmid pDB1417 was designed by insertion of *nfuA,* flanked by *Nde*I and *Bam*HI restriction sites, into the *Nde*I and *Bam*HI sites of pT7-7 for recombinant expression. Similarly, plasmids pDB1582 and pDB1583 were constructed for recombinant expression of $NfuA^{152CA}$ and $NfuA^{155CA}$, respectively.

Cell Growth at Ambient and Elevated Oxygen Levels: All strains used in this study were cultured in Burk's media supplemented with 13 mM ammonium acetate (25). When appropriate, media were also supplemented with 20 mM L-arabinose. To expose cells to elevated oxygen concentrations, Petri plates were placed in BBL GasPak jars and filled with a gas mixture containing 40% O_2 as described previously (5).

Aconitase and Isocitrate Dehydrogenase Assays of A. vinelandii Crude Extracts: A. vinelandii cells were grown in liquid cultures containing Burk's media supplemented with 13 mM ammonium acetate until they reached OD_{600} = 0.5. Cells were subsequently harvested by centrifugation at 5000 rpm for 5 min and stored at –20°C, if not used immediately. To prepare crude extracts, cells were first resuspended in degassed buffer containing 25 mM Tris at pH 7.4 and were lysed using a French Pressure Cell at 12,000 psi. Lysed cells, which were maintained in airtight vials filled with Argon gas, were centrifuged at 35,000 rpm for 45 min. Crude extracts were separated from the cell debris pellet inside a Coy anaerobic glove box containing 4% H_2 gas and 96% N_2 to minimize exposure to oxygen. Aconitase assays were prepared in 1 mL quartz cuvettes – sealed airtight with rubber septa – containing 700 µL of 100 mM Tris-HCl buffer at pH 8.0 and 0.1 mg of crude extract. The reaction was initiated with the addition of 25 mM

sodium citrate and activity was monitored at 240 nm (26). Isocitrate dehydrogenase assays of crude extracts were performed in quartz cuvettes containing 900 µL of 50 mM MOPS buffer at pH 7.3, 2.5 mM $MgCl_2$, 0.45 mM $NADP^+$, and 0.1 mg of crude extract. The reaction was started with the addition of 80 mM *DL* – Isocitric acid (trisodium salt) in the MOPS/$MgCl_2$ buffer described above and monitored at 340 nm (27).

Purification of NfuA and Its Variants: E. coli BL21(DE3) cells transformed with plasmids pDB1417, pDB1582, or pDB1583 were used for the heterologous expression of NfuA, $NfuA^{152CA}$, or $NfuA^{155CA}$ respectively. Cells were grown in LB media containing 0.1mg/mL ampicillin until they reached OD_{600} = 0.5, at which point, they were induced with 29 mM lactose and allowed to continue to grow for 3 hours at 30°C. Cells were then harvested by centrifugation at 5000 rpm for 5 min and stored in –20°C until used.

Cells expressing recombinant NfuA or its alanine-substituted variants were resuspended in de-gassed 50 mM Tris-HCl, pH 7.4 buffer (buffer A) and lysed either by sonication (1 min pulse/30 sec pause for a total of 20 min) or by the use of a French Pressure Cell. Crude extracts were prepared as described above. All purification procedures were conducted anaerobically by the use of Schlenk lines filled with Argon gas. Crude extracts were loaded at 2.5 mL/min using a peristaltic pump into a 25 mL Q-Sepharose column previously equilibrated with 5 bed volumes of buffer A. The column was, subsequently, washed with 50 mL of buffer A and 75 mL of buffer A containing 100 mM NaCl. To elute NfuA, a 200 mL of 0.1 - 1.0 M NaCl gradient was applied and the contents of each fraction were analyzed by 15% SDS-PAGE. The fractions containing NfuA, which eluted between 40 mL and 94 mL of the gradient, were consolidated and $(NH_4)_2SO_4$ was added to a final concentration of 1 M. This sample was then loaded onto a 25 mL Phenyl-Sepharose column that was previously equilibrated with buffer A containing 1 M

$(NH_4)_2SO_4$. Following binding of the sample onto the column, the latter was washed with 125 mL buffer A containing 1 M $(NH_4)_2SO_4$ followed by 25 mL of 0.5 M $(NH_4)_2SO_4$ in buffer A. The protein was then eluted using a 100 mL gradient of 0.5 - 0.0 M $(NH_4)_2SO_4$ followed by 50 mL of buffer A. The fractions containing NfuA eluted in the last 28 mL of the gradient as well as during the final wash with buffer A and were concentrated by Amicon ultrafiltration with a YM10 membrane. The resulting sample was loaded onto a 320 mL Superdex S75 gel filtration column equilibrated with 100 mM Tris-HCl buffer (pH 8.0) with 1 mM DTT (buffer B) and 150 mM NaCl. The purest fractions of NfuA as judged by SDS PAGE were pooled and concentrated by Amicon ultrafiltration using a YM10 membrane, and frozen as pellets in liquid N_2 until used. The resulting samples of NfuA were >95% pure as judged by gel densitometry.

In vitro Reconstitution of NfuA: Purified NfuA, $NfuA^{152CA}$, or $NfuA^{155CA}$ (0.24 mM) were incubated with NifS (12 μM), ferrous ammonium sulfate (4.8 mM) and L-cysteine (4.8 mM) in buffer B for 3 hours at room temperature under argon inside a Vaccum Atmospheres glove box (< 2 ppm O_2). Excess reagents were removed by loading onto a High-trap Q-Sepharose column and eluting with a 0 to 1.0 M NaCl gradient using buffer B. The holo protein eluted between 0.45-0.55 M NaCl and was concentrated using Amicon ultrafiltration using a YM10 membrane. ^{57}Fe-enriched ferrous sulfate (>95% enrichment) was used in place of natural abundance ferrous ammonium sulfate in the preparation of Mössbauer samples.

Determination of Oligomeric State of Apo and Holo NfuA: The oligomeric states of both apo and holo NfuA were determined by gel-filtration chromatography using a 25 mL Superdex S75 column. The elution buffer was buffer B with 100 mM KCl, which was applied to the column at a flow rate of 0.4 mL/min. Molecular weight standards used were blue dextran (M_r

2,000,000), β-amylase (M_r 200,000), alcohol dehydrogenase (M_r 150,000), bovine serum albumin (M_r 66,000), carbonic anhydrase (M_r 29,000), and cytochrome *c* (M_r 12,400).

Analytical and Spectroscopic Analyses: Protein concentrations were determined by the *DC* protein assay (Bio-Rad) using BSA as the standard. Iron concentrations were determined colorimetrically using bathophenanthroline under reducing conditions, after digestion of the protein in 0.8% $KMnO_4$/0.2 M HCl (28) or by using the commercial Quantichrom™ iron assay kit (DIFE-250) from Bioassay Systems. Samples for spectroscopic studies were prepared and handled under Ar in a Vacuum Atmospheres glove box (O_2 < 2 ppm). UV-visible absorption was recorded at room temperature using a Shimadzu UV-3101PC or Cary 50 Bio spectrophotometer. Resonance Raman spectra were recorded as previously described, using an Instruments SA Ramanor U1000 spectrometer coupled with a Coherent Sabre argon ion laser, with 20 μL frozen droplets of 2-3 mM sample mounted on the cold finger of an Air Products Displex Model CSA-202E closed cycle refrigerator (29). Signal-to-noise was improved by multiple scans and bands due to the frozen buffer solution were subtracted from all the spectra shown in this work after normalization of lattice modes of ice centered at 230 cm^{-1}. VTMCD spectra were recorded using samples containing 55% (v/v) ethylene glycol in 1 mm cuvettes using an Oxford Instruments Spectromag 4000 (0-7 T) split-coil superconducting magnet (1.5-300 K) mated to a Jasco J-715 spectropolarimeter (30). X-band (~9.6 GHz) EPR spectra were recorded using a Bruker ESP-300E EPR spectrometer equipped with a dual-mode ER-4116 cavity and an Oxford Instruments ESR-9 flow cryostat. Mössbauer spectra were recorded by using the previously described instrumentations (31). Analysis of the Mössbauer data was performed with the program WMOSS (Web Research).

Activation of Apo-aconitase by Reconstituted NfuA: Apo-aconitase was prepared by incubating recombinantly expressed and purified *A. vinelandii* aconitase A (AcnA) (32) with EDTA and potassium ferricyanide as described previously (33). Activation mixtures contained 4 μM apo-AcnA and between 0-12 μM of [4Fe-4S] cluster-loaded NfuA in buffer B. The concentration of [4Fe-4S] cluster-loaded NfuA corresponds to the concentration of $[4Fe\text{-}4S]^{2+}$ clusters calculated using a molar extinction coefficient of ε_{400} = 15.0 $mM^{-1}cm^{-1}$ per $[4Fe\text{-}4S]^{2+}$ cluster. Activation mixtures were incubated at room temperature (22°C) under anoxic conditions, and 10 μL samples were taken at different time points and assayed for AcnA activity. AcnA activity was measured spectrophotometrically at 240 nm at 22°C by following the formation of *cis*-aconitate from citrate or isocitrate, using a molar absorption coefficient ε_{240} of 3400 mM^{-1} cm^{-1} for *cis*-aconitate (26). Assays (1 mL) were carried out in sealed anoxic cuvettes containing 900 μL of 100 mM Tris/HCl (pH 8.0) and initiated by addition of 100 μL of 200 mM citrate or isocitrate. Anaerobically reconstituted samples of *A. vinelandii* AcnA containing one [4Fe-4S] cluster per protein monomer exhibited maximal specific activity of 25 units/mg using citrate (~100% activity) and 79 units/mg using isocitrate (~100% activity) (32). The time course of holo-AcnA formation at 22°C was analyzed by fitting to second-order kinetics, based on the initial concentrations of apo-AcnA and $[4Fe\text{-}4S]^{2+}$ clusters on NfuA, using the Chemical Kinetics Simulator software package (IBM).

Results

Figure 2-1 shows the genomic organization of genes from *A. vinelandii* whose products have been shown, or are suspected, to participate in some aspect of [Fe-S] protein maturation. NifU is located within a gene cluster that also encodes $IscA^{Nif}$ and NifS. Nif genes are only

expressed in the absence of a fixed nitrogen source. NifU is a modular protein that includes a central domain, which harbors a stable [2Fe-2S] cluster, as well as N-terminal and C-terminal domains (15), both of which have respectively been shown by *in vitro* experiments to accommodate NifS-directed formation of labile [Fe-S] clusters (2, 3). The N-terminal domain of NifU bears primary sequence identity when compared to IscU, an essential protein upon which [Fe-S] clusters can also be assembled *in vitro* (8, 16). Three other proteins, VnfU, AnfU and NfuA, all encoded within separate regions of the genome, bear primary sequence identity when compared to each other and when compared to the C-terminal domain of NifU. The sequence conservation among this family of proteins extends to a Cys-X-X-Cys motif, which is required for *in vitro* [Fe-S] cluster assembly within the NifU C-terminal domain (2, 3). VnfU and AnfU are respectively contained within gene clusters whose expression is required to support nitrogen fixation under conditions where Mo or Mo and V are absent from the growth medium. The N-terminal half of NfuA also exhibits primary sequence identity when compared to the IscA family of proteins (Figure 2-1). The IscA-like domain found within NfuA is not present in NifU, VnfU or AnfU or other NfuA-like proteins described in the literature.

It has been previously shown that [Fe-S] clusters can be assembled on the C-terminal domain of the *A. vinelandii* NifU protein (2, 3). It has also been shown that proteins from different organisms that bear primary sequence identity when compared to NfuA can be used as *in vitro* scaffolds for [Fe-S] cluster assembly (17-20). These proteins, which have been given various designations in the literature (most commonly Nfu or CnfU for chloroplastic Nfu), also contain the Cys-X-X-Cys signature, but do not include an N-terminal IscA-like domain.

When *A. vinelandii* NfuA is heterologously produced in *E. coli* and then purified under anoxic conditions it does not contain an [Fe-S] cluster. Gel exclusion chromatography indicates

that as-isolated recombinant NfuA is an approximately equal mixture of dimeric and tetrameric species (data not shown). When as-isolated NfuA is incubated with NifS, L-cysteine and Fe^{2+}, an [Fe-S] species is rapidly assembled. Gel exclusion chromatography revealed that upon cluster assembly NfuA is resolved into a single dimeric species. Analytical data, coupled with the UV-visible absorption spectrum and extinction coefficients (Figure 2-2), indicate that the reconstituted sample contains approximately one $[4Fe\text{-}4S]^{2+}$ cluster per NfuA dimer. Repurified samples of reconstituted NfuA contained 2.0 ±0.3 Fe/NfuA monomer and the visible absorption comprises a broad shoulder centered at 400 nm (A_{400}/A_{280} = 0.23 ±0.2) with a molar extinction coefficient (ε_{400} = 7.5 ±0.5 $mM^{-1}cm^{-1}$ based on the concentration of NfuA monomer) that is indicative of approximately 0.5 $[4Fe\text{-}4S]^{2+}$ clusters/NfuA monomer (8). More definitive assessments of the Fe-S cluster type and content were provided by analysis of the Mössbauer spectrum of a ^{57}Fe reconstituted NfuA shown in Figure 2-3 (vertical bars), which revealed that 90% of the Fe is associated with a $[4Fe\text{-}4S]^{2+}$ cluster and the remaining 10% of the Fe with an adventitiously bound Fe^{2+} species. The spectrum of the $[4Fe\text{-}4S]^{2+}$ cluster (dashed line) is simulated as a superposition of two equal intensity quadrupole doublets arising from the two valence delocalized pairs with δ = 0.47 mm/s, ΔE_Q =1.25 mm/s for doublet 1 and δ = 0.45/mm/s, ΔE_Q = 0.99 mm/s for doublet 2. The spectrum of the Fe^{2+} species (dotted line) is simulated with an asymmetric quadrupole doublet with δ = 1.38 mm/s and ΔE_Q = 3.25 mm/s. The presence of [2Fe-2S] clusters was not detected.

While the absorption and Mössbauer results provide unambiguous evidence for anaerobic reconstitution of a $[4Fe\text{-}4S]^{2+}$ cluster on NfuA, the vibrational properties as determined by resonance Raman spectroscopy are somewhat atypical compared to well-characterized biological $[4Fe\text{-}4S]^{2+}$ centers (34-36) and exhibit characteristics that have only previously been observed

for the subunit bridging $[4Fe\text{-}4S]^{2+}$ cluster in the MgATP-bound nitrogenase Fe protein (37). This is illustrated in Figure 2-4 which shows a comparison of the resonance Raman spectra of the $[4Fe\text{-}4S]^{2+}$ centers in reconstituted forms of *A. vinelandii* IscU and NfuA in the Fe-S stretching region using 457-nm excitation. The major difference lies in the anomalously high frequency for the most intense band in the spectrum (353 cm^{-1} for the NfuA $[4Fe\text{-}4S]^{2+}$ center compared to 335-343 cm^{-1} in other biological $[4Fe\text{-}4S]^{2+}$ centers), which is generally assigned to the symmetric breathing mode of the [4Fe-4S] cubane core. Analogous spectra with similar band frequencies and relative intensities were observed for the reconstituted NfuA using 488- and 514-nm excitation, indicating that the anomalous behavior cannot be attributed to anomalous excitation profiles for discreet bands. One possible explanation is that the intense bands at 353 and 359 cm^{-1} for the $[4Fe\text{-}4S]^{2+}$ center in NfuA correspond to asymmetric Fe-S(Cys) stretching modes and that the symmetric breathing modes primarily involving the [4Fe-4S] core and the Fe-S(Cys) bonds are only weakly enhanced as a result of distortions of the core and/or the cluster environment. This is tentatively supported by the observation of similar frozen-solution resonance Raman spectra for $[4Fe\text{-}4S]^{2+}$ center in MgATP-bound nitrogenase Fe protein which was found to be split into two [2Fe-2S] fragments separated by ~5 Å in the crystalline state (37). Normal mode calculations coupled with $^{57/54}Fe$ and $^{34/32}S$ isotope shifts and measurement of depolarization ratios are planned to test this hypothesis and provide vibrational assignments for the $[4Fe\text{-}4S]^{2+}$ center in NfuA.

The nature of the cluster ligation for the [4Fe-4S] center on NfuA was addressed by amino acid substitution studies. On the basis of UV-visible spectroscopy, it was not possible to reconstitute an [Fe-S] cluster on variant forms of NfuA proteins that have either of the conserved cysteine residues within the Cys-X-X-Cys motif substituted by alanine (data not shown). Taken

together, the analytical, spectroscopic and mutagenesis data are reasonably interpreted in terms of cluster-loaded NfuA having a $[4Fe\text{-}4S]^{2+}$ cluster that is symmetrically bridged between two identical subunits, although other arrangements are possible and have not been excluded.

The redox properties of the $[4Fe\text{-}4S]^{2+}$ cluster assembled on NfuA were assessed using the combination of UV-visible absorption, EPR and variable-temperature magnetic circular dichroism (VTMCD) spectroscopies, see Figures 2-2 and 2-5. Anaerobic addition of 1 reducing equivalent of dithionite results in reversible bleaching of the visible absorption (Figure 2-2) due to partial reduction to yield a S = 1/2 $[4Fe\text{-}4S]^{+}$ cluster as evidenced by parallel EPR and VTMCD studies. EPR revealed a near-axial resonance (g = 2.03, 1.93, 1.89) with relaxation properties (observable only below 40 K) indicative of a $[4Fe\text{-}4S]^{+}$ cluster, that accounts for 0.4 spins/NfuA dimer (see inset in Figure 2-2). The low spin quantification is in accord with the partial bleaching of the visible absorption and appears to reflect partial reduction. No low-field EPR signals indicative of a S = 3/2 $[4Fe\text{-}4S]^{+}$ clusters were observed. In accord with the EPR results, the VTMCD spectrum is consistent with a S = 1/2 $[4Fe\text{-}4S]^{+}$ cluster rather than a S = 3/2 $[4Fe\text{-}4S]^{+}$ cluster (38) and the intensity indicates ~0.4 $[4Fe\text{-}4S]^{+}$ clusters/NfuA dimer. Partial reduction by one reducing equivalent of dithionite implies a redox potential for the $[4Fe\text{-}4S]^{2+,+}$ couple that is close to that of dithionite at pH 8.0 (–450 mV). Such a low potential redox process is unlikely to be physiologically relevant. Moreover, the reduced cluster is unstable and is rapidly degraded within minutes in the presence of excess dithionite even under strictly anaerobic conditions. Similar redox behavior has recently been reported for the subunit bridging [4Fe-4S] cluster on IscU (16). Hence only the oxidized form of the subunit-bridging [4Fe-4S] cluster on NfuA is likely to be relevant *in vivo.*

In vitro experiments have demonstrated that a [4Fe-4S] cluster-loaded form of IscU can be used for the activation of apo aconitase (32). This observation is in agreement with *in vivo* data where physiological depletion of IscU results in a deficiency in the maturation of aconitase and a loss in the capacity to sustain growth (5). However, IscU-directed *in vitro* activation of apo-aconitase is not stoichiometric and too slow to represent a true physiological process, indicating the likely participation of other components in the [Fe-S] protein maturation process. Among other components that are likely to be involved in stimulating the IscU-directed [Fe-S] protein maturation process are HscB and HscA, which have been shown to catalyze the nucleotide-dependent release of [2Fe-2S] clusters preassembled on the IscU scaffold (39) and which have also been shown to be necessary to sustain *A .vinelandii* growth. However, initial experiments on the effects of HscA/HscB/ATP on the rate of cluster transfer from [4Fe-4S]-IscU to apo-aconitase A (Apo-AcnA) failed to demonstrate any significant rate enhancement (32, 40). This raises the possibility for the participation of intermediate [Fe-S] cluster carriers. In order to test whether or not NfuA might serve as an intermediate [Fe-S] cluster carrier, which could assist the effective maturation of [Fe-S] proteins, we asked if a [4Fe-4S] cluster-loaded form of NfuA can be used for *in vitro* activation of apo-aconitase.

Figure 2-6A shows the time-dependent activation of apo-aconitase that occurs when it is mixed with [4Fe-4S] cluster-loaded NfuA. Initial experiments duplicated the conditions established to achieve optimal aconitase activation using [4Fe-4S] cluster-loaded IscU (32) and involved incubation of cluster-loaded NfuA (12 μM in [4Fe-4S] clusters) with 4 μM of apo-aconitase, i.e. a 3-fold stoichiometric excess of [4Fe-4S] clusters. The activation is remarkably rapid, having a second order rate constant of $7 \times 10^4\ M^{-1}min^{-1}$, a rate which is almost 10 times faster than observed for analogous conditions using the [4Fe-4S] cluster-loaded form of IscU

(32). Such rates are only consistent with intact cluster transfer as activation with equivalent amounts of Fe^{2+} and S^{2-} ions is at least 15 times slower. Moreover, unlike [4Fe-4S]-IscU to apo-AcnA cluster transfer which is optimal with a 3:1 stoichiometry, [4Fe-4S] cluster transfer from NfuA to apo-AcnA occurs with a 1:1 stoichiometry. This is illustrated in Figure 2-6B which shows apo-aconitase activation after 20 min of incubation as a function of the molar ratio of [4Fe-4S] clusters on NfuA to apo-AcnA. The data is well simulated by theoretical data constructed for [4Fe-4S] cluster transfer from NfuA to apo-AcnA that occurs with a 1:1 stoichiometry and has a second order rate constant of 7.0×10^4 $M^{-1}min^{-1}$. Hence cluster transfer and activation of apo-aconitase is much faster and more efficient with [4Fe-4S]-NfuA than with [4Fe-4S]-IscU.

To examine the physiological consequences associated with loss of NfuA function a strain (designated DJ1707) was constructed where the *nfuA* gene is disrupted by a combined deletion and kanamycin gene cartridge insertion. DJ1707 has no obvious phenotypic traits with respect to growth rate when cultured in liquid medium or colony size when cultured on agar plates. However, when cell extracts of DJ1707 were examined for aconitase activity they exhibited only ~50% of activity when compared to the isogenic wild type strain. This relative loss in aconitase activity contrasted with no loss in isocitrate dehydrogenase activity. Isocitrate dehydrogenase, like aconitase, is a TCA cycle enzyme but it does not require an [Fe-S] cluster for its activity. A modest, but reproducible reduction in the activity of an [Fe-S] cluster-containing enzyme, with no apparent effect on the capacity for growth is similar to the phenotype associated with loss of IscA function in *A. vinelandii* (5). Another phenotype associated with loss of IscA function is a complete loss in capacity for growth when cells are cultured under a 40% oxygen atmosphere (5). This same phenotype is also associated with loss of NfuA function

(Figure 2-7). To test the functional importance of the two conserved cysteine residues contained within NfuA, strains were constructed where these residues, Cys^{152} and Cys^{155} were individually substituted by alanine. These strains, DJ1759 and DJ1769, also exhibited the same oxygen-sensitive growth phenotype associated with DJ1707, which has both a deletion and kanamycin gene cartridge insertion within *nfuA* (Figure 2-7).

In previous work it was shown that cells functionally depleted for IscU are unable to sustain growth even when cultured under nitrogen fixing conditions where NifU is expressed. This result indicates target specificity with respect to Isc- and Nif-directed [Fe-S] protein maturation. However, if the accumulation of NifU and NifS is elevated far above normal physiological levels by placing their expression under control of the strong *E. coli ara* regulatory elements, the requirement for a functional IscU can be bypassed (7). In the present work, we also found that the oxygen-sensitive phenotype of cells lacking NfuA could not be rescued by culturing cells under nitrogen fixing conditions. Thus, when expressed at normal physiological levels, NifU is unable to supplant the function of NfuA. However, when *nifUS* expression is placed under control of the strong *ara* regulatory elements (Figure 2-8) the oxygen-sensitive phenotype associated with loss of NfuA function is fully corrected. Thus, there is a capacity for functional cross-talk between NifU and NfuA, but only when NifU is expressed at high levels. In separate experiments we asked whether or not the IscU-like [Fe-S] cluster assembly site contained within the N-terminal region of NifU or the NfuA-like [Fe-S] cluster assembly site contained within the C-terminal domain of NifU is required to correct the phenotype associated with loss of NfuA function (Figure 2-8). This was accomplished by constructing two different strains, one having the NifU-Cys^{35} residue substituted by alanine (DJ1773) and the other having the NifU-Cys^{275} residue substituted by alanine (DJ1791), in combination with inactivation of

NfuA. Previous work has shown that such substitutions respectively eliminate the capacity for [Fe-S] cluster formation within the IscU-like and NfuA-like domains of NifU. As can be seen in Figure 2-8, a capacity for the assembly of [Fe-S] clusters on both the IscU-like and NfuA-like domains of NifU is required for correction of the oxygen-sensitive phenotype associated with loss of NfuA function.

Discussion

The potential of Nfu proteins with sequence homology to the C-terminal domain of NifU to act as scaffold proteins for the assembly of [2Fe-2S] or [4Fe-4S] clusters has previously been demonstrated via spectroscopic and analytical studies of recombinant forms of cyanobacterial, plant chloroplast and human Nfu proteins (17-20). UV-visible absorption and analytical studies of cyanobacterial and plant chloroplast Nfu proteins as purified were indicative of one [2Fe-2S]$^{2+}$ cluster per dimer (18,20). In contrast, recombinant human Nfu was purified in an apo form that assembled one [4Fe-4S]$^{2+}$ cluster per dimer under anaerobic reconstitution conditions as evidenced by UV-visible absorption, Mössbauer and analytical studies (17). In both cases the clusters were tentatively considered to be symmetrically ligated by the conserved CXXC motif of each monomer, although this mode of coordination was not based on structural, spectroscopic or mutagenesis data. Both cluster-bound forms are likely to be physiologically relevant as *in viv*o studies indicate that Nfu is required for maturation of both [2Fe-2S] and [4Fe-4S] cluster-containing proteins in plant chloroplasts (21). The ability to assembly both [2Fe-2S] and [4Fe-4S] clusters is a common and desirable attribute of [Fe-S] cluster scaffold proteins (1). By analogy with recent *in vitro* studies of *A. vinelandii* IscU (16), the specific cluster assembled on

Nfu proteins is likely to be determined by cellular environment, with significant O_2 levels favoring the assembly of the more O_2-tolerant [2Fe-2S] clusters.

In this work, we report *in vitro* and *in vivo* characterization of *A. vinelandii* NfuA, which constitutes a distinct class of Nfu proteins comprising a N-terminal A-type domain and a C-terminal Nfu-type domain, but lacking the three conserved cysteines generally associated with the A-type scaffold proteins. The accompanying paper describes the characterization of a similar protein from *E. coli*. It is shown that a [4Fe-4S] cluster can be readily assembled on *A. vinelandii* NfuA *in vitro* when supplied with a source of S^{2-} and Fe^{2+} under strictly anaerobic conditions. On the basis of cysteine mutagenesis studies, analytical data and extensive spectroscopic characterization (UV-visible absorption, Mössbauer, resonance Raman, EPR and VTMCD), it is concluded that the [4Fe-4S] cluster assembled within NfuA *in vitro* is symmetrically bridged between identical subunits and coordinated by both cysteines in the CXXC motif. Loss of NfuA function results in a reproducible reduction in the activity of aconitase, a [4Fe-4S] cluster-dependent enzyme. Furthermore, [4Fe-4S] clusters assembled on NfuA *in vitro* can be used for the very efficient *in vitro* activation of apo-aconitase. Finally, loss of NfuA function does not exhibit an overt physiological phenotype unless cells are cultured under conditions of elevated oxygen. From these data it is clear that NfuA has some function related to the maturation or maintenance of [Fe-S] proteins, but what is the specific function of NfuA?

The most pertinent observations in relation to this question are summarized as follows. (*i*) IscU is essential for the *in vivo* maturation of [Fe-S] proteins. (*ii*) The [4Fe-4S] cluster-loaded form of IscU is a poor *in vitro* donor for aconitase maturation (32) whereas the [4Fe-4S] cluster loaded form of NfuA is very effective for *in vitro* activation of aconitase. (*iii*) NfuA is not essential for *in vivo* [Fe-S] protein maturation but loss of NfuA results in a lower activity of at

least one key [4Fe-4S] protein, i.e. aconitase. (*iv*) The same phenotypical relationship observed between IscU and NfuA is also observed for the IscU-like and NfuA-like domains of NifU. Namely, loss of the IscU-like domain of NifU nearly eliminates the capacity for the *in vivo* maturation of nitrogenase, whereas functional loss of the NfuA-like domain has no obvious effect on nitrogenase maturation (3). Furthermore, the IscU-like domain of NifU is a relatively poor [4Fe-4S] donor for maturation of the nitrogenase Fe protein. (*v*) The correction of the oxygen-sensitive phenotype associated with loss of NfuA that can be achieved by elevated expression of NifU requires functionality of both the IscU-like and NfuA-like domains within NifU.

These results lead us to propose a model where IscU and the IscU-like domain within NifU have essential roles in the *de novo* formation of [Fe-S] clusters, whereas NfuA and the NfuA-like domain of NifU could have auxiliary roles related to the effective transfer of [Fe-S] clusters to specific target proteins. This model suggests that [Fe-S] clusters initially formed on the IscU type of scaffolds in *A. vinelandii* are subsequently transferred to NfuA type proteins. In this context NfuA type proteins would be considered to serve as intermediate [Fe-S] cluster carriers or, perhaps, as [Fe-S] cluster reservoirs. Given that IscU appears to be required for the maturation of housekeeping [Fe-S] proteins in *A. vinelandii*, the participation of intermediate carriers is a reasonable possibility. Namely, it is difficult to imagine that IscU would have the capacity to directly and effectively interact with the large variety of cellular [Fe-S] proteins present in cells. This proposed lack of direct physiological delivery of [Fe-S] clusters from IscU to various client proteins is supported by the relatively poor capacity for cluster-loaded forms of IscU to effect *in vitro* [Fe-S] protein maturation. Nevertheless, the observation that NfuA is dispensable indicates that IscU can serve at some level as a primary [Fe-S] cluster donor to client

proteins, or that IscU is able to deliver [Fe-S] clusters to a suite of intermediate carriers, some of which have overlapping functions. We favor the latter possibility and suggest that a variety of proteins, which have recently been shown to have the capacity to harbor [Fe-S] clusters, for example, Nfu (17-20), IscA (9, 41, 42), and glutaredoxins (43-45) could collectively serve as a physiological [Fe-S] cluster reservoir. This possibility is in line with the manifestation of a clear phenotype for NfuA and IscA (5) in *A. vinelandii* under conditions of oxygen stress where a demand for the capacity for [Fe-S] cluster formation would be enhanced. Also, the fact that functionality of both the IscU-like and NfuA-like domains within NifU is required to rescue the NfuA-minus phenotype when NifU is expressed at high levels, suggest that the physiological function of the NfuA-domain is strictly dependent on having an intact IscU-like domain. Namely, the observed phenotype is consistent with the preassembly of [Fe-S] clusters on the IscU-like domain with subsequent transfer to the NfuA-like domain. The converse is unlikely to occur because maturation of nitrogenase does not require an intact NfuA-like domain within NifU.

Another interesting feature of NfuA is that it bears primary sequence identity when compared to the IscA family of proteins, but this sequence conservation does not include cysteine residues that are conserved among the IscA family. This comparison suggests that primary sequence conservation between the IscA family and NfuA could be related to target specificity, rather than [Fe-S] cluster assembly, and supports the possibility that IscA and NfuA could have some overlapping functions. Given the large number of client [Fe-S] proteins within the cell, as well as the variety of potential environmental conditions a cell might encounter, a hierarchy of intermediate [Fe-S] cluster carriers that could control the distribution of [Fe-S] clusters would be a reasonable strategy for maximizing metabolic capacity. There is already

precedent for such a strategy in the case of *E. coli* where there are at least two different systems that can function for [Fe-S] protein maturation under different conditions. One of these, the Isc system operates under standard laboratory conditions whereas the Suf system operates under conditions of Fe limitation or oxygen stress (13). It should be noted that *A. vinelandii* does not encode a Suf system for [Fe-S] cluster assembly. Other cases of apparent specialized targeting of preassembled [Fe-S] clusters involves the role of ErpA, an IscA-like protein, in the maturation of IspG (12) and the role of the NifU and NifS in maturation of nitrogenase (46). Our future studies will be aimed at testing the hypothesis that NfuA and the NfuA-like domain of NifU function as intermediate carriers of [Fe-S] clusters preformed on the respective IscU and IscU-like scaffolds. In particular we are interested in testing whether or not clusters formed on the proposed primary scaffold can be captured by the proposed NfuA and NfuA-like carriers. Clearly, this could be a complicated process that might involve a variety of other components.

Acknowledgements

This work was supported by grants from the National Science Foundation (MCB0717710 to DRD) and National Institute of Health (GM47295 to BHH and GM62524 to MKJ). We thank B. Py, F. Barras, and M. Fontecave for providing their results on the *E. coli* NfuA homolog prior to publication.

References

1. Johnson, D. C., Dean, D. R., Smith, A. D., and Johnson, M. K. (2005) *Annu. Rev. Biochem.* **74**, 247-281

2. Smith, A. D., Jameson, G. N., Dos Santos, P. C., Agar, J. N., Naik, S., Krebs, C., Frazzon, J., Dean, D. R., Huynh, B. H., and Johnson, M. K. (2005) *Biochemistry* **44**, 12955-12969

3. Dos Santos, P. C., Smith, A. D., Frazzon, J., Cash, V. L., Johnson, M. K., and Dean, D. R. (2004) *J. Biol. Chem.* **279**, 19705-19711

4. Zheng, L., Cash, V. L., Flint, D. H., and Dean, D. R. (1998) *J. Biol. Chem.* **273**, 13264-13272.

5. Johnson, D. C., Unciuleac, M. C., and Dean, D. R. (2006) *J. Bacteriol.* **188**, 7551-7561

6. Johnson, D. C., Dos Santos, P. C., and Dean, D. R. (2005) *Biochem. Soc. Trans.* **33**(Pt 1), 90-93

7. Dos Santos, P. C., Johnson, D. C., Ragle, B. E., Unciuleac, M. C., and Dean, D. R. (2007) *J. Bacteriol.* **189**, 2854-2862

8. Agar, J. N., Krebs, C., Frazzon, J., Huynh, B. H., Dean, D. R., and Johnson, M. K. (2000) *Biochemistry* **39**, 7856-7862.

9. Krebs, C., Agar, J. N., Smith, A. D., Frazzon, J., Dean, D. R., Huynh, B. H., and Johnson, M. K. (2001) *Biochemistry* **40**, 14069-14080

10. Yang, J., Bitoun, J. P., and Ding, H. (2006) *J. Biol. Chem.* **281**, 27956-27963

11. Takahashi, Y., and Tokumoto, U. (2002) *J. Biol. Chem.* **277**, 28380-28383.

12. Loiseau, L., Gerez, C., Bekker, M., Ollagnier-de Choudens, S., Py, B., Sanakis, Y., Teixeira de Mattos, J., Fontecave, M., and Barras, F. (2007) *Proc. Natl. Acad. Sci. U. S. A.* **104**, 13626-13631

13. Outten, F. W., Djaman, O., and Storz, G. (2004) *Mol. Microbiol.* **52**, 861-872

14. Ollagnier-De Choudens, S., Nachin, L., Sanakis, Y., Loiseau, L., Barras, F., and Fontecave, M. (2003) *J. Biol. Chem.* **278**, 17993-18001.

15. Agar, J. N., Yuvaniyama, P., Jack, R. F., Cash, V. L., Smith, A. D., Dean, D. R., and Johnson, M. K. (2000) *J. Biol. Inorg. Chem.* **5**, 167-177.

16. Chandramouli, K., Unciuleac, M. C., Naik, S., Dean, D. R., Huynh, B. H., and Johnson, M. K. (2007) *Biochemistry* **46**, 6804-6811

17. Tong, W. H., Jameson, G. N., Huynh, B. H., and Rouault, T. A. (2003) *Proc. Natl. Acad. Sci. U. S. A.* **100**, 9762-9767

18. Nishio, K., and Nakai, M. (2000) *J. Biol. Chem.* **275**, 22615-22618.

19. Leon, S., Touraine, B., Ribot, C., Briat, J. F., and Lobreaux, S. (2003) *Biochem. J.* **371**, 823-830.

20. Yabe, T., Morimoto, K., Kikuchi, S., Nishio, K., Terashima, I., and Nakai, M. (2004) *Plant Cell* **16**, 993-1007

21. Touraine, B., Boutin, J. P., Marion-Poll, A., Briat, J. F., Peltier, G., and Lobreaux, S. (2004) *Plant J.* **40**, 101-111

22. Schilke, B., Voisine, C., Beinert, H., and Craig, E. (1999) *Proc. Natl. Acad. Sci. U. S. A.* **96**, 10206-10211

23. Balasubramanian, R., Shen, G., Bryant, D. A., and Golbeck, J. H. (2006) *J. Bacteriol.* **188**, 3182-3191

24. Jacobson, M. R., Brigle, K. E., Bennett, L. T., Setterquist, R. A., Wilson, M. S., Cash, V. L., Beynon, J., Newton, W. E., and Dean, D. R. (1989) *J. Bacteriol.* **171**, 1017-1027.

25. Strandberg, G. W., and Wilson, P. W. (1968) *Can. J. Microbiol.* **14**, 25-31

26. Saas, J., Ziegelbauer, K., von Haeseler, A., Fast, B., and Boshart, M. (2000) *J. Biol. Chem.* **275**, 2745-2755

27. Cribbs, R., and Englesberg, E. (1964) *Genetics* **49**, 95-108

28. Fish, W. W. (1988) *Methods Enzymol.* **158**, 357-364

29. Cosper, M. M., Jameson, G. N., Hernandez, H. L., Krebs, C., Huynh, B. H., and Johnson, M. K. (2004) *Biochemistry* **43**, 2007-2021

30. Johnson, M. K. (2000) CD and MCD Spectroscopy. In Que, L., Jr., editor. *Physical methods in bioinorganic chemistry. Spectroscopy and magnetism*, University Science Books, Sausalito, CA

31. Ravi, N., Moore, V., Lloyd, S. G., Hales, B. J., and Huynh, B. H. (1994) *J. Biol. Chem.* **269**, 20920-20924

32. Unciuleac, M. C., Chandramouli, K., Naik, S., Mayer, S., Huynh, B. H., Johnson, M. K., and Dean, D. R. (2007) *Biochemistry* **46**, 6812-6821

33. Kennedy, M. C., and Beinert, H. (1988) *J. Biol. Chem.* **263**, 8194-8198.

34. Czernuszewicz, R. S., Macor, K. A., Johnson, M. K., Gewirth, A., and Spiro, T. G. (1987) *J. Am. Chem. Soc.* **109**, 7178-7187

35. Spiro, T. G., Czernuszewicz, R. S., and Han, S. (1988) Iron-sulfur proteins and analog complexes. In Spiro, T. G., editor. *Resonance Raman spectra of heme and metalloproteins*, John Wiley & Sons, New York

36. Brereton, P. S., Duderstadt, R. E., Staples, C. R., Johnson, M. K., and Adams, M. W. (1999) *Biochemistry* **38**, 10594-10605.

37. Sen, S., Igarashi, R., Smith, A., Johnson, M. K., Seefeldt, L. C., and Peters, J. W. (2004) *Biochemistry* **43**, 1787-1797

38. Onate, Y. A., Finnegan, M. G., Hales, B. J., and Johnson, M. K. (1993) *Biochim. Biophys. Acta* **1164**, 113-123.

39. Chandramouli, K., and Johnson, M. K. (2006) *Biochemistry* **45**, 11087-11095.

40. Vickery, L. E., and Cupp-Vickery, J. R. (2007) *Crit. Rev. Biochem. Mol. Biol.* **42**, 95-111.

41. Ollagnier-De-Choudens, S., Sanakis, Y., and Fontecave, M. (2004) *J. Biol. Inorg. Chem.* **9**, 828-38

42. Morimoto, K., Yamashita, E., Kondou, Y., Lee, S. J., Arisaka, F., Tsukihara, T., and Nakai, M. (2006) *J. Mol. Biol.* **360**, 117-132

43. Rouhier, N., Unno, H., Bandyopadhyay, S., Masip, L., Kim, S. K., Hirasawa, M., Gualberto, J. M., Lattard, V., Kusunoki, M., Knaff, D. B., Georgiou, G., Hase, T., Johnson, M. K., and Jacquot, J. P. (2007) *Proc. Natl. Acad. Sci. U. S. A.* **104**, 7379-7384

44. Lillig, C. H., Berndt, C., Vergnolle, O., Lonn, M. E., Hudemann, C., Bill, E., and Holmgren, A. (2005) *Proc. Natl. Acad. Sci. U. S. A.* **102**, 8168-8173

45. Rodriguez-Manzaneque, M. T., Tamarit, J., Belli, G., Ros, J., and Herrero, E. (2002) *Mol. Biol. Cell.* **13**, 1109-1121

46. Jacobson, M. R., Cash, V. L., Weiss, M. C., Laird, N. F., Newton, W. E., and Dean, D. R. (1989) *Mol. Gen. Genet.* **219**, 49-57

Figure 2-1: *A. vinelandii* Fe-S cluster biosynthetic genes. *Top*: Schematic representation of the *A. vinelandii* genes known or suspected to be involved in the maturation of [Fe-S] proteins and their relative location in the *A. vinelandii* chromosome. Proteins containing same functional domains are color-coded accordantly. *Bottom:*Primary amino acid sequence of NfuA. Identical amino acids in $IscA^{nif}$ and NifU are highlighted in pink and blue respectively. The conserved cysteines present in the CXXC motif are indicated with black dots.

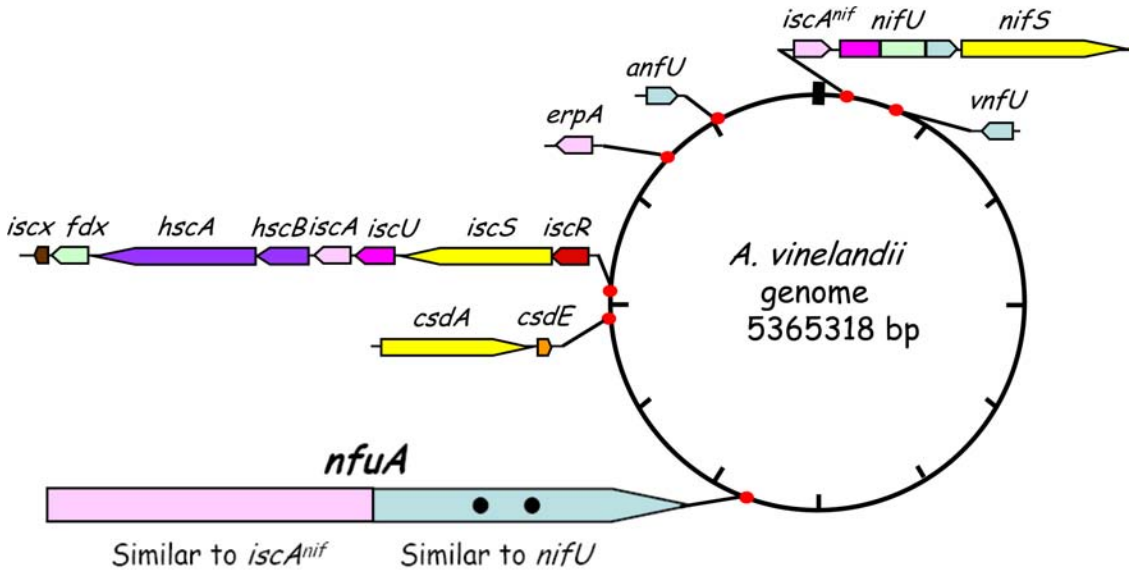

MSAITITDAAHDYLAELLAKQNGTDIGIRIFITQPGTPAAETCLAYCKPHERHPDDIAQALKSFT
LWIDAVSEPFLEDAIVDYANDRMGGQLTIKAPNAKVPMIDEDSPLGERINYYLQTEINPGLASHG
GQVSLVDIVEEGIAVLRFGGGCQGCGMVDMTLKDGVEKTLLERIPDLKGVRDATDHSNRENAYY

Figure 2-2: UV-visible absorption spectra of reconstituted *A. vinelandii* NfuA as prepared (solid line) and after anaerobic reduction with 1 reducing equivalent of dithionite (dashed line). Molar extinction coefficients are expressed per NfuA monomer. The inset shows the X-band EPR spectrum of the sample reduced with 1 reducing equivalent of dithionite. EPR conditions: microwave frequency, 9.60 GHz; microwave power, 10 mW; modulation amplitude, 0.63 mT; temperature, 10 K.

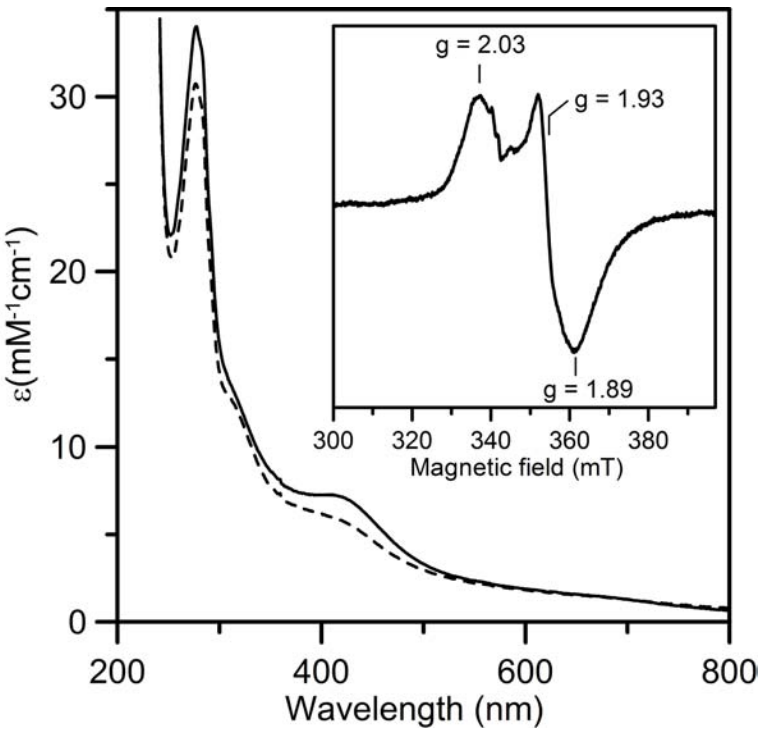
g = 2.03
g = 1.93
g = 1.89
300
320
340
360
380
Magnetic field (mT)
30
20
10
0
ε(mM-1cm-1)
200
400
600
800
Wavelength (nm)

Figure 2-3: Mössbauer spectrum of ^{57}Fe reconstituted *A. vinelandii* NfuA recorded at 4.2 K with a field of 50 mT applied parallel to the γ-radiation. The solid black line is the composite spectrum including the simulated spectrum of a [4Fe-4S]$^{2+}$ cluster (dashed line), scaled to 90% of the total Fe absorption, and the simulated spectrum of a Fe^{2+} species (dotted line), accounting for 10% of the Fe absorption. The parameters used for the simulations are provided in the text.

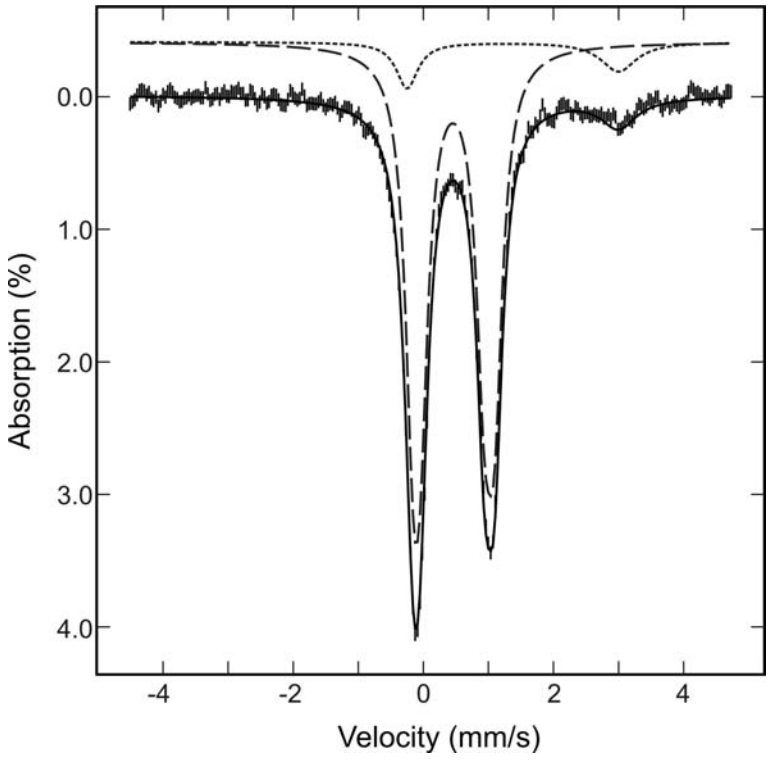
0.0
1.0
2.0
3.0
4.0
Absorption (%)
-4
-2
0
2
4
Velocity (mm/s)

Figure 2-4: Comparison of the resonance Raman spectra for $[4Fe\text{-}4S]^{2+}$ cluster-loaded forms of *A. vinelandii* IscU and NfuA. The samples (~3 mM in [4Fe-4S] clusters) were in the form of frozen droplets at 17 K. The spectra were recorded using 457-nm excitation with 100-mW of laser power at the sample. Each spectrum is the sum of 100 scans, with each scan involving photon counting for 1 s at 1-cm^{-1} increments, with 7 cm^{-1} resolution. Bands due to lattice modes of the frozen buffer solution have been subtracted from both spectra.

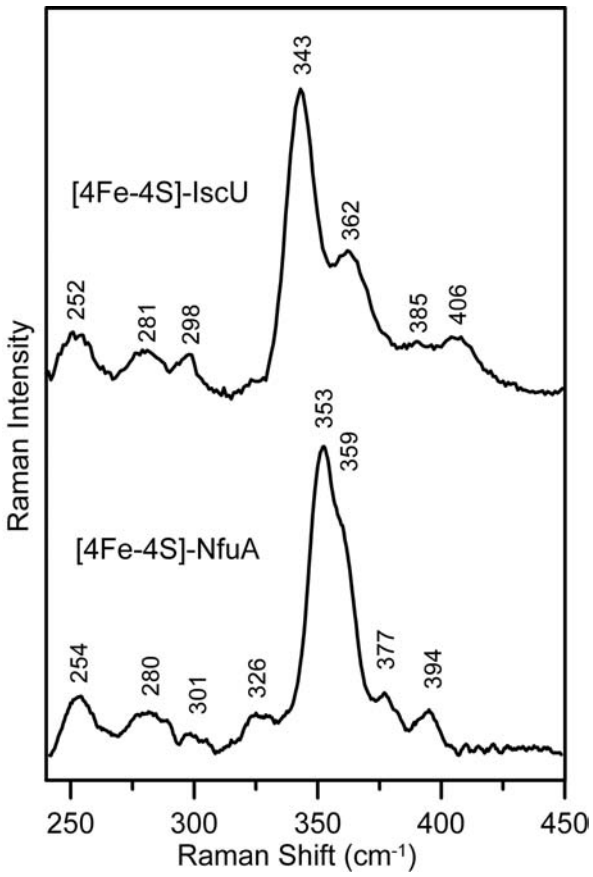
[4Fe-4S]-IscU
343
362
252
281
298
385
406
[4Fe-4S]-NfuA
353
359
254
280
301
326
377
394
Raman Intensity
250
300
350
400
450
Raman Shift (cm-1)

Figure 2-5: VTMCD spectra of dithionite-reduced reconstituted *A. vinelandii* NfuA. Reconstituted NfuA (0.25 mM in [4Fe-4S] clusters) was reduced with 1 reducing equivalent of dithionite after addition of 55% (v/v) ethylene glycol. MCD spectra recorded in a 1 mm cell with a magnetic field of 6 T at 1.7, 4.2 and 15 K. All bands increase in intensity with decreasing temperature and $\Delta\varepsilon$ values are expressed per NfuA monomer.

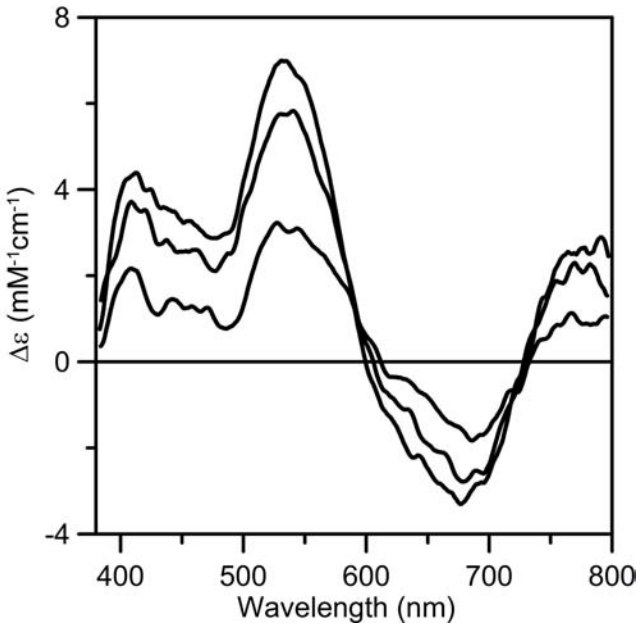
8
4
0
-4
Δε (mM-1cm-1)
400
500
600
700
800
Wavelength (nm)

Figure 2-6: Activation of apo-AcnA activity using [4Fe-4S] cluster-loaded NfuA. (A) Apo-AcnA (4 μM) was incubated with [4Fe-4S] cluster-loaded NfuA (12 μM in $[4Fe\text{-}4S]^{2+}$ clusters) at room temperature under anaerobic conditions. Aliquots containing 4 μM AcnA were withdrawn after 100, 460, 820, 1140, 1480 and 1800 s, and AcnA activity was immediately measured. The solid line is the best fit to second-order kinetics based on the initial concentrations of $[4Fe\text{-}4S]^{2+}$ clusters on NfuA and apo-AcnA, and corresponds to a rate constant of 7.0×10^4 $M^{-1}min^{-1}$. (B) Apo-AcnA activation as a function of the concentration of NfuA-ligated $[4Fe\text{-}4S]^{2+}$ clusters. The concentration of apo-AcnA was kept constant at 4 μM, and the concentration of NfuA-ligated $[4Fe\text{-}4S]^{2+}$ clusters was varied as indicated on the *x* axis. After 1200 s, aliquots were withdrawn and assayed for AcnA activity. The solid line is theoretical data for second order kinetics with a rate constant of 7.0×10^4 $M^{-1}min^{-1}$ assuming quantitative [4Fe-4S] cluster transfer from NfuA to apo-AcnA with a 1:1 stoichiometry.

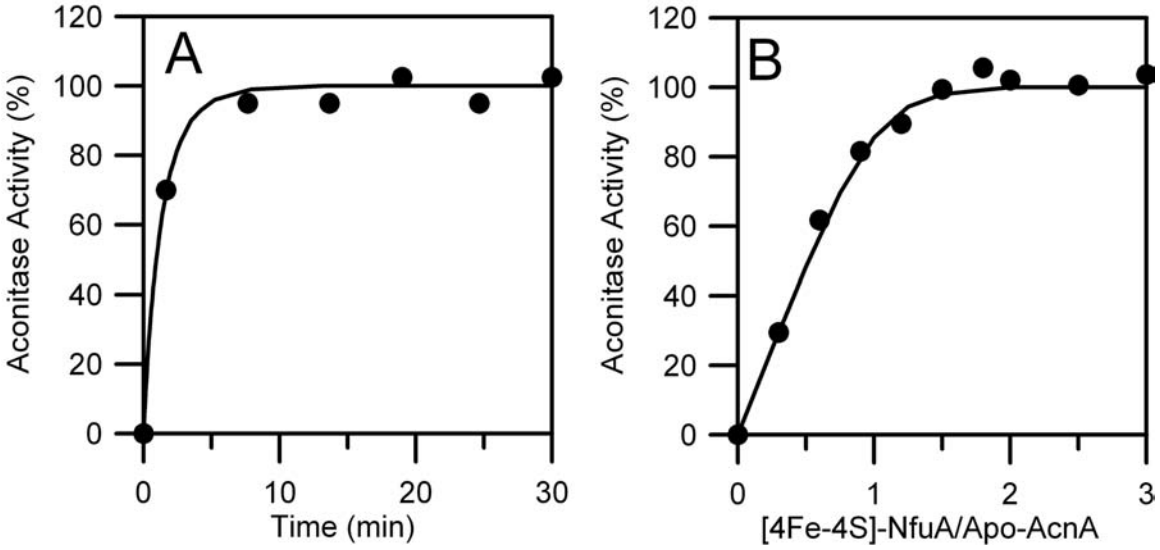
A
B
Aconitase Activity (%)
Time (min)
[4Fe-4S]-NfuA/Apo-AcnA
0
20
40
60
80
100
120
10
30
1
2
3

Figure 2-7: Inactivation of *nfuA* and its conserved cysteines results in a null-growth phenotype under elevated oxygen conditions. Strains were cultured in Burk's medium supplemented with 13 mM ammonium acetate under ambient (~20%) O_2 or 40% O_2 for three days. The standard laboratory strain designated as DJ was used as a wild-type control (WT). Strain DJ1707 has a deletion and kanamycin gene cartridge insertion within the *nfuA* gene (Δ*nfuA::kan*). Strain DJ1759 and DJ1769 have respectively NfuA Cys^{152} and NfuA Cys^{155} substituted by alanine.

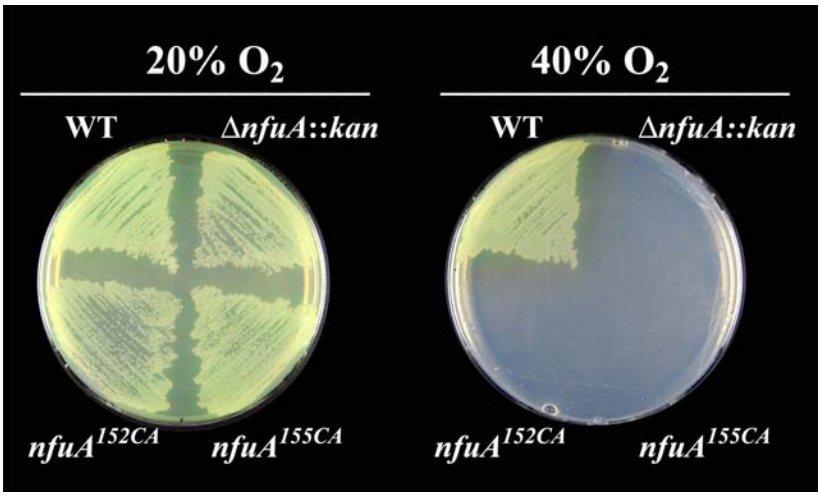
20% O2
WT
ΔnfuA::kan
nfuA152CA
nfuA155CA
40% O2
WT
ΔnfuA::kan
nfuA152CA
nfuA155CA

Figure 2-8: Rescue of the null growth phenotype associated with the functional loss of NfuA by elevated *ara*-directed expression of NifUS. (*top*) Schematic representation of the genetic organizations of DJ1707, DJ1772, DJ1773, and DJ1791. (*bottom*) Growth of strains when cultured in Burk's medium supplemented with 13 mM ammonium acetate and 20 mM arabinose and cultured under a 40% O_2 atmosphere. NifU and NifS expression is under control of the *ara*-regulatory elements and accumulate at high levels when arabinose is added to the growth medium.

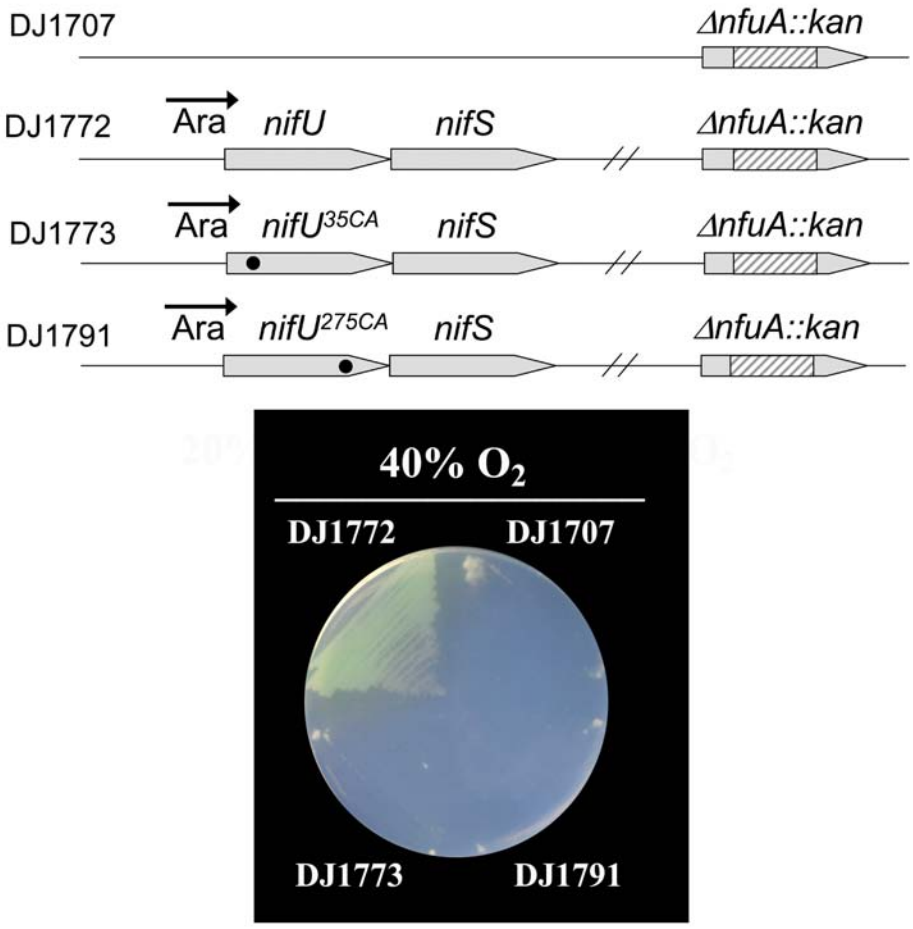
DJ1707
ΔnfuA::kan
DJ1772
Ara
nifU
nifS
ΔnfuA::kan
DJ1773
Ara
nifU35CA
nifS
ΔnfuA::kan
DJ1791
Ara
nifU275CA
nifS
ΔnfuA::kan
40% O2
DJ1772
DJ1707
DJ1773
DJ1791

CHAPTER 3

CHLOROPLAST MONOTHIOL GLUTAREDOXINS ACT AS SCAFFOLD PROTEINS FOR THE ASSEMBLY AND DELIVERY OF [2FE-2S] CLUSTERS

Sibali Bandyopadhyay , Filipe Gama , Maria Micaela Molina-Navarro, José Manuel Gualberto, Ronald Claxton, Sunil G. Naik, Boi Hanh Huynh, Enrique Herrero, Jean Pierre Jacquot, Michael K. Johnson, Nicolas Rouhier
Submitted to *EMBO J.*

Abstract

Glutaredoxins (Grxs) are small oxidoreductases able to reduce disulfide bonds or protein-glutathione mixed disulfides. More than 30 distinct grx genes are expressed in higher plants, but little is currently known concerning their functional diversity. This study presents biochemical and spectroscopic evidence for incorporation of a [2Fe-2S] cluster in two heterologously expressed chloroplastic Grxs, GrxS14 and GrxS16, and *in vitro* cysteine desulphurase-mediated assembly of an identical [2Fe-2S] cluster in apo-GrxS14. These Grxs possess the same monothiol CGFS active site as yeast Grx5, which has been shown to be involved in mitochondrial Fe-S cluster biogenesis, and both were able to complement a yeast *grx5* mutant defective in Fe-S cluster assembly. *In vitro* kinetic studies monitored by CD spectroscopy indicate that [2Fe-2S] clusters on GrxS14 are rapidly and quantitatively transferred to apo chloroplast ferredoxin. These data demonstrate that chloroplast CGFS Grxs can function as scaffold proteins for the assembly of [2Fe-2S] clusters that can be transferred intact to physiologically relevant acceptor proteins. Alternatively, they may function in the storage and/or delivery of preformed Fe-S clusters.

Introduction

Iron sulphur proteins (Fe-S proteins) are intimately involved in numerous essential biological processes, such as photosynthesis, respiration and the metabolism of carbon, oxygen, hydrogen, nitrogen and sulphur (Beinert et al, 1997; Johnson & Smith, 2005). However, little is currently known concerning the mechanism of Fe-S cluster biogenesis in plants. Much of the current understanding of Fe-S cluster biogenesis stems from investigation of components of the bacterial *isc* (*iron-sulphur cluster assembly*), *suf* (*sulfur mobilization*) and *nif* (*nitrogen fixation*) operons (Johnson et al, 2005) and identification and characterization of homologous ISC-type proteins in yeast and mammalian mitochondria (Lill & Mühlenhoff, 2005). The ISC, SUF, and NIF Fe-S cluster assembly machineries share a common basic mechanism involving cysteine desulphurase (IscS, SufS, and NifS) mediated assembly of [2Fe-2S] or [4Fe-4S] clusters on U-type (IscU, SufU, N-terminal domain of NifU), A-type (IscA, SufA, ^{Nif}IscA) and Nfu-type (corresponding to the C-terminal domain of NifU) scaffold proteins, and subsequent intact cluster transfer into acceptor apo-proteins. In the case of the ISC machinery, [2Fe-2S] cluster transfer from IscU has been shown to be facilitated by specific molecular co-chaperones (HscA and HscB) in an ATP-dependent reaction (Chandramouli & Johnson, 2006) and [4Fe-4S] cluster assembly on dimeric IscU has been shown to occur at the subunit interface via reductive coupling of two [2Fe-2S] clusters (Chandramouli et al, 2007). However, little is currently known concerning the detailed mechanism of Fe-S cluster assembly and transfer involving scaffold proteins. In plants, Fe-S cluster biosynthesis primarily occurs in mitochondria, using the ISC machinery with Isu, IscA and Nfu as potential scaffold proteins, and in chloroplasts using the SUF machinery with SufA, SufB and Nfu proteins as potential scaffold proteins (Balk & Lobreaux, 2005; Ye et al, 2006b;

Layer et al, 2007). In this work, we present evidence in support of a role for chloroplastic monothiol glutaredoxins in the assembly or transfer of Fe-S clusters in plants.

Glutaredoxins (Grxs) are small ubiquitous oxidoreductases that normally function in the reduction of disulfide bridges or glutathionylated proteins. However, recent studies in *Saccharomyces cerevisiae* and *Escherichia coli* have indicated specific roles for some glutaredoxins in facilitating Fe-S cluster biosynthesis (Rodriguez-Manzaneque et al, 1999, 2002; Mulhenhoff et al, 2003; Achebach et al, 2004). Yeast mutant cells deleted for the *grx5* gene were found to be more sensitive to oxidative stress, to accumulate free iron, and to have impaired mitochondrial Fe-S cluster biogenesis and respiratory growth (Rodriguez-Manzaneque et al, 1999, 2002). Other prokaryotic and eukaryotic monothiol Grxs with analogous CGFS active-site sequences have recently been shown to be efficient functional substitutes for yeast Grx5 (Molina-Navarro et al, 2006 ; Cheng et al, 2006). While the specific role of yeast Grx5 in Fe-S cluster biogenesis remains to be elucidated, ^{55}Fe radiolabelling studies of knockout mutants suggest that it likely facilitates the transfer of clusters preassembled on the Iscu1p scaffold protein into acceptor proteins (Mülhenhoff et al, 2003). Another hypothesis formulated from *in silico* analysis suggests that Grx5 may play a role in regulating the initial assembly of Fe-S cluster on scaffold proteins (Alves et al, 2004). The recent discovery that Grx5 is also required for vertebrate heme synthesis is also particularly interesting, since it raises the possibility that Grx5 is a key determinant for channeling Fe into heme and Fe-S cluster biosynthesis in mammals (Wingert et al, 2005). In *E. coli*, some Grxs have been shown to increase the incorporation of a [4Fe-4S] cluster into the oxygen sensor fumarate nitrate reductase regulator, presumably by reducing disulfides involving cluster-ligating cysteines in the apoprotein (Achebach et al, 2004).

The most obvious role for Grxs in Fe-S cluster biogenesis lies in facilitating Fe-S cluster assembly or transfer by reducing disulfides on scaffold or apo forms of Fe-S proteins. However, the recent discovery that some Grxs can assembly Fe-S clusters suggests the possibility of alternative roles in Fe-S cluster assembly or transfer. Poplar Grx C1 (CGYC active site) and human Grx2 (CSYS active site) were recently shown to be holodimers with a subunit-bridging [2Fe-2S] cluster ligated by one active-site cysteine of each monomer and the cysteines of two external glutathione molecules (Feng et al, 2006; Johansson et al, 2006; Rouhier et al, 2007). The cluster-containing dimeric form of human Grx2 was proposed to function as a redox sensor for the activation of Grx2 in case of oxidative stress (Lillig et al, 2005). Although this is a viable hypothesis, mutagenesis studies on poplar Grx C1 indicate that incorporation of a [2Fe-2S] cluster is likely to be a general feature of plant Grxs possessing a glycine adjacent to the catalytic cysteine (Rouhier et al, 2007). Hence monothiol Grxs with CGFS active sites (such as yeast Grx5) might also have the capability to incorporate an Fe-S cluster. Moreover, the requirement of glutathione for the export of an Fe-S cluster (or a precursor thereof) from mitochondria to facilitate the assembly of cytosolic Fe-S proteins in *S. cerevisiae* (Lill & Mühlenhoff, 2005) provides further circumstantial evidence in support of a role for glutathione- and Grx-ligated [2Fe-2S] clusters in Fe-S biogenesis.

In higher plants, around 30 different Grx isoforms can be classified into three distinct subgroups depending on their active site sequences (Rouhier et al, 2004, 2006). The first class, which contains Grxs with C[P/G/S][Y/F][C/S] motifs other than CGFS, is homologous to the classical dithiol Grxs such as *Escherichia coli* Grx1 and 3, yeast Grx1 and 2 and mammalian Grx1 and 2. The second class has a strictly conserved CGFS active-site sequence and includes Grxs homologous to yeast Grx3, 4 and 5 or *E. coli* Grx4. Plants have generally four members in

this group (Grx S14 to Grx S17). The properties of proteins of the third class which is specific to higher plants and involves a CC[M/L][C/S] active site, are largely unknown. Little is currently known concerning the roles of Grxs in plant metabolism. Most documented functions of Grxs in plants are for subgroup I as part of the oxidative stress response, by directly reducing peroxides or dehydroascorbate, by reducing peroxiredoxins (Prx), a group of thiol-dependent peroxidases, and also by protecting thiol groups on other enzymes via glutathionylation/deglutathionylation mechanisms (Rouhier et al, 2004, 2006).

This study presents biochemical, spectroscopic and analytical evidence for the incorporation of [2Fe-2S] clusters in two plant chloroplast Grxs with CGFS active sites, Grx S14 and S16, and both *in vivo* and *in vitro* evidence for their involvement in the maturation of Fe-S proteins. The results strongly suggest that these proteins function either as scaffold proteins for *de novo* synthesis and transfer of Fe-S clusters or as Fe-S cluster delivery or storage proteins for mediating the transfer of Fe-S clusters from ISC or SUF scaffold proteins to acceptor proteins.

Materials and methods

Heterologous Expression and Purification of CGFS Grxs in E. coli: The open reading frames of poplar and A. thaliana Grx S14, S15 and S16 were amplified from poplar or A. thaliana leaf RT PCR product, and were cloned into the expression plasmid pET-3d between NcoI and BamHI restriction sites (underlined) using the primers presented in Table 3-1. The first 63 and 34 amino acids of poplar or Arabidopsis Grx S14 (At3g54900) and of poplar or Arabidopsis Grx S15 (At3g15660), which encode respectively the putative transit peptide sequences were excluded to express the mature form of the proteins. For poplar Grx S16, three different cleavage sites, removing 51 (S16a), 61 (S16b) and 84 (S16c) amino acids, have been

tested to obtain a soluble protein, while a fully soluble AtGrx S16 protein was obtained by removing the first 62 amino acids. In addition, for improved expression, an alanine was sometimes added just behind the initiator methionine. Mutated proteins in which cysteines were replaced by serines have been generated by PCR site-directed mutagenesis for poplar and Arabidopsis Grx S14 and for Grx S15 using two complementary primers described in Table 3-1. Although not exactly at the same position in the primary sequences, to facilitate understanding, the cysteine residues in all these proteins has been similarly numbered based on recombinant poplar Grx S14. The cysteine-to-serine mutants are thus called poplar or Arabidopsis Grx S14 C33S, C87S, C108S or C87/108S and Grx S15 C33S. Conversely, a serine to cysteine mutation was introduced in Grx S15 S87C.

The *E. coli* expression strain BL21(DE3), containing the helper plasmid pSBET, was transformed with each recombinant plasmid. LB cultures of 2 to 3 liters were grown at 37 °C and induced in exponential phase by adding 100 µM IPTG (isopropyl-β-D-thiogalactopyranoside). The bacteria were pelleted by centrifugation for 15 minutes at 5000 *g* and resuspended in buffer A (30 mM Tris HCl pH 8.0, 200 mM NaCl) in the presence or absence of 1 mM glutathione. The culture expressing all Grx S14 and Grx S16 constructions except poplar and *A. thaliana* Grx S14 C33S and poplar Grx S16b constructions exhibited a brown coloration, characteristic of the presence of an Fe-S cluster, while the culture expressing the three Grx S15 constructions exhibited normal coloration. Grx S14 and S15 from poplar and Arabidopsis were mostly soluble, with the poplar proteins precipitating between 0 and 40% ammonium sulfate saturation and the Arabidopsis proteins between 40 and 80%. Poplar Grx S16a and AtGrx S16 were produced as soluble proteins whereas poplar Grx S16b did not produce significant amounts of soluble protein and poplar Grx S16c was completely insoluble. Almost all of the coloration linked to the

holoproteins was lost during aerobic purification, irrespective of the presence of glutathione during the chromatography steps. After breaking the cells by sonication, aerobic purification of the apoproteins from the soluble fraction was carried out in three steps: (i) ammonium sulfate precipitation (two successive cuts between 40 and 80% saturation), (ii) exclusion size chromatography (ACA44, PALL BioSepra), and (iii) ion exchange (DEAE sepharose, Sigma) chromatography. This latter step cannot be realized in the presence of glutathione which strongly modifies the behaviour and separation of the proteins.

Anaerobic purification of poplar Grx S14 and AtGrx S16 was carried out under Ar in a Vacuum Atmospheres glove box at oxygen levels < 2 ppm. The cell pellet was resuspended in 100 mM Tris-HCl pH 8.0 with 1 mM glutathione (buffer B), sonicated and centrifuged at 39700 *g* for one hour at 4 ºC to remove the cell debris. The reddish-brown cell-free extract containing holo Grx S14 was subjected to 40% ammonium sulfate cut followed by centrifugation. The brown pellet was resolubilized in buffer B and loaded onto a 10 ml Phenyl Sepharose column (GE Healthcare). The protein was eluted with a 1.0-0.0 M $(NH_4)_2SO_4$ gradient using buffer B. The purest fractions, as judged by SDS-PAGE analysis, were pooled and $(NH_4)_2SO_4$ was removed by ultrafiltration dialysis using a YM10 membrane and buffer B.

Reconstitution of an Fe-S Cluster in Apo Poplar Grx S14: Reconstitution of poplar apo Grx S14, 0.4 mM in buffer B, was accomplished in the glove box under anaerobic conditions by incubating at room temperature for 150 min with 5 mM glutathione, 2 mM DTT, 12-fold excess of Fe(II) (ferrous ammonium sulfate), L-cysteine, and catalytic amounts of *E. coli* IscS (20 µM). Reagents in excess were removed by loading onto a High-Trap Q-Sepharose column (GE-Healthcare) and eluting with a 0 to 1.0 M NaCl gradient in buffer B. The holo protein eluted between 0.45-0.55 M NaCl and was desalted using ultrafiltration dialysis.

Yeast Plasmids and Strains: New *S. cerevisiae* plasmids employed in this work are described in Table 3-2. They are derived from pMM221 (Molina et al, 2004), which contains the *S. cerevisiae* mitochondrial targeting sequence of Grx5 plus a C-terminal 3HA/His_6 tag, under the control of the doxycycline-regulatory $tetO_2$ promoter. Oligonucleotides employed for PCR amplification of the Grx sequences from the *E. coli* expression plasmids were designed to allow in-frame cloning of the amplified sequences in pMM221. pMM54 (Rodriguez-Manzaneque et al, 2002) contains a yeast *GRX5-3HA* construction under its own promoter. *S. cerevisiae* strains are described in Table 3-3. Plasmids were linearized by *Cla*I digestion previous to chromosomal integration. Crosses between yeast strains, sporulation and tetrad analyses were carried out by standard genetic techniques.

Growth Conditions for S. cerevisiae Cells: *S. cerevisiae* cultures were grown as described in (Molina et al, 2004). Samples for further analyses were taken from cultures grown exponentially for at least ten generations at 30ºC. Sensitivity to oxidants was determined onto YPD plates containing the indicated concentration of the agent, by spotting 1:5 serial dilutions of exponential cultures and recording growth after 2 days of incubation at 30ºC.

Other Methods: Mitochondria were purified and subfractionated (Diekert et al, 2001) from exponential yeast cultures in YPLactate medium at 30 ºC. Aconitase and malate dehydrogenase were assayed as described in (Robinson et al, 1987), in extracts prepared (Molina-Navarro et al, 2006) from cells growing exponentially in YP Galactose medium.

In vivo Subcellular Localization by GFP fusions: Full-length open reading frames were cloned in 5' of the GFP sequence under the control of a double 35S promoter into the plasmid pCK S65C between *Nco*I and *BamH*I sites (underlined) (Menand et al, 1998) using the primers described in Table 3-1 (Grx S14 pCK for and rev, Grx S15 pCK for and rev, Grx S16 pCK for

and rev). *Nicotiana benthamiana* cells were transfected by bombardment of leaves with tungsten particles coated with plasmid DNA and images were obtained with a Zeiss LSM510 confocal microscope.

Analytical and Spectroscopic Methods: Protein concentrations were determined by the *DC* protein assay (Bio-Rad), using BSA as the standard. Iron concentrations were determined colorimetrically using bathophenanthroline under reducing conditions, after digestion of the protein in 0.8% $KMnO_4$/0.2 M HCl (Fish, 1988). Sample concentrations and extinction coefficients are based on protein monomer unless indicated otherwise. Samples for spectroscopic studies were prepared under Ar in a Vacuum Atmospheres glove box (O_2 < 2 ppm). UV-visible absorption and CD spectra were recorded at room temperature using a Shimadzu UV-3101PC spectrophotometer and Jasco J-715 spectropolarimeter, respectively. Resonance Raman spectra were recorded as previously described (Cosper et al, 2004), using an Instruments SA Ramanor U1000 spectrometer coupled with a Coherent Sabre argon ion laser, with 20 μL frozen droplets of 2-3 mM sample mounted on the cold finger of an Air Products Displex Model CSA-202E closed cycle refrigerator. Mössbauer spectra were recorded by using the previously described instrumentations (Ravi et al, 1994). The zero velocity of the spectra refers to the centroid of a room temperature spectrum of a metallic Fe foil. Analysis of the Mössbauer data was performed with the WMOSS program (Web Research).

Fe-S Cluster Transfer Experiments: Synechocystis ferredoxin for cluster transfer experiments was heterologously expressed in *E. coli* and purified according to published procedures (Glauser et al, 2004). Apo Fd was prepared by treating the holo protein with EDTA and potassium ferricyanide at room temperature under anaerobic conditions and removing excess reagents by ultrafiltration dialysis using a YM10 membrane and buffer B. The time course of

cluster transfer from [2Fe-2S] Grx S14 to apo Fd was monitored under anaerobic conditions in 1 cm cuvettes at 23°C using UV-visible CD spectroscopy. The reactions were carried out in buffer B and apo Fd was treated with 5 mM DTT in buffer B for 60 min prior to use in cluster transfer reactions. The zero-time point corresponds to the addition of apo Fd to yield a cluster transfer reaction mixture that was 1 mM in DTT. Changes in the CD spectra at 423 nm were used to assess the concentration of holo Fd formed as a function of time. The time course of holo-Fd formation was analyzed by fitting to second-order kinetics, based on the initial concentrations of Grx S14 [2Fe–2S] clusters and apo-Fd in the reaction mixture, using the Chemical Kinetics Simulator software package (IBM).

Results

The Plant CGFS containing Grx Subgroup: In silico analysis of glutaredoxins from different kingdoms reveals that four or five Grxs with CGFS active site are generally present in higher plants and in *Chlamydomonas reinhardtii*, while only three are present in *Saccharomyces cerevisiae*, two in most other fungi, in nematodes and in mammals, one in *Synechocystis* and most bacteria including *E. coli* (Lemaire, 2004; Rouhier et al, 2006). In *Populus trichocarpa*, Grx S14 and S15 are small proteins (171 and 172 amino acids, respectively, including the transit peptide sequence) with a single repeat of the Grx module. Grx S16 is larger (296 amino acids including the transit peptide sequence) with a N-terminal extension linked to the Grx module. Grx S17 is larger (492 amino acids) and displays a N-terminal Trx-like domain with a WCDAS active site followed by three successive Grx modules. A careful examination of amino acid sequence alignments (Figure 3-10), indicates that although not present in all CGFS Grxs, a second cysteine is found at a conserved position in the C-terminus (Cys 87 in Grx S14 and Cys

221 in Grx S16, numbering based on the recombinant mature protein sequences). In plants, it is absent in Grx S15 and in some Grx domains of Grx S17. Analysis of the 250 sequences found in the Genbank database reveals that this second cysteine is present in 60% of sequences. In *S. cerevisiae* Grx5, these two cysteines are able to form a disulfide bridge in the presence of oxidized glutathione, but the physiological reductant of this disulfide is not known (Tamarit et al, 2003). The identity between Grxs of the same family for the three sequenced plant organisms ranges from 50 to 58%, from 46 to 54%, from 54 to 64%, and from 67 to 74%, respectively within plant Grx S14, Grx S15, Grx S16 and Grx S17 and from 18 to 38% between families.

Subcellular Localization of the CGFS Grxs: In order to gain additional information concerning the subcellular localization of the CGFS Grxs, we have determined the localisation of all the isoforms which possess an N-terminal transit sequence. Grx S17, predicted to be cytosolic, does not seem to possess such an extension and its localization has not been characterized further. The full-length sequences of the three other Grxs devoid of the stop codon were introduced in frame before the GFP sequence and the construction used to bombard tobacco leaves. As shown in Figure 3-1, the fluorescence of Grx S14 and S16 strictly coincides with the one of the chlorophyll, while the fluorescence of Grx S15 superimposed well with the one of the mitochondrial marker. Therefore Grx S14 and S16 are chloroplastic and Grx S15 is mitochondrial.

Some Poplar Monothiol but not Dithiol Glutaredoxins Rescue the Defects of a Yeast Mutant Lacking Grx5: It has been recently shown that different bacterial, animal and plant monothiol glutaredoxins are able to substitute for the Grx5 function in Fe-S cluster biosynthesis (Molina-Navarro et al, 2006 ; Wingert et al, 2005 ; Cheng et al, 2006). In order to determine whether the four poplar monothiol Grxs were able to rescue the defects of a *S. cerevisiae Δgrx5*

mutant, we cloned the respective open reading frame sequences deprived of their own transit sequences in the yeast vector pMM221 which allows compartmentalisation at the mitochondrial matrix (Molina et al, 2004). All the studied proteins were adequately compartmentalized in the mitochondrial matrix (Figure 3-2A). Of the two poplar Grxs with a single monothiol glutaredoxin domain, chloroplast Grx S14 and mitochondrion Grx S15, only the chloroplast one rescued the mutant *grx5* defects in respiratory growth (Figure 3-2B) and sensitivity to oxidants (Figure 3-2C). These defects were also efficiently rescued by Grx S16 and S17 which both have N-terminal extensions in their mature forms. To test whether a single glutaredoxin domain is sufficient for the function of Grx S17, we made a pMM221-based construction with the last domain of S17 (from aa 398 to 492) fused to the mitochondrial targeting sequence of Grx5 ($S17_{398\text{-}492}$). This protein was also compartmentalized at the mitochondrial matrix (Figure 3-2A), although a double band appeared corresponding to the matrix and intermembrane fractions. The one of lower mobility probably corresponds to unprocessed precursor. $S17_{398\text{-}492}$ suppressed partially the growth phenotypes of the *grx5* mutant, in particular growth in respiratory conditions (Figure 3-2C). The ratio of activities of the mitochondrial enzymes aconitase (containing Fe-S clusters) and malate dehydrogenase (without Fe-S clusters) provides a measure of the efficiency of the Fe-S cluster assembly in mitochondrial proteins (Molina et al, 2004). This ratio was measured in strains carrying all these constructions in a chromosomal *grx5* background (Figure 3-2D). Ratios were proximal to wild type in strains expressing the mitochondrial forms of S14, S16 and S17, in accordance with the growth phenotypes. In contrast, both S15 and the truncated form of S17 attained enzyme ratios about one fourth to one fifth of wild type cells (Figure 3-2D). For all the strains tested, absolute malate dehydrogenase levels were basically similar, and doxycycline addition to growth media lowered aconitase activity to basal levels (data not

shown). For the monothiol glutaredoxins analysed, there appears to be a correlation between efficiency to express active aconitase and growth phenotypes, except that poplar mitochondrial S15 does not rescue at all the growth defects of the yeast mutant, while still being able to synthesise low levels of mature aconitase. These observations may indicate that different functions directly or indirectly affected in the mutant lacking Grx5 may have different stringencies when partially substituted by heterologous glutaredoxins, as would be the case of S15 and $S17_{398-492}$. The same situation has already been observed with chicken Grx5 (Molina-Navarro et al, 2006).

In order to determine whether the capacity to bind an Fe-S cluster is sufficient for complementation, we have assessed the ability of poplar dithiol glutaredoxins Grx C1 (CGYC), Grx C1 G32P (CPYC) and Grx C4 (CPYC) to rescue the defects of a *S. cerevisiae Δgrx5* mutant. Grx C1 is able to incorporate a [2Fe-2S] centre, but not Grx C1 G32P and Grx C4 (Rouhier et al, 2007). Although all these Grx were targeted to the matrix compartment (Figure 3-3A), neither the C1 and C4 mitochondrial forms nor the G32P substitution derivative of C1 rescued the inability of a *grx5* mutant for respiratory growth on glycerol medium (Fig. 4-3B), which indicates the absence of a functional Fe-S cluster-containing Rieske protein in the yeast respiratory chain (Molina et al, 2004; Molina-Navarro et al, 2006). Also, the three strains expressing these three Grxs were as sensitive to oxidants such as *t*-BOOH or diamide as the *grx5* mutant (Figure 3-3C). In accordance with the above results, Grx C1, C1 G32P or C4 displayed similar malate dehydrogenase to aconitase enzyme ratios as the *grx5* mutant, which were much lower than in cells expressing wild type Grx5 (Figure 3-3D). Again, absolute malate dehydrogenase activity did not significantly vary from one genetic background to another (data not shown). Altogether, these results indicate that none of the three dithiol Grxs, even the one

binding a Fe-S cluster, is functional in yeast mitochondria for the maturation of Fe-S containing proteins. To determine whether this is caused by structural incompatibility of the dithiol glutaredoxins with the Fe-S cluster biosynthetic machinery or more specifically by the different active site sequences between dithiol and monothiol, we replaced the CGYC active site of Grx C1 into CGFS (Grx C1 Y33F/C34S mutant) to mimic the active site sequence of Grx5. The resulting Grx fully substituted for yeast Grx5 with respect to all the phenotypes analysed (Figure 3-3). These rescuing effects did not occur when expression of Grx C1 Y33F/C34S from the *tet* promoter was switched-off by doxycycline addition to the growth medium (data not shown). We therefore conclude that it is the requirement for a monothiol glutaredoxin active site which precludes poplar dithiol glutaredoxins for functionally rescuing a *grx5* mutant.

Heterologous Expression of plant CGFS glutaredoxins: The mature form of the three organellar poplar CGFS Grxs was expressed in *E. coli* to check their ability to incorporate Fe-S clusters. Based on our previous experience with Grx C1, glutathione, which was shown to stabilize and ligate the [2Fe-2S] cluster, was added during the first steps of an aerobic purification procedure (Rouhier et al, 2007). Although the presence of a brownish coloration typical of a Fe-S cluster prosthetic group was clearly evident in cells containing overexpressed poplar and *A. thaliana* (At) Grx S14 and S16, almost no holoprotein was obtained at the end of aerobic purification, even in the presence of reduced glutathione, suggesting that the cluster degrades quickly in air. In contrast, there was no indication of an Fe-S cluster prosthetic group in recombinant poplar or *A. thaliana* Grx S15.

Purification and Spectroscopic Characterization of Fe-S Cluster-containing Poplar Grx S14 and AtGrx S16: Purification of poplar Grx S14 inside a glove box under strictly anaerobic conditions was undertaken to address the type, stoichiometry and properties of the putative Fe-S

centre. The reddish-brown purified samples were >95% pure as judged by gel electrophoresis and contained 0.40 ± 0.05 cluster/monomer (average of 6 preparations). The UV-visible absorption and CD spectra of anaerobically purified poplar Grx S14 are shown in Figure 3-4 and are both characteristic of a $[2Fe\text{-}2S]^{2+}$ centre (Stephens et al, 1978; Dailey et al, 1994). On the basis of the theoretical and experimental ε_{280} values for the apo protein (9.9 $mM^{-1}cm^{-1}$), the ε_{280} and ε_{411} values for the $[2Fe\text{-}2S]^{2+}$ centre are estimated to be 3.9 and 4.4 $mM^{-1}cm^{-1}$, respectively, and the A_{411}/A_{280} was found to be 0.31 ± 0.04. In accord with the analytical data, these extinction coefficients are indicative of 0.4-0.5 $[2Fe\text{-}2S]^{2+}$ clusters per monomer. Hence the analytical, absorption and CD data are consistent with approximately one $[2Fe\text{-}2S]^{2+}$ per dimeric Grx S14. Anaerobically purified At Grx S16 contained an analogous $[2Fe\text{-}2S]^{2+}$ centre as judged by very similar UV-visible absorption and CD spectra, see Figure 3-4.

In vitro reconstitution of aerobically purified apo Grx S14 was attempted under strictly anaerobic conditions in the presence of 5 mM glutathione and 2mM DTT, using Fe(II), L-cysteine and catalytic amounts of *E. coli* IscS. After chromatographic removal of excess reagents, the resulting cluster-loaded form of Grx S14 was essentially identical to anaerobically purified [2Fe-2S] Grx S14, as judged by Fe analyses and UV-visible absorption and CD spectra (data not shown). Glutathione was required for successful reconstitution of a [2Fe-2S] cluster on Grx S14. Samples of apo Grx S14 reconstituted using the same procedure in a reaction mixture containing 2 mM DTT, but no glutathione, showed no evidence of the presence on a bound Fe-S cluster following repurification. Hence *in vitro* Fe-S cluster reconstitution studies confirm the potential of poplar Grx S14 to act as a scaffold for the assembly of [2Fe-2S] clusters in a cysteine desulphurase-mediated reaction and indicate that glutathione is required for cluster assembly.

Resonance Raman and Mössbauer studies of anaerobically purified poplar Grx S14 confirm the presence of a $[2Fe\text{-}2S]^{2+}$ centre and provide insight into the cluster ligation. Resonance Raman spectra obtained using 457- and 514-nm excitation reveal Fe-S stretching modes at 288, 332, 347, 365, 402, and 424 cm^{-1} (Figure 3-5). The vibrational frequencies are generally similar to those of structurally characterized [2Fe-2S] ferredoxins with complete cysteinyl cluster ligation and are readily assigned to vibrational modes of the $Fe_2S^b{}_2S^t{}_4$ unit (S^b = bridging S and S^t = terminal or cysteinyl) by direct analogy with published data (Han et al, 1989; Fu et al, 1992). Figure 3-6 compares the Mössbauer spectra of poplar Grx S14 with those of the all cysteinyl-ligated $[2Fe\text{-}2S]^{2+}$ cluster in poplar Grx C1 and the IscU $[2Fe\text{-}2S]^{2+}$ cluster which has one non-cysteinyl ligand (Agar et al, 2000). Each spectrum is indicative of a $S = 0$ $[2Fe\text{-}2S]^{2+}$ centre that results from antiferromagnetic coupling of two high-spin Fe(III) ions and is simulated as the sum of quadrupole doublets from each Fe site using the parameters listed in the figure legend. The similarity and values of the isomer shift (δ) and quadrupole splitting (ΔE_Q) parameters for each Fe site of the $[2Fe\text{-}2S]^{2+}$ clusters in Grx C1 and Grx S14 are consistent with approximately tetrahedral S ligation at each Fe site. Non-cysteinyl ligation is generally manifested by anomalous isomer shifts and quadrupole splittings for the unique Fe site which results in marked asymmetry in the observed spectrum, as is apparent in the spectrum of $[2Fe\text{-}2S]^{2+}$ centre in IscU (Agar et al, 2000). Hence the Mössbauer data indicate a $[2Fe\text{-}2S]^{2+}$ cluster as the sole Fe-containing prosthetic group in anaerobically purified poplar Grx S14, and the Mössbauer and resonance Raman data taken together provide support for complete cysteinyl ligation.

Cluster Ligation in Grx S14 and S16: The two structurally characterized $[2Fe\text{-}2S]^{2+}$ centres in dithiol Grxs, human Grx2 (CSYC active site) and poplar Grx C1 (CGYC active site)

have very similar absorption and CD spectra and have analogous coordination environments, involving the active-site cysteines of two Grxs and the cysteines of two glutathiones as determined by X-ray crystallography (Johansson et al, 2006 ; Rouhier et al, 2007). On the basis of UV-visible absorption and CD spectra shown in Figure 3-4, a distinct type of $[2Fe\text{-}2S]^{2+}$ centre is clearly present in the monothiol plant Grxs (Grx S14 and S16) investigated in this work. Marked differences in the excited-state electronic properties and ground-state vibrational properties of the $[2Fe\text{-}2S]^{2+}$ centres in poplar Grx C1 and Grx S14 are evident in comparing the UV-visible absorption/CD and resonance Raman spectra shown in Figures 3-4 and 3-5, respectively. Differences in the relative intensities of corresponding Raman bands reflect changes in excitation profiles resulting from perturbation of the excited state electronic structure. Nevertheless it is clear that corresponding Fe-S stretching frequencies are upshifted by 2-8 cm^{-1} in Grx S14 compared to Grx C1, suggesting stronger Fe-S bonds for both terminal and bridging S. This is consistent with the general increase in the energies of S→Fe(III) charge transfer bands which suggests greater covalency in the Fe-S bonds for the $[2Fe\text{-}2S]^{2+}$ centre in Grx S14. The observed differences in vibrational and excited state electronic properties can be interpreted in terms of differences in the ligation and/or environment of the $[2Fe\text{-}2S]^{2+}$ centres in monothiol and dithiol Grxs.

Since the spectroscopic properties of the $[2Fe\text{-}2S]^{2+}$ centers in monothiol Grxs indicate complete cysteinyl ligation, mutagenesis studies were undertaken to address the possibility that glutathione is replaced as a ligand by an intrinsic cysteine residue in Grx S14 and S16. Three cysteine residues are present in Grx S14 at positions 33, 87 and 108 (recombinant poplar Grx S14 numbering). The active site cysteine (Cys33) is conserved in all CGFS monothiol Grxs. Cys87 is present in all S14- and S16-type plant Grxs, but not in S15-type plant Grxs, while

Cys108 is even not conserved in all S14-type plant Grxs (see Figure 3-10). Hence in order to address the cluster ligation in Grx S14 and check whether the inability for Grx S15 to incorporate an Fe-S cluster is a consequence of the absence of the second conserved cysteine residue, single or double cysteine mutants both on poplar and AtGrx S14 and on poplar Grx S15 have been generated by site-directed mutagenesis. AtGrx S14 was used for these mutation studies because introducing these mutations in poplar Grx S14 led mostly to insoluble proteins. On the basis of the color of the cells and supernatant following sonication and centrifugation, it was clear that AtGrx S14 C33S was no longer able to incorporate the cluster, while AtGrx S14 C87S, AtGrx S14 C108S and AtGrx S14 C87/108S were still able to incorporate the cluster. Further confirmation that the second conserved cysteine residue is not a ligand came from the observation that poplar Grx S15 S87C was still unable to accommodate an Fe-S cluster. Taken together, the mutagenesis and spectroscopic data, coupled with the requirement for glutathione in cluster reconstitution experiments, strongly support similar cluster ligation in monothiol and dithiol Grxs (as typified by Grx S14 and Grx C1, respectively), involving the catalytic cysteines of two monomers and two external glutathione molecules. The structural origin of the differences in spectroscopic properties of the $[2Fe\text{-}2S]^{2+}$ clusters in monothiol and dithiol Grxs is therefore likely to result from differences in ligand arrangement or cluster environment.

In vitro Cluster Transfer from [2Fe-2S] Grx S14 to Apo Chloroplast Ferredoxin: The results presented above provide *in vitro* evidence in support of a role for monothiol Grxs as scaffolds for the assembly of [2Fe-2S] clusters. However, functional Fe-S cluster scaffold proteins need to be capable both of assembling clusters and transferring them to apo forms of physiologically relevant acceptor proteins. We have therefore investigated the ability of [2Fe-2S] Grx S14, which is localized in chloroplasts, to transfer its cluster to an apo form of *Synechocystis*

[2Fe-2S] ferredoxin, one of the most abundant and highly conserved of all chloroplastic Fe-S proteins.

Direct evidence for rapid and quantitative cluster transfer from [2Fe-2S] Grx S14 to apo Fd was provided by anaerobic CD studies as a function of time using a reaction mixture involving stoichiometric [2Fe-2S] Grx S14 and apo Fd (Figure 3-7). The marked difference in the CD spectra of $[2Fe\text{-}2S]^{2+}$ centres in Grx S14 and holo Fd in the reaction mixture facilitates direct monitoring of cluster transfer and assessment of the extent of intact cluster transfer via concomitant decrease and increase of the CD spectra of the cluster donor and acceptor, respectively. Comparison of the time course of CD changes in the reaction mixture (Figure 3-7A) with simulated data for 0-100% intact cluster transfer (Figure 3-7B) indicates quantitative cluster transfer from [2Fe-2S] Grx S14 to apo Fd that is 60% complete after 5 min and 100% complete after ~ 60 min. The agreement between the observed and simulated data is inconsistent with cluster degradation and reassembly on Fd and can only be explained by direct cluster transfer. Furthermore parallel CD studies of reconstitution of apo *Synechocystis* Fd with equivalent amounts of S^{2-} and Fe^{3+} or Fe^{2+} under identical conditions did not result in significant cluster assembly over a 60 min period (data not shown). Parallel studies using poplar [2Fe-2S] Grx C1 under identical conditions showed no indication of cluster transfer to apo *Synechocystis* Fd, indicating specificity in the ability of Grxs to transfer [2Fe-2S] clusters to acceptor proteins.

Quantitative assessment of the rate of cluster transfer as a function of [2Fe-2S] Grx S14 to apo Fd stoichiometry (0.22:1 to 1.5:1 based on cluster content of Grx S14) was obtained by continuous monitoring of the CD changes at 423 nm (Figure 3-8). Based on the initial concentrations of Grx S14 [2Fe-2S] clusters and apo Fd, the data in each case are well fit by second order kinetics with a rate constant of 20000 $M^{-1}min^{-1}$. To put this into context, the fastest

intact [2Fe-2S] cluster transfer reported so far is for HscA/HscB/ATP-mediated [2Fe-2S] cluster transfer from [2Fe-2S] IscU to apo-IscFdx, which had a second order rate constant of 800 $M^{-1}min^{-1}$ (Chandramouli & Johnson, 2006). Hence, the results demonstrate that [2Fe-2S] cluster transfer from [2Fe-2S] Grx S14 to apo Fd is quantitative and occurs at a rate that is 25× faster than *in vitro* cluster transfer studies using the IscU scaffold protein. On the basis of the *in vitro* experiments reported herein, we conclude that monothiol glutaredoxins with CGFS active sites have the potential to function as scaffold proteins for the assembly and delivery of [2Fe-2S] clusters.

Discussion

Involvement of Chloroplastic CGFS Grxs in Iron-Sulphur Cluster Assembly: Grxs with a CGFS active site constitute a recently described subgroup of the glutaredoxin family, whose functions are largely unknown at the present time. In mammals, PICOT, a bimodular Trx-Grx protein, is implicated in signal transduction via the negative regulation of a protein kinase C activity. In yeast, Grx5, a simple single module Grx, was originally identified as playing a central role in protecting against oxidative damage (Rodriguez Manzaneque et al, 1999). Subsequent more detailed investigations of the effects of *S. cerevisiae grx5* deletion refined the role to mitochondrial Fe-S cluster biogenesis (Rodriguez Manzaneque et al, 2002) and immunoprecipitation studies suggested that Grx5 facilitates transfer of clusters assembled on the Isu scaffold protein to acceptor proteins (Mulhenhoff et al, 2003). In contrast, the other two CGFS Grxs in yeast, Grx3 and Grx4, were found to be nuclear proteins mainly involved in the nuclear localization regulation of the transcriptional iron regulators Aft1 and Aft2 (Herrero & de la Torres-Ruiz, 2007).

In plants, the CGFS Grx subgroup is expanded to four members, but the only functional information stems from *in vivo* analysis of *A. thaliana* Grx S14 (aka AtGRXcp), which was shown to be a chloroplastic protein probably involved in the oxidative stress response (Cheng et al, 2006). In this work, the subcellular locations of each of the poplar CGFS Grxs were assessed and yeast Δ*grx5* complementation studies of mitochondrial-targeted forms were used to assess the possibility that plant CGFS Grxs are also involved in Fe-S cluster assembly. All the CGFS Grxs, except Grx S15, but not the dithiol Grxs (even Grx C1, which contains a [2Fe-2S] cluster as purified), were able to complement the defects of the *S. cerevisiae* Δ*grx5* mutant, although not always to a similar extent. These results were somewhat surprising because the two chloroplastic Grxs (Grx S14 and S16) are the most efficient proteins, while the mitochondrial Grx S15 is essentially not effective. In addition, the proteins involved in plant and yeast mitochondrial Fe-S cluster assembly belong to the ISC type of machinery, while plant chloroplasts contain essentially the SUF system. Nevertheless, it is evident that both Grx S14 and S16 have the ability to assume a role analogous to that of Grx5 in mitochondrial Fe-S cluster biosynthesis. Whether Grx S15 is involved in plant mitochondria Fe-S cluster assembly is still uncertain, but out of a total of 27 to 36 plant Grxs, only one or two other Grxs, displaying a CCMS active site, are predicted to be present in mitochondria and could fulfil an analogous role. As discussed below, a major difference between Grx S14 or Grx S16 and Grx S15 that could explain their different behaviour is the capacity of the two chloroplastic Grxs to incorporate an Fe-S cluster when expressed in *E. coli*.

Grx S14 and S16 as Fe-S Cluster Scaffold Proteins: The observation that both plant Grx S14 and S16 contain analogous $[2Fe\text{-}2S]^{2+}$ centres when heterologously expressed in *E. coli* raises the possibility of a role for monothiol CGFS-type Grxs as scaffolds for the assembly of

chloroplastic Fe-S clusters. Additional support for a scaffolding role comes from the ability to assemble spectroscopically identical clusters on apo Grx S14 in a cysteine desulphurase-mediated reaction in the presence of L-cysteine, Fe^{2+} ion and glutathione. Cysteine mutagenesis studies, analytical and spectroscopic data, and the requirement of glutathione to effect cluster assembly on apo Grx S14, indicate the presence of a subunit-bridging $[2Fe\text{-}2S]^{2+}$ cluster ligated by the first active site cysteine of two Grxs and the cysteines of two glutathione molecules. A similar ligation has been structurally established in the dithiol poplar Grx C1 (Rouhier et al, 2007). However, pronounced differences in the ground-state vibrational and excited-state electronic properties for the [2Fe-2S] centres in monothiol and dithiol plant Grxs, indicate differences in the cluster environment or the arrangement of coordinating cysteine residues that will require crystallographic studies of monothiol Grxs for complete structural elucidation.

A functional Fe-S cluster scaffold protein must also be effective in transferring clusters to physiologically relevant acceptor proteins. Hence the observation of rapid and stoichiometric cluster transfer from [2Fe-2S] Grx S14 to apo ferredoxin, the most abundant [2Fe-2S] cluster-containing soluble chloroplast protein, provides support for a role for monothiol CGFS Grxs as [2Fe-2S] cluster donors for maturation of chloroplast Fe-S proteins. Moreover, analogous cluster transfer experiments using the structurally characterized [2Fe-2S] cluster-bound dithiol Grx C1 failed to show any evidence of cluster transfer to apo ferredoxin. This indicates specificity in the cluster transfer process and further demonstrates structural difference in cluster environment for the subunit-bridging [2Fe-2S] centres in Grx S14 and C1. The proposed role for monothiol CGFS Grxs as Fe-S cluster scaffold proteins also provides a rationalization for the apparent disparity concerning the role of the second partly conserved cysteine residue in yeast Grx5 in *in vivo* and *in vitro* activity data. Mutagenesis results indicated that the second conserved cysteine

is required for *in vitro* deglutathionylation activity, but is not required for *in vivo* Fe-S cluster assembly activity or the assembly of a [2Fe-2S] cluster on Grx S14 (Belli et al, 2002).

Two pieces of evidence argue against a scaffolding role for monothiol CGFS Grxs in *de novo* Fe-S cluster assembly. First, gene disruptions of other known scaffold proteins (such as the Nfu proteins) or other components of the chloroplastic Fe-S assembly machinery are generally associated with a dwarf phenotype or abnormal development (Touraine et al, 2004; Yabe et al, 2004; Xu & Möller, 2006; Van Hoewyk et al, 2007). For example, in cyanobacteria, the deletion of SufA and/or IscA, but not Nfu, is possible without affecting Fe-S assembly leading to the proposal that these proteins are involved in iron homeostasis and stress response rather than scaffolds for *de novo* Fe-S cluster biosynthesis (Balasubramanian et al, 2006). In the case of Grx S14, the phenotype consists in a defect in early seedling growth under oxidative stress (Cheng et al, 2006) and is not as strong as that associated with *nfu* gene disruptions. Taking into account the large number of Fe-S proteins in the chloroplast, one possibility is that Grx S14 has specific target proteins whose function is not essential for plant development. Alternatively, the absence of Grx S14 may be compensated by other scaffold proteins in the loss-of-function mutant. Clearly, there is a pressing need to investigate the phenotypes of gene disruptions resulting in depletion of other chloroplast proteins, both individually and together, e.g. Grx S16, Grx S14/Grx S16, SufA/Grx S14, and SufA/Grx S16. Second, the role of Grx5 in yeast mitochondrial Fe-S cluster biogenesis does not appear to be dependent on glutathione which is required for the assembly of a [2Fe-2S] cluster on Grx S14. Depletion of glutathione was found to affect the maturation of cytosolic Fe-S proteins, but had no significant effect on mitochondrial Fe-S cluster biogenesis (Sipos et al, 2002). However, it should be emphasized that there is currently no

information on the type of cluster or the requirements for cluster assembly on Grx5, or the level of glutathione that is required to support mitochondrial Fe-S cluster assembly.

Alternative Functions for Monothiol CGFS Grxs: The ability of monothiol CGFS Grxs to accommodate [2Fe-2S] clusters and transfer them to acceptor proteins is also consistent with a role in storage of preformed Fe-S clusters or as Fe-S cluster delivery systems that mediate cluster transfer from other potential scaffold proteins (i.e. SufA, SufB, and Nfu in chloroplasts and Isa/IscA, Nfu, and Isu in mitochondria) to specific acceptor proteins. Such a role is consistent with yeast Δ*grx5* immunoprecipitation studies which suggested that Grx5 facilitates transfer of clusters assembled on the Isu scaffold protein to acceptor proteins (Mulhenhoff et al, 2003). This would also explain why a strong phenotype may not be associated with gene disruption, because the transfer would still occur although at a lower rate. In addition, yeast two-hybrid studies indicate an *in vivo* interaction between Grx5 and Isa1 (Vilella et al, 2004) and the crystal structure of an IscA protein with an asymmetrical subunit-bridging [2Fe-2S] cluster has recently been published (Morimoto et al, 2006). Hence it is possible that IscA/SufA-type proteins hand off clusters to monothiol Grxs for delivery to acceptor proteins and that this cluster assembly pathway would only be completely shut down by deletion of both genes. *In vitro* cluster transfer experiments involving chloroplast [2Fe-2S] SufA and [2Fe-2S] Nfu proteins and apo Grx S14 and kinetic studies of the effect on apo Grx S14 on the rates of cluster transfer from chloroplast [2Fe-2S] SufA and [2Fe-2S] Nfu to apo ferredoxin are in progress to test this hypothesis.

Acknowledgements

This research was supported by grants from the National Institutes of Health (GM62524 to M.K.J and GM47295 to B.H.H) and grants BFU2004-03167 and 2005SGR00677 to E.H..

Financing from the ANR programs (GNP05010G and JC07_204825) to N.R., F.G., J.P.J. is acknowledged.

References

Abdel-Ghany SE, Ye H, Garifullina GF, Zhang L, Pilon-Smits EA, Pilon M (2005) Ironsulfur cluster biogenesis in chloroplasts. Involvement of the scaffold protein CpIscA. *Plant Physiol* **138**: 161-172

Achebach S, Tran QH, Vlamis-Gardikas A, Mullner M, Holmgren A, Unden G (2004) Stimulation of Fe-S cluster insertion into apoFNR by *Escherichia coli* glutaredoxins 1, 2 and 3 *in vitro*. *FEBS Lett* **565**: 203-206

Agar JN, Krebs B, Frazzon J, Huynh BH, Dean DR, Johnson MK (2000) IscU as a scaffold for iron-sulfur cluster biosynthesis: Sequential assembly of [2Fe-2S] and [4Fe-4S] clusters in IscU, *Biochemistry* **39**: 7856-7862.

Alves R, Herrero E, Sorribas A (2004) Predictive reconstruction of the mitochondrial ironsulfur cluster assembly metabolism. II. Role of glutaredoxin Grx5. *Proteins* **57**: 481-492.

Balasubramanian R, Shen G, Bryant DA, Golbeck JH (2006) Regulatory roles for IscA and SufA in iron homeostasis and redox stress responses in the cyanobacterium *Synechococcus* sp. strain PCC 7002. *J Bacteriol* **88**:3182-3191

Balk J, Lobreaux S (2005) Biogenesis of iron-sulfur proteins in plants. *Trends Plant Sci* **10**: 324-331

Beinert H, Holm RH, Munck E (1997) Iron-sulfur clusters: nature's modular, multipurpose structures. *Science* **277**: 653-659

Belli G, Polaina J, Tamarit J, De La Torre MA, Rodriguez-Manzaneque MT, Ros J, Herrero E (2002) Structure-function analysis of yeast Grx5 monothiol glutaredoxin defines essential amino acids for the function of the protein. *J Biol Chem* **277**: 37590-37596

Chandramouli K., Johnson MK (2006) HscA and HscB stimulate [2Fe-2S] cluster transfer from IscU to apoferredoxin in an ATP-dependent reaction. *Biochemistry* **45**: 11087-11095

Chandramouli K, Unciuleac M-C, Naik S, Dean DR, Huynh BH, Johnson MK (2007) Formation and properties of [4Fe-4S] clusters on the IscU scaffold protein. *Biochemistry* **46**, 6804-6811

Cheng NH, Liu JZ, Brock A, Nelson RS, Hirschi KD (2006) AtGRXcp, an Arabidopsis chloroplastic glutaredoxin, is critical for protection against protein oxidative damage. *J Biol Chem* **281**: 26280-26288

Cosper MM, Krebs C, Hernandez H, Jameson GNL, Eidsness MK, Huynh BH, Johnson MK (2004) Characterization of the cofactor content of *Escherichia coli* biotin synthase. *Biochemistry* **43**: 2007-2021

Dailey HA, Finnegan MG, Johnson MK (1994) Human ferrochelatase is an iron-sulfur protein. *Biochemistry* **33**: 403-407

Diekert K, de Kroon AIPM, Kispal G, Lill R (2001) Isolation and subfractionation of mitochondria from the yeast *Saccharomyces cerevisiae*. *Methods Cell Biol* **65**: 37-51

Feng Y, Zhong N, Rouhier N, Hase T, Kusunoki M, Jacquot JP, Jin C, Xia B (2006) Structural insight into poplar glutaredoxin C1 with a bridging iron-sulfur cluster at the active site. *Biochemistry* **45**: 7998-8008

Fernandes AP, Fladvad M, Berndt C, Andresen C, Lillig CH, Neubauer P, Sunnerhagen M, Holmgren A, Vlamis-Gardikas A (2005) A novel monothiol glutaredoxin (Grx4) from *Escherichia coli* can serve as a substrate for thioredoxin reductase. *J Biol Chem* **280**: 24544-24552

Fish WW (1988) Rapid colorimetric micromethod for the quantitation of complexed iron in biological samples. *Meth Enzymol* **158**: 357-364

Fladvad M, Bellanda M, Fernandes AP, Mammi S, Vlamis-Gardikas A, Holmgren A, Sunnerhagen M (2005) Molecular mapping of functionalities in the solution structure of reduced Grx4, a monothiol glutaredoxin from *Escherichia coli*. *J Biol Chem* **280**: 24553-24561

Fu W, Drozdzewski PM, Davies MD, Sligar SG, Johnson MK (1992) Resonance Raman and magnetic circular dichroism studies of reduced [2Fe-2S] proteins. *J Biol Chem* **267**: 15502-15510

Glauser DA, Bourquin F, Manieri W, Schürmann P (2004) Characterization of ferredoxin:thioredoxin reductase modified by site-directed mutagenesis. *J Biol Chem* **279**: 16662-16669

Han S, Czernuszewicz RS, Kimura T, Adams MWW, Spiro TG (1989) Fe_2S_2 protein resonance Raman revisited: Structural variations among adrenodoxin, ferredoxin, and red paramagnetic protein. *J Am Chem Soc* **111**: 3505-3511

Herrero E, de la Torre-Ruiz MA (2007) Monothiol glutaredoxins: a common domain for multiple functions. *Cell Mol Life Sci* **64**: 1518-1530

Johansson C, Kavanagh KL, Gileadi O, Oppermann U (2007) Reversible sequestration of active site cysteines in a 2Fe-2S-bridged dimer provides a mechanism for glutaredoxin 2 regulation in human mitochondria. *J Biol Chem* **282**: 3077-3082

Johnson DC, Dean DR, Smith AD, Johnson MK (2005) Structure, function, and formation of biological iron-sulfur clusters. *Annu Rev Biochem* **74**: 247-81

Johnson MK, Smith AD (2005) Iron-sulfur proteins. In *Encyclopedia of Inorganic Chemistry, Second Edition* (King RB, ed.) pp 2589-2619. John Wiley & Sons, Chichester, UK

Layer G, Gaddam SA, Ayala-Castro CN, Ollagnier-de Choudens S, Lascoux D, Fontecave M, Outten FW (2007) SufE transfers sulfur from SufS to SufB for iron-sulfur cluster assembly. *J Biol Chem* **282**: 13342-1350

Lemaire SD (2004) The glutaredoxin family in oxygenic photosynthetic organisms. *Photosynth Res* **79**: 305-318

Leon S, Touraine B, Briat JF, Lobreaux S (2002) The AtNFS2 gene from *Arabidopsis thaliana* encodes a NifS-like plastidial cysteine desulfurase. *Biochem J* **366**: 557-564

Leon S, Touraine B, Ribot C, Briat JF, Lobreaux S (2003) Iron-sulphur cluster assembly in plants: distinct NFU proteins in mitochondria and plastids from *Arabidopsis thaliana*. *Biochem J* **371**: 823-830

Leon S, Touraine B, Briat JF, Lobreaux S (2005) Mitochondrial localization of *Arabidopsis thaliana* Isu Fe-S scaffold proteins. *FEBS Lett* **579**: 1930-1934

Lill R, Muhlenhoff U (2005) Iron-sulfur-protein biogenesis in eukaryotes. *Trends Biochem Sci* **30**: 133-141

Lillig CH, Berndt C, Vergnolle O, Lonn ME, Hudemann C, Bill E, Holmgren A (2005) Characterization of human glutaredoxin 2 as iron-sulfur protein: a possible role as redox sensor. *Proc Natl Acad Sci USA* **102**: 8168-8173

Menand B, Marechal-Drouard L, Sakamoto W, Dietrich A, Wintz H (1998) A single gene of chloroplast origin codes for mitochondrial and chloroplastic methionyl-tRNA synthetase in *Arabidopsis thaliana*. *Proc Natl Acad Sci USA* **95**: 11014-11019

Molina MM, Bellí G, de la Torre MA, Rodríguez-Manzaneque MT, Herrero E (2004) Nuclear monothiol glutaredoxins of *Saccharomyces cerevisiae* can function as mitochondrial glutaredoxins. *J Biol Chem* **279**: 51923-51930

Molina-Navarro MM, Casas C, Piedrafita L, Bellí G, Herrero, E (2006) Prokaryotic and eukaryotic monothiol glutaredoxins are able to perform the functions of Grx5 in the biogenesis of Fe/S clusters in yeast mitochondria. *FEBS Lett* **580**: 2273-2280

Morimoto K, Yamashita E, Kondou Y, Lee SJ, Arisaka F, Tsukihara T, Nakai M. (2006) The asymmetric IscA homodimer with an exposed [2Fe-2S] cluster suggests the structural basis of the Fe-S cluster biosynthetic scaffold, *J. Mol. Biol.* **360**: 117-132

Muhlenhoff U, Gerber J, Richhardt N, Lill R (2003) Components involved in assembly and dislocation of iron-sulfur clusters on the scaffold protein Isu1p. *EMBO J* **22**: 4815-4825

Ojeda L, Keller G, Muhlenhoff U, Rutherford JC, Lill R, Winge DR (2006) Role of glutaredoxin-3 and glutaredoxin-4 in the iron regulation of the Aft1 transcriptional activator in *Saccharomyces cerevisiae*. *J Biol Chem* **281**: 17661-17669

Ravi N, Bollinger JM, Huynh BH, Edmondson DE, Stubbe J (1994) Mechanism of assembly of the tyrosyl radical-diiron(III) cofactor of *E. coli* ribonucleotide reductase. 1. Mössbauer characterization of the diferric radical precursor. *J Am Chem Soc* **116**: 8007-8014

Robinson JB Jr, Brent LG, Sumegi B, Srere PA (1987) An enzymatic approach to the study of the Krebs tricarboxylic acid cycle. In *Mitochondria: A Practical Approach* (Darley-Usmar WM, Rickwood D, Wilson MT, eds), pp 153-170. IRL Press, Oxford, UK

Rodríguez-Manzaneque MT, Ros J, Cabiscol E, Sorribas A, Herrero E (1999) Grx5 glutaredoxin plays a central role in protection against protein oxidative damage in *Saccharomyces cerevisiae*. *Mol Cell Biol* **19**: 8180-8190

Rodríguez-Manzaneque MT, Tamarit J, Bellí G, Ros J, Herrero E (2002) Grx5 is a mitochondrial glutaredoxin required for the activity of iron/sulfur clusters. *Mol Biol Cell* **13**: 1109-1121

Rouhier N, Gelhaye E, Jacquot JP (2004) Plant glutaredoxins: still mysterious reducing systems. *Cell Mol Life Sci* **61**: 1266-1277

Rouhier N, Couturier J, Jacquot JP (2006) Genome-wide analysis of plant glutaredoxin systems. *J Exp Bot* **57**: 1685-1696

Rouhier N, Unno H, Bandyopadhyay S, Masip L, Kim SK, Hirasawa M, Gualberto JM, Lattard V, Kusunoki M, Knaff DB, Georgiou G, Hase T, Johnson MK, Jacquot JP (2007) Functional, structural and spectroscopic characterization of a glutathione-ligated [2Fe.2S] cluster in poplar glutaredoxin C1. *Proc Natl Acad Sci USA* **104**: 7379-7384

Sipos K, Lange H, Fekete Z, Ullmann P, Lill R, Kispal G (2002) Maturation of cytosolic ironsulfur proteins requires glutathione. *J Biol Chem* **277**: 26944-26949

Stephens PJ, Thomson AJ, Dunn JBR, Keiderling TA, Rawlings J, Rao KK, Hall DO (1978) Circular dichroism and magnetic circular dichroism of iron-sulfur proteins. *Biochemistry* **17**: 4770-4778

Tamarit J, Bellí G, Cabiscol E, Herrero E, Ros J (2003) Biochemical characterization of yeast mitochondrial Grx5 monothiol glutaredoxin. *J Biol Chem* **278**: 25745-25751

Touraine B, Boutin JP, Marion-Poll A, Briat JF, Peltier G, Lobreaux S (2004) Nfu2: a scaffold protein required for [4Fe-4S] and ferredoxin iron-sulfur cluster assembly in Arabidopsis chloroplasts. *Plant J* **40**: 101-111

Van Hoewyk D, Abdel-Ghany SE, Cohu CM, Herbert SK, Kugrens P, Pilon M, Pilon-Smits EA (2007) Chloroplast iron-sulfur cluster protein maturation requires the essential cysteine desulfurase CpNifS. *Proc Natl Acad Sci USA* **104**: 5686-5691

Vilella F, Alves R, Rodríguez-Manzaneque MT, Bellí G, Swaminathan S, Sunnerhagen P, Herrero E (2004) Evolution and cellular function of monothiol glutaredoxins: involvement in iron-sulfur cluster assembly. *Comp Funct Genom* **5**: 328-341

Wingert RA, Galloway JL, Barut B, Foott H, Fraenkel P, Axe JL, Weber GJ, Dooley K (2005) Deficiency of glutaredoxin 5 reveals Fe-S clusters are required for vertebrate haem synthesis. *Nature* **436**: 1035-1039

Xu XM, Moller SG (2006) AtSufE is an essential activator of plastidic and mitochondrial desulfurases in *Arabidopsis*. *EMBO J* **25**: 900-909

Yabe T, Morimoto K, Kikuchi S, Nishio K, Terashima I, Nakai M (2004) The Arabidopsis chloroplastic NifU-like protein CnfU, which can act as an iron-sulfur cluster scaffold protein, is required for biogenesis of ferredoxin and photosystem I. *Plant Cell* **16**: 993-1007

Ye H, Abdel-Ghany SE, Anderson TD, Pilon-Smits EA, Pilon M (2006a) CpSufE activates the cysteine desulfurase CpNifS for chloroplastic Fe-S cluster formation. *J Biol Chem* **281**:8958-8969

Ye H, Pilon M, Pilon-Smits EA (2006b) CpNifS-dependent iron-sulfur cluster biogenesis in chloroplasts. *New Phytol* **171**: 285-292

Table 3-1: Primers used in this study for the production of recombinant proteins. For cloning primers, the restriction is underlined. All the primers were for amplification of poplar sequences except those labelled At or Sc, which served to amplify *A. thaliana* or *S. cerevisiae* sequences.

Grx S14 FOR	5'CCCCCCATGGCTTTGACTCCTGCGCTGAAG 3'
Grx S14 REV	5'CCCCGGATCCTCAAGAGCACATTGCCTT 3'
Grx S14 C33S FOR	5'AAGGACTTCCCTCAATCTGGATTTTCACAAACT 3'
Grx S14 C33S REV	5'AGTTTGTGAAAATCCAGATTGAGGGAAGTCCTT 3'
Grx S14 C87S FOR	5'GAATTCTTTGGTGGCTCTGATATCACTGTTGAG 3'
Grx S14 C87S REV	5'CTCAACAGTGATATCAGAGCCACCAAAGAATTC 3'
Grx S14 C108S REV	5' 5'CCCCGGATCCTCAAGAGGACATTGCCTTTTCCAC 3'
Grx S15 FOR	5'CCCCCCATGGCTTCTACCAACATTCCCAAT 3'
Grx S15 REV	5'CCCCGGATCCTTATTCGGACTCCTCTTT 3'
Grx S15 C33S FOR	5'CCTGACCTTCCTCAATCTGGATTTAGTGCTCTG 3'
Grx S15 C33S REV	5'CAGAGCACTAAATCCAGATTGAGGAAGGTCAGG 3'
Grx S15 S87C FOR	5'GAGTTTATTGGTGGCTGTGATATAATTATGAAT 3'
Grx S15 S87C REV	5'ATTCATAATTATATCACAGCCACCAATAAACTC 3'
Grx S16 FORa	5'CCCCCCATGGCTTTCAAAACCCTCTCA 3'
Grx S16 FORb	5'CCCCCCATGGCTCCGTCAGATTGTGGCGTTTAC 3'
Grx S16 FORc	5'CCCCCATGGCTTCTAAACCTCGCTCTTTAAGT 3'
Grx S16 REV	5' CCCCGGATCCTTATTTTTTGAAGTGACCGGCGAG 3'
Grx S14 PCK FOR	5' CCCCCCATGGGTTCCCAGTCATTGCTT 3'
Grx S14 PCK REV	5'CCCCGGATCCGAGCACATTGCCTTTTCCAC 3'
Grx S15 PCK FOR	5' CCCCCCATGGCAAGGTTACTGTCG 3'
Grx S15 PCK REV	5'CCCCGGATCCTCGGACTCCTCTTTTCC 3'
Grx S16 PCK FOR	5' CCCCCCATGGCTACCATCACCATC3'
Grx S16 PCK REV	5'CCCCGGATCCTTTTTGAAGTGACCGGCGAG 3'
AtGrx S14 FOR	5'CCCCCCATGGCTTCGGCTCTTACGCCGCAA
AtGrx S14 REV	5'CCCCGGATCCTCAAGAGCACATAGCTTTCTC 3'
AtGrx S14 C33S FOR	5'AGAGACTTCCCGATGTCTGGATTCTCCAACACT 3'
AtGrx S14 C33S REV	5'AGTGTTGGAGAATCCAGACATCGGGAAGTCTCT 3'
AtGrx S14 C8S FOR	5'GAGTTTTTCGGTGGTTCTGATATTACTCTTGAG
AtGrx S14 C87S REV	5'CTCAAGAGTAATATCAGAACCACCGAAAAACTC
AtGrx S14 C108S REV	5'CCCCGGATCCTCAAGAGGACATAGCTTTCTCCAC 3'
AtGrx S15 FOR	5'CCCCCCATGGCTAGATTTTCCTCAACAGTGCCA 3'
AtGrx S15 REV	5'CCCCGGATCCTCAATCTTGGTTTCCGGA 3'
AtGrx S16 FOR	5'CCCCCCATGGCTTCCGCCGTCAAATCTCTAACG 3'
AtGrx S16 REV	5'CCCCGGATCCCTAGTTCAAGATATTGGC 3'
ScGrx5 FOR	5'CCCCCCATGGCTTTGAGCACAGAGATAAGA 3'
ScGrx5 REV	5'CCCCGGATCCTCAACGATCTTTGGTTTC 3'

Table 3-2: New plasmids employed in this work

Plasmid	Characteristics
pMM628	Sequence coding from amino acid 2 to 117 of Grx C1 cloned between *Not*I-*Pst*I sites of pMM221
pMM630	Sequence coding from amino acid 2 to 117 of Grx C1(G32P) cloned between *Not*I-*Pst*I sites of pMM221
pMM632	Sequence coding from amino acid 2 to 113 of Grx C4 cloned between *Not*I-*Pst*I sites of pMM221
pMM634	Sequence coding from amino acid 37 to 174 of Grx S15 cloned between *Not*I-*Pst*I sites of pMM221
pMM657	Sequence coding from amino acid 66 to 173 of Grx S14 cloned between *Not*I-*Pst*I sites of pMM221
pMM676	Derivative of pMM628 with the sequence coding for CGFS instead of C31GYC in Grx C1
pMM712	Sequence coding from amino acid 85 to 296 of Grx S16 cloned between *Not*I-*Pst*I sites of pMM221
pMM713	Sequence coding from amino acid 1 to 492 of Grx S17 cloned between *Not*I-*Pme*I sites of pMM221
pMM714	Sequence coding from amino acid 398 to 492 of Grx S17 cloned between *Not*I-*Pme*I sites of pMM221

Table 3-3: Yeast strains employed in this work

Strain	Relevant phenotype	Comments
W303-1A	*MAT***a** *ura3-1 ade2-1 leu2-3,112 trp1-1 his3-11,15*	Wild type
W303-1B	As W303-1A but *MATα*	Wild type
MML100	*MAT***a** *grx5::kanMX4*	Ref. 2
MML240	*MAT***a** *grx5::kanMX4* [pMM54(*GRX5-3HA*)]::*LEU2*	Ref. 2
MML755	*MATα* [pMM628(*GRX C1-3HA*)]::*LEU2*	Integration of linear pMM628 in W303-1B
MML756	*MATα* [pMM630(*GRX C1*$_{G32P}$*-3HA*)]::*LEU2*	Integration of linear pMM630 in W303-1B
MML757	*MATα* [pMM632(*GRX C4-3HA*)]::*LEU2*	Integration of linear pMM632 in W303-1B
MML758	*MATα* [pMM634(*GRX S15-3HA*)]::*LEU2*	Integration of linear pMM634 in W303-1B
MML759	*MATα* [pMM657(*GRX S14-3HA*)]::*LEU2*	Integration of linear pMM657 in W303-1B
MML761	*MAT***a** *grx5::kanMX4* [pMM628(*GRX C1-3HA*)]::*LEU2*	Spore from a cross MML100 x MML755
MML763	*MAT***a** *grx5::kanMX4* [pMM630(*GRX C1*$_{G32P}$*-3HA*)]::*LEU2*	Spore from a cross MML100 x MML756
MML765	*MAT***a** *grx5::kanMX4* [pMM632(*GRX C4-3HA*)]::*LEU2*	Spore from a cross MML100 x MML757
MML767	*MAT***a** *grx5::kanMX4* [pMM634(*GRX S15-3HA*)]::*LEU2*	Spore from a cross MML100 x MML758
MML769	*MAT***a** *grx5::kanMX4* [pMM657(*GRX S14-3HA*)]::*LEU2*	Spore from a cross MML100 x MML759
MML779	*MATα* [pMM676(*GRX C1*$_{CGFS}$*-3HA*)]::*LEU2*	Integration of linear pMM676 in W303-1B
MML780	*MAT***a** *grx5::kanMX4* [pMM676(*GRX C1*$_{CGFS}$*-3HA*)]::*LEU2*	Spore from a cross MML100 x MML779
MML786	*MATα* [pMM712(*GRX S16-3HA*)]::*LEU2*	Integration of linear pMM712 in W303-1B
MML787	*MATα* [pMM713(*GRX S17-3HA*)]::*LEU2*	Integration of linear pMM713 in W303-1B
MML788	*MATα* [pMM714(*GRX S17*$_{398\text{-}492}$*-3HA*)]::*LEU2*	Integration of linear pMM714 in W303-1B
MML806	*MAT***a** *grx5::kanMX4* [pMM712(*GRX S16-3HA*)]::*LEU2*	Spore from a cross MML100 x MML786
MML808	*MAT***a** *grx5::kanMX4* [pMM713(*GRX S17-3HA*)]::*LEU2*	Spore from a cross MML100 x MML787
MML810	*MAT***a** *grx5::kanMX4* [pMM714(*GRX S17*$_{398\text{-}492}$*-3HA*)]::*LEU2*	Spore from a cross MML100 x MML788

Figure 3-1: Subcellular localization of CGFS Grxs by GFP fusion. The full-length sequences of Grx S14 (A), Grx S16 (B) and Grx S15 (C) were fused to the GFP and used to bombard tobacco cells. The pictures presented here are guard cells. From the left to the right: visible light, autofluorescence of chlorophyll (red) and mitochondrial marker (white); fluorescence of the constructions and merged images.

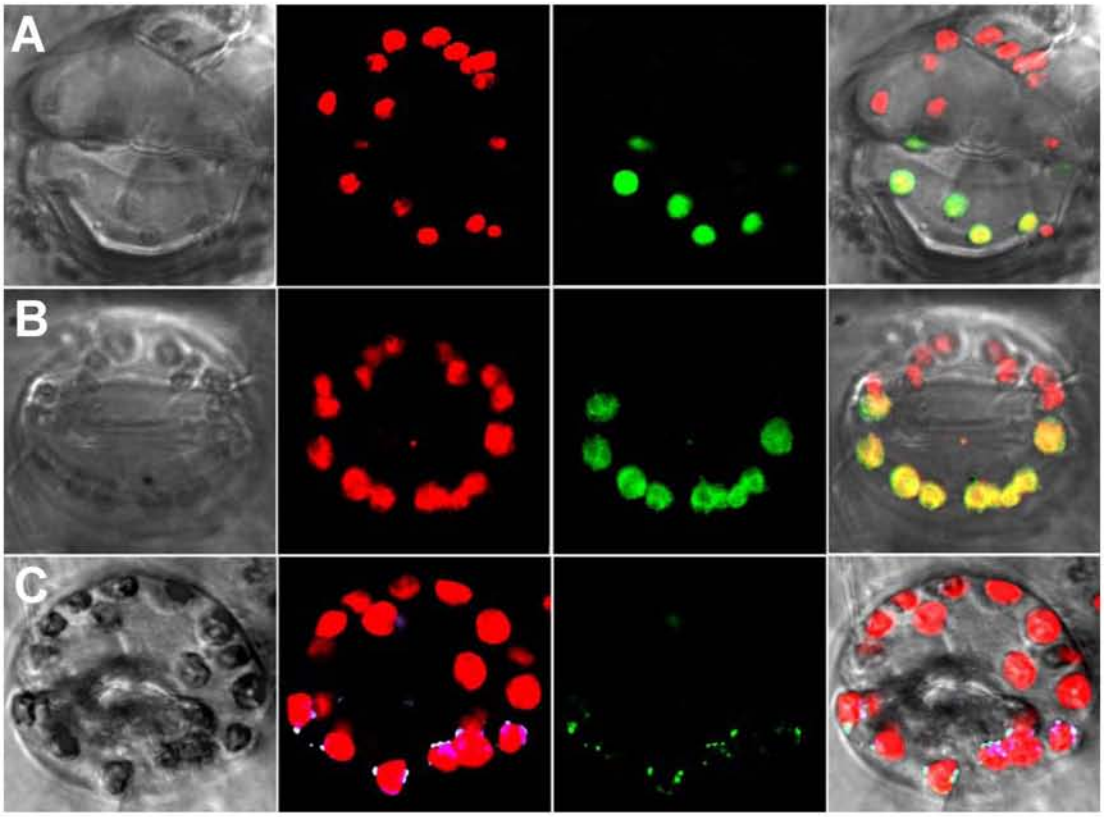
A
B
C

Figure 3-2: Rescue of the *S. cerevisiae grx5* mutant defects by mitochondrial forms of poplar monothiol glutaredoxins. (A) Derivatives of pMM221 are able to compartmentalise Grx S14 (pMM657, integrated in strain MML759), S15 (pMM634, strain MML758), S16 (pMM712, strain MML786), S17 (pMM713, strain MML787) and $S17_{398\text{-}492}$ (pMM714, strain MML788) in the mitochondrial matrix of *S. cerevisiae* cells. Cultures were grown exponentially in YPLactate medium at 30ºC to about 3 x 10^7 cells per ml, before mitochondrial isolation and subfractionation. TE, total cell extract; MT, mitochondrial fraction; IMS, intermembrane space; MX, matrix. Twenty micrograms of proteins were loaded in the TE lanes, and 5 µg were loaded in the other lanes. Anti-HA antibodies were used in the Western blot analyses to detect the HA-tagged proteins, and anti-lipoic acid antibodies were used to detect the matrix marker α-ketoglutarate dehydrogenase (α-KGDH). (B) Growth on glucose (YPD plates) or glycerol (YPGly plates), after 3 days at 30ºC, of chromosomal *grx5* strains expressing no mitochondrial (No Grx) or the mitochondrial forms of *S. cerevisiae* Grx5 ($Grx5_{Sc}$, MML240), S14 (MML769), S15 (MML767), S16 (MML806), S17 (MML808) or $S17_{398\text{-}492}$ (MML810). (C) Sensitivity to *t*-BOOH or diamide of the strains described in (B), after 3 days at 30ºC on YPD plates. (D) Ratio between aconitase and malate dehydrogenase activities in exponential cultures at 30ºC in YP Galactose medium. The same strains were employed as in (B). Values are normalized with respect to strain MML240 that expresses yeast Grx5 under its own promoter (unit value).

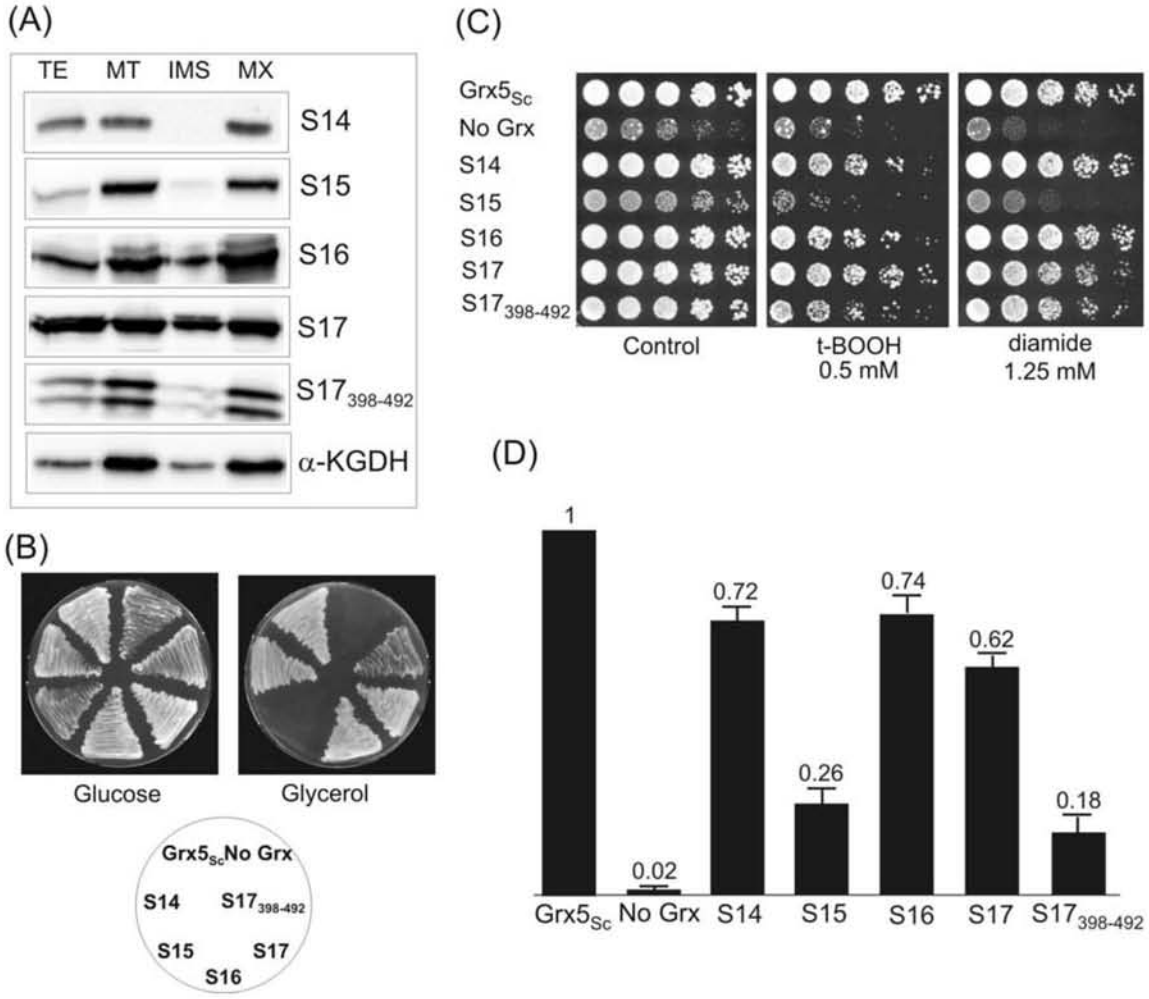
(A)
TE
MT
IMS
MX
S14
S15
S16
S17
S17 398-492
α-KGDH
(B)
Glucose
Glycerol
Grx5Sc
No Grx
S14
S17 398-492
S15
S17
S16
(C)
Grx5Sc
No Grx
S14
S15
S16
S17
S17 398-492
Control
t-BOOH 0.5 mM
diamide 1.25 mM
(D)
1
0.02
0.72
0.26
0.74
0.62
0.18
Grx5Sc
No Grx
S14
S15
S16
S17
S17 398-492

Figure 3-3: Rescue of the *S. cerevisiae grx5* mutant defects by mitochondrial forms of poplar dithiol glutaredoxins. (A) Derivatives of pMM221 are able to compartmentalise Grx C1 (pMM628, integrated in strain MML755), C1$_{G32P}$ (pMM630, strain MML756), C4 (pMM632, strain MML757) and C1$_{CGFS}$ (pMM676, strain MML779) in the mitochondrial matrix of *S. cerevisiae* cells. Growth conditions and western blot analyses are similar to those described in Figure 3-2. TE, total cell extract; MT, mitochondrial fraction; IMS, intermembrane space; MX, matrix. (B) Growth on glucose (YPD plates) or glycerol (YPGly plates), after 3 days at 30ºC, of chromosomal *grx5* strains expressing no mitochondrial (No Grx) or the mitochondrial forms of *S. cerevisiae* Grx5 (Grx5$_{Sc}$, MML240), C1 (MML761), C1$_{G32P}$ (MML763), C4 (MML765) or C1$_{CGFS}$ (MML780). (C) Sensitivity to *t*-BOOH or diamide of the strains described in (B), after 3 days at 30ºC on YPD plates. (D) Ratio between aconitase and malate dehydrogenase activities in exponential cultures at 30ºC in YPGalactose medium. The same strains were employed as in (B). Values are normalized with respect to strain MML240 that expresses yeast Grx5 under its own promoter (unit value).

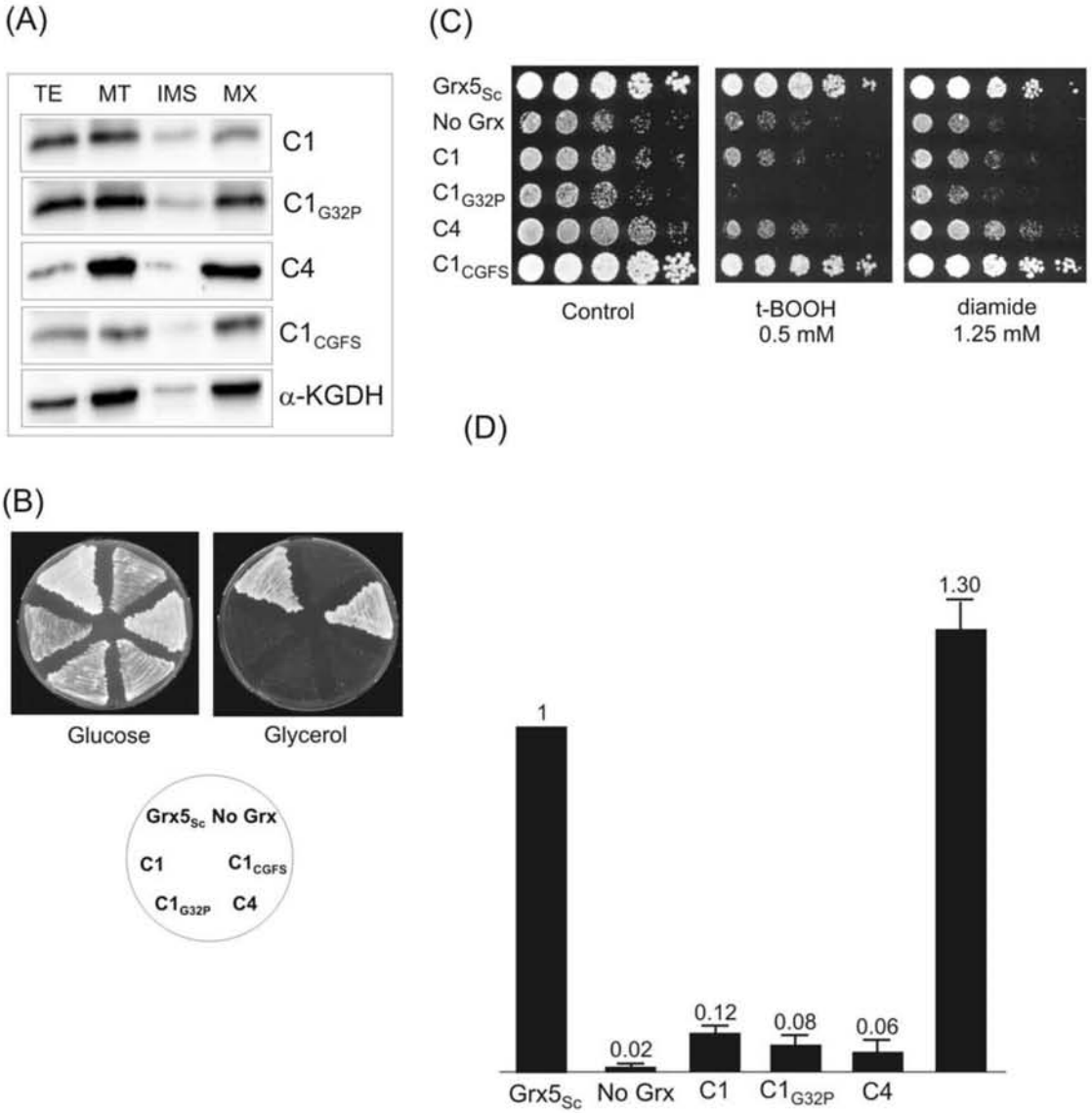
(A)
TE
MT
IMS
MX
C1
C1G32P
C4
C1CGFS
α-KGDH
(C)
Grx5Sc
No Grx
C1
C1G32P
C4
C1CGFS
Control
t-BOOH
0.5 mM
diamide
1.25 mM
(B)
Glucose
Glycerol
Grx5Sc
No Grx
C1
C1CGFS
C1G32P
C4
(D)
1
0.02
0.12
0.08
0.06
1.30
Grx5Sc
No Grx
C1
C1G32P
C4

Figure 3-4: Comparison of the UV-visible absorption and CD spectra of [2Fe-2S] cluster-bound forms of poplar Grx S14 (thick line), At Grx S16 (broken line) and poplar Grx C1 (thin line). Spectra were recorded under anaerobic conditions in 0.1 cm cuvettes using Grx samples (0.4 mM in monomer) in 100 mM Tris-HCl pH 8.0 with 1mM glutathione.

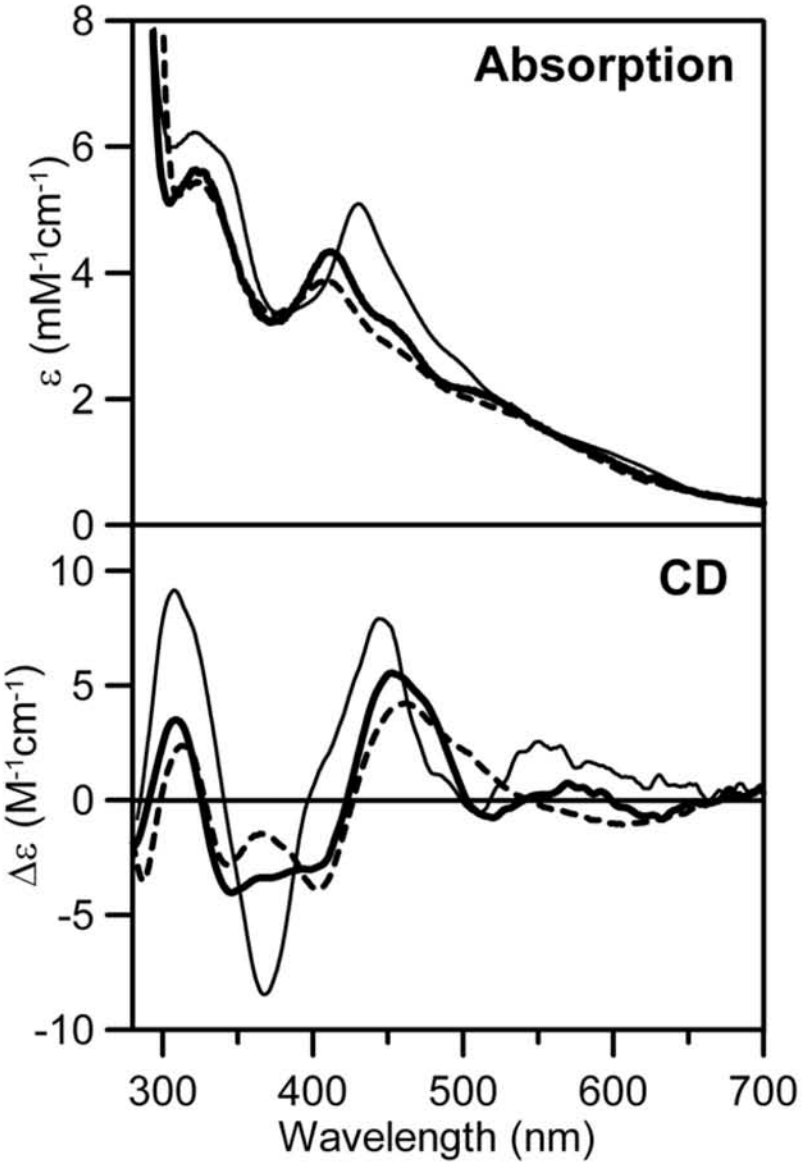
Absorption
CD
ε (mM-1cm-1)
Δε (M-1cm-1)
Wavelength (nm)
8
6
4
2
0
10
5
0
-5
-10
300
400
500
600
700

Figure 3-5: Comparison of the resonance Raman spectra of [2Fe-2S] cluster-bound forms of poplar Grx S14 (thick line) and Grx C1 (thin line) with 514- and 457-nm laser excitation. Samples were ~ 4 mM in Grx and were in the form of a frozen droplet at 17 K. Each spectrum is the sum of 100 scans, with each scan involving counting photons for 1 s each 0.5 cm^{-1} with 6 cm^{-1} spectral resolution. Lattice modes of ice have been subtracted.

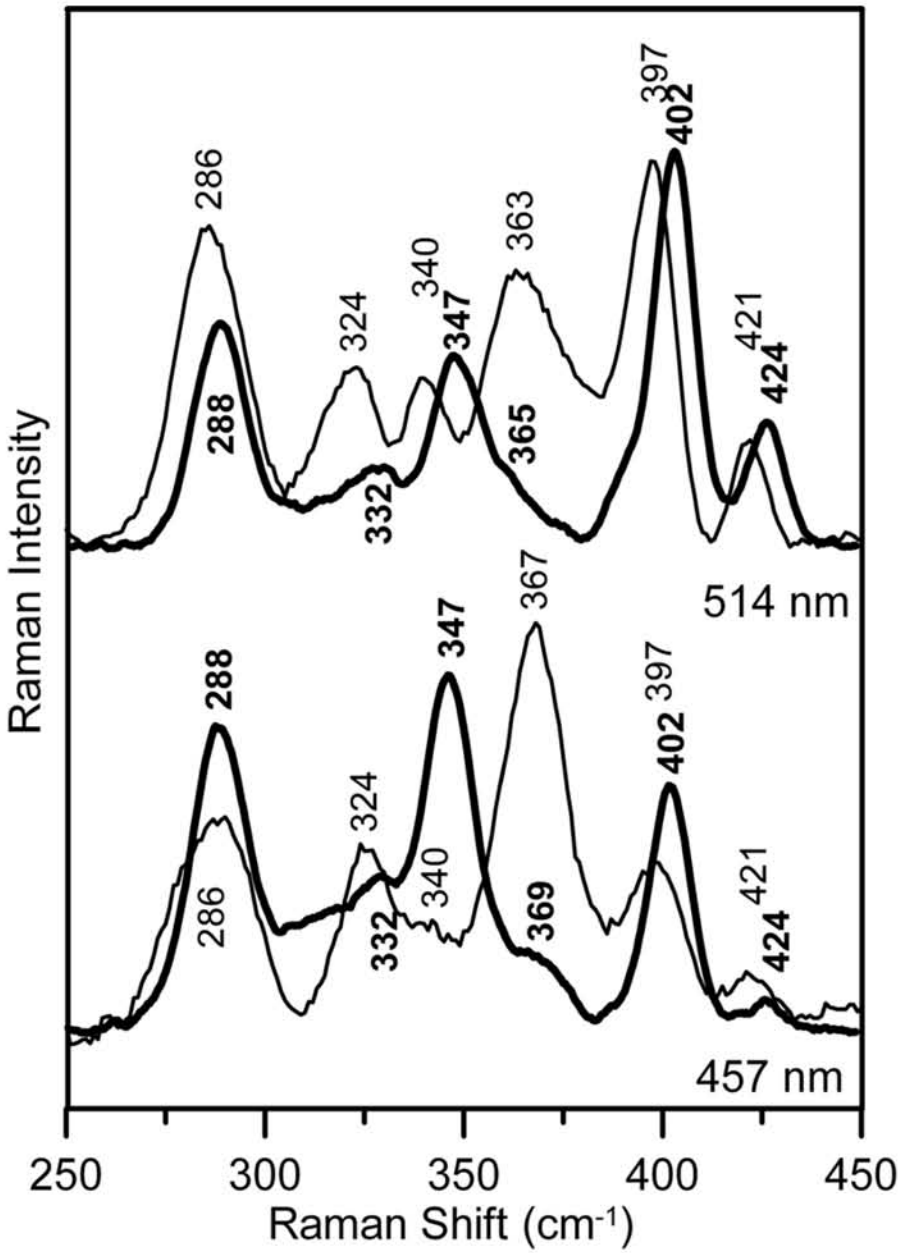
Raman Intensity
286
324
340
347
363
397
402
421
424
288
332
365
514 nm
288
347
367
397
402
324
286
332
340
369
421
424
457 nm
250
300
350
400
450
Raman Shift (cm-1)

Figure 3-6: Comparison of the Mössbauer spectra of [2Fe-2S] cluster-bound forms of poplar Grx S14 (blue), poplar Grx C1 (red), and *A. vinelandii* IscU (green). The Grx S14 and C1 Mössbauer samples were prepared by growing cells on ^{57}Fe-enriched media and the IscU sample was prepared by IscS-mediated reconstitution using 57Fe(II) (Agar et al, 2000). The Mössbauer spectra were recorded at 4.2 K with a magnetic field of 50 mT applied parallel to the γ-beam. Each spectrum is best simulated as the sum of two overlapping quadrupole doublets with the following parameters: ΔE_Q = 0.56 mm/s and δ = 0.26 mm/s for doublet 1 and ΔE_Q = 0.76 mm/s, δ = 0.28mm/s for doublet 2 of Grx S14; ΔE_Q = 0.54 mm/s and δ = 0.27 mm/s for doublet 1 and ΔE_Q = 0.76 mm/s, δ= 0.28 mm/s for doublet 2 of Grx C1; ΔE_Q = 0.66 mm/s and δ= 0.27 mm/s for doublet 1 and ΔE_Q = 0.94 mm/s, δ = 0.32 mm/s for doublet 2 of IscU.

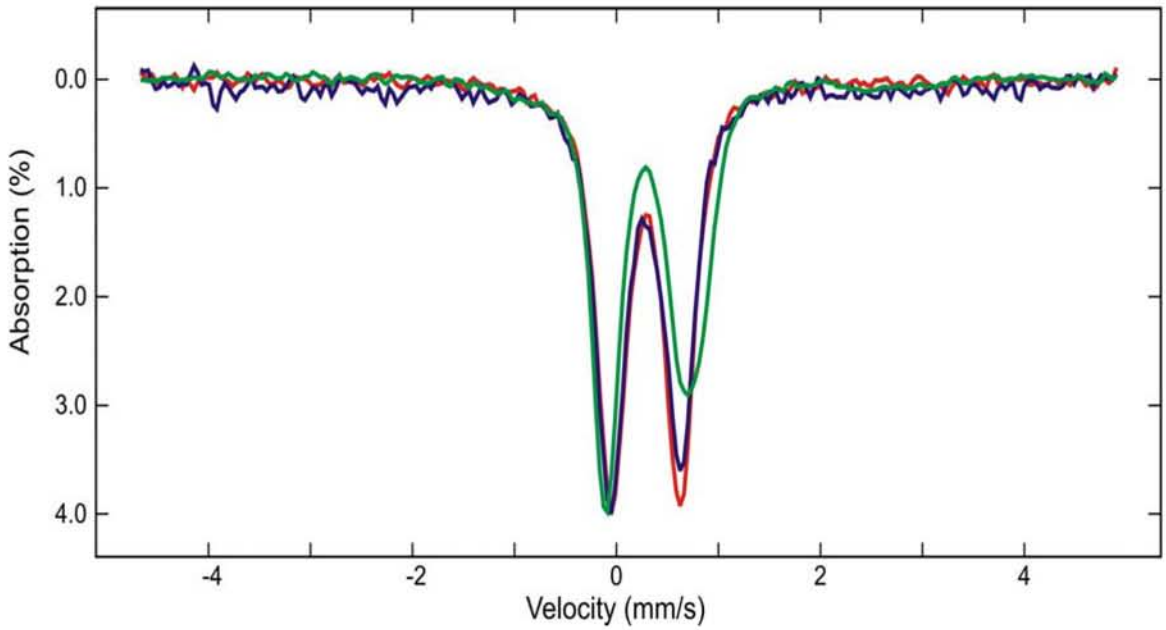
Absorption (%)
0.0
1.0
2.0
3.0
4.0
-4
-2
0
2
4
Velocity (mm/s)

Figure 3-7: Time course of cluster transfer from poplar Grx S14 to apo *Synechocystis* Fd monitored by UV-visible CD spectroscopy at 23°C in 1 cm cuvettes. (A) CD spectra recorded at 5 min intervals for a period of 60 min for a reaction mixture that was initially 15 μM in Grx S14 [2Fe-2S] clusters and 15 μM apo Fd. The spectrum at zero time (thick line) corresponds to [2Fe-2S] Grx S14 in the same reaction mixture in the absence of apo Fd. The arrows indicate the direction of intensity change with time at selected wavelengths. (B) Predicted changes in the CD spectra during quantitative cluster transfer. Thick lines correspond to holo forms of *Synechocystis* [2Fe-2S] Fd and [2Fe-2S] Grx S14 and thin lines correspond to simulated CD spectra corresponding to 10% to 90% [2Fe-2S] cluster transfer from Grx S14 to Fd in 10% increments. In both panels, $\Delta\varepsilon$ values are expressed per $[2Fe\text{-}2S]^{2+}$ cluster.

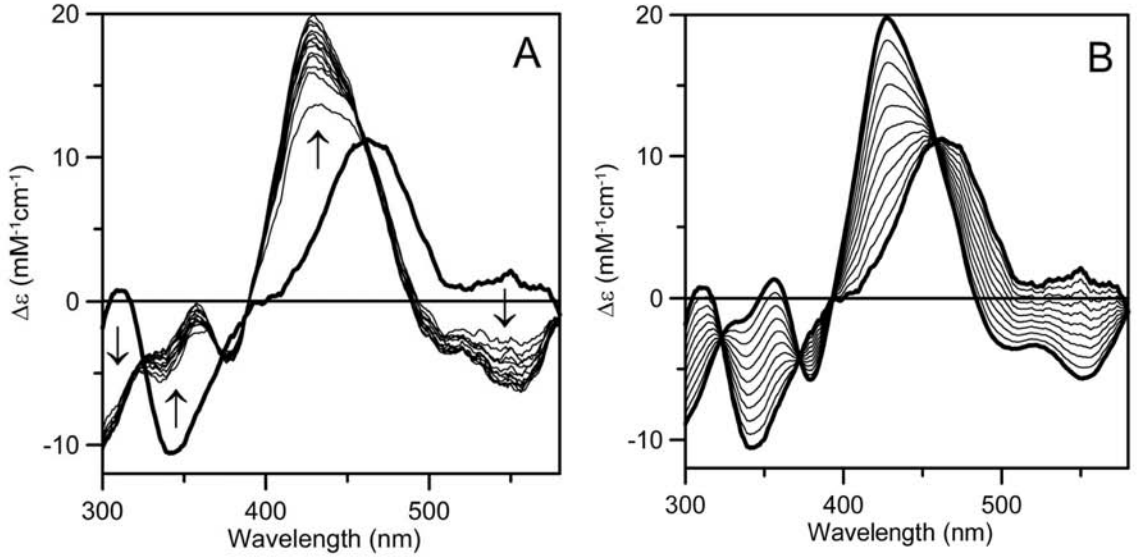
A
B
20
10
0
-10
300
400
500
Wavelength (nm)
Δε (mM-1cm-1)

Figure 3-8: Kinetics of cluster transfer from poplar Grx S14 to apo *Synechocystis* Fd at 23°C as a function of the stoichiometry of Grx S14 [2Fe-2S] clusters to apo Fd. The experimental conditions are as described in Figure 3-7, except that the concentration of Grx S14 [2Fe-2S] clusters was varied to give the indicated Grx S14 [2Fe-2S] to apo Fd ratios. Reactions were continuously monitored at 423 nm and converted to percent Fd reconstitution based on the simulated data shown in Figure 3-7. Solid lines correspond to second order kinetics with k = 20000 $M^{-1}min^{-1}$ based on the initial concentrations of Grx S14 [2Fe-2S] clusters and apo Fd.

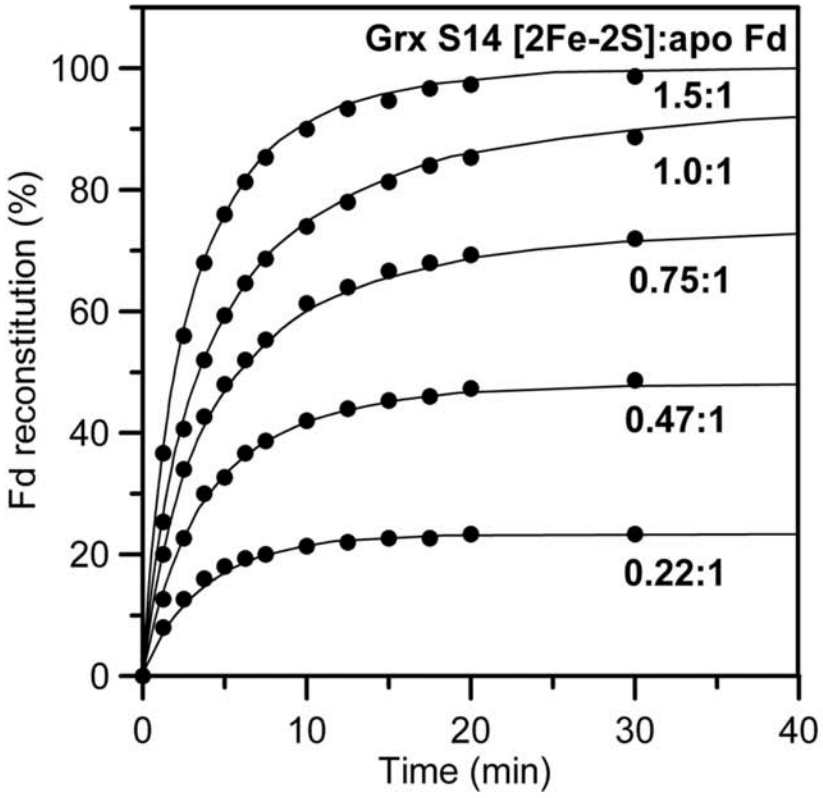
Grx S14 [2Fe-2S]:apo Fd
1.5:1
1.0:1
0.75:1
0.47:1
0.22:1
Fd reconstitution (%)
Time (min)
0
20
40
60
80
100
0
10
20
30
40

Figure 3-9: Working model for the potential roles of Grx S14 in the chloroplastic iron-sulphur assembly machinery. Grx S14 could function as a scaffold protein for *de novo* synthesis and transfer of Fe-S clusters, as a Fe-S cluster delivery protein for mediating the transfer of Fe-S clusters from other potential scaffold proteins (IscA, Nfu1, 2 and 3, and SufB) to acceptor proteins.

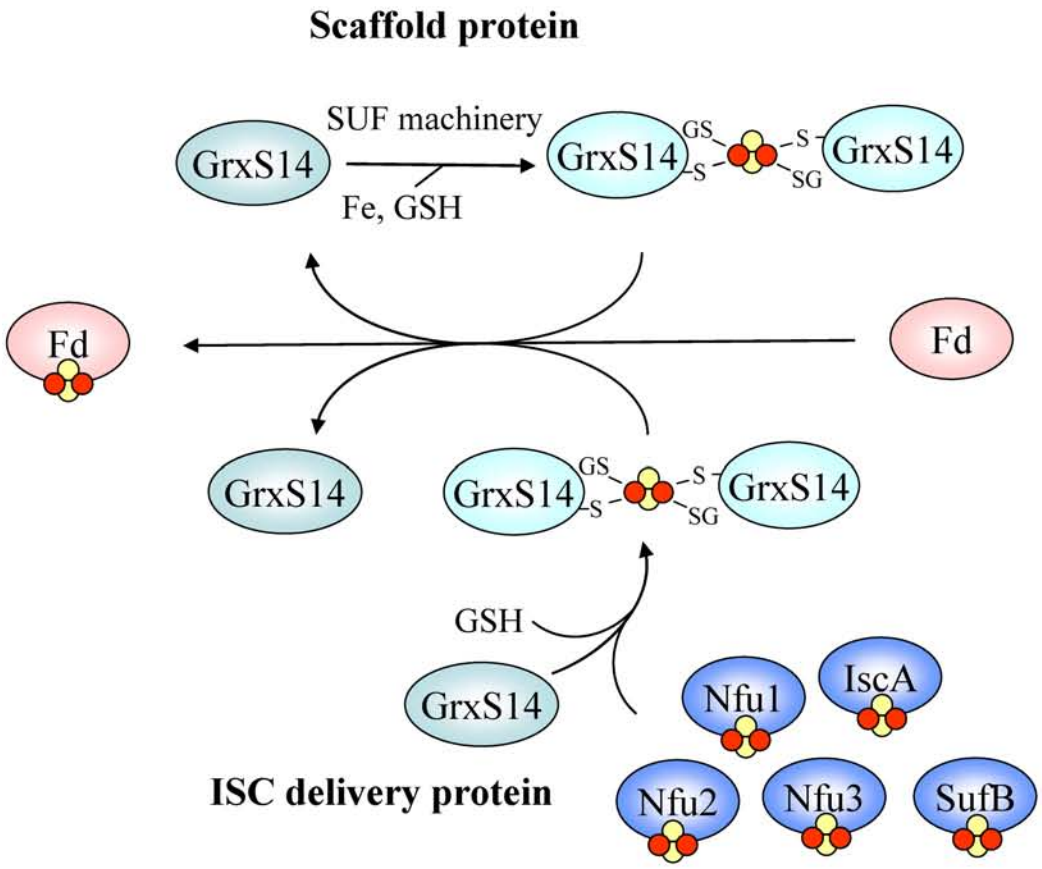
Scaffold protein
SUF machinery
GrxS14
Fe, GSH
GrxS14
GS
S
S
SG
GrxS14
Fd
Fd
GrxS14
GrxS14
GS
S
S
SG
GrxS14
GSH
GrxS14
Nfu1
IscA
Nfu2
Nfu3
SufB
ISC delivery protein

Figure 3-10: Amino acid sequence alignment of selected CGFS-containing Grxs from different kingdoms. The asterisks are showing totally or partially conserved cysteines in Grx S14. Accession numbers are as follows: PtGrx S14 : BU827308, PtGrx S15 : BU827149, PtGrx S16 : xx, AtGrx S14 : At3g54900, AtGrx S15 : At3g15660, AtGrx S16 : At2g38270, SynGrx3 (*Synechocystis s*p. PCC6308 (slr1846) : NP_440398, HsGrx5 (*Homo sapiens*): NP_057501, ScGrx3 (*S. cerevisiae*): NP_010383, ScGrx4 : NP_011101, ScGrx5 : NP_015266, EcGrx4 (*E. coli*): P0AC69.


PtGrxS14 --NKLASSIRCLTPALKTTLDKVVTSHKVVLFMKGTKDFPQCGFSQTVVQILKSLNVP--
AtGrxS14 KPTKFRCSASALTPQLKDTLEKLVNSEKVVLFMKGTRDFPMCGFSNTVVQILKNLNVP--
PtGrxS15 NNKAVNESGSCSGINIKELVDKDVKEHPIVIYMKGYPDLPQCGFSALAVRVLKQYNVP--
AtGrxS15 TQKVPPDS----TDSLKDIVENDVKDNPVMIYMKGVPESPQCGFSSLAVRVLQQYNVP--
PtGrxS16 DLRLTPGRHVQLTVPLEELIDRLVKENKVVAFIKGSRSAPMCGFSQKVVGILESEGVDYE
AtGrxS16 DIRLTPGRHVELTVPLEELIDRLVKESKVVAFIKGSRSAPQCGFSQRVVGILESQGVDYE
SynGrx3 1 ----------MNPETKARIDQLVTANKVMVFMKGTKLMPQCGFSNNVVQILNMLGIP--
HsGrx5 GPGVRAAGSGAGGGGSAEQLDALVKKDKVVVFLKGTPEQPQCGFSNAVVQILRLHGVRD-
EcGrx4 1 ----------MSTTIEKIQRQIAENPILLYMKGSPKLPSCGFSAQAVQALAACGER--
ScGrx4 DD-----EEDETEEEINARLVKLVQAAPVMLFMKGSPSEPKCGFSRQLVGILREHQIR--
ScGrx3 EDDDDEEEEEETEEQINARLTKLVNAAPVMLFMKGSPSEPKCGFSRQLVGILREHQVR--
ScGrx5 ----------EIRKAIEDAIESAPVVLFMKGTPEFPKCGFSRATIGLLGNQGVDPA
PtGrxS14 -FESVNILENELLRQGLKDYSSWPTFPQLYIDGEFFGGCDITVEAYKSGELQEQVEKAMC 169
AtGrxS14 -FEDVNILENEMLRQGLKEYSNWPTFPQLYIGGEFFGGCDITLEAFKTGELQEEVEKAMC 172
PtGrxS15 -ITARNILEYPDLRTGVKAYSNWPTFPQIFIKGEFIGGSDIIMNMHQTGELKEKLQDIAG 167
AtGrxS15 -ISSRNILEDQELKNAVKSFSHWPTFPQIFIKGEFIGGSDIILNMHKEGELEQKLKDVSG 166
AtGrxS16 TVDVLDDEYNHGLRETLKNYSNWPTFPQIFVKGELVGGCDILTSMYENGELANILN---- 293
PtGrxS16 SVDVLDEEYNYGLRETLKKYSNWPTFPQIFMNGELVGGCDILTSMHEKGELAGHFKK--- 296
SynGrx3 -FETLDVLADAEIRQGIKEYSNWPTIPQVYVNGEFVGGSDIMIELYQNGELQEMLEVALA 106
HsGrx5 -YAAYNVLDDPELRQGIKDYSNWPTIPQVYLNGEFVGGCDILLQMHQNGDLVEELKKLGI 143
EcGrx4 -FAYVDILQNPDIRAELPKYANWPTFPQLWVDGELVGGCDIVIEMYQRGELQQLIKETAA 105
ScGrx4 -FGFFDILRDENVRQSLKKFSDWPTFPQLYINGEFQGGLDIIKESIEEDPEYFQHALQ-- 244
ScGrx3 -FGFFDILRDESVRQNLKKFSEWPTFPQLYINGEFQGGLDIIKESLEEDPDFLQHALQS- 285
ScGrx5 KFAAYNVLEDPELREGIKEFSEWPTIPQLYVNKEFIGGCDVITSMARSGELADLLEEAQA 138
PtGrxS14 S---------- 170
AtGrxS14 S---------- 173
PtGrxS15 KEESE------- 172
AtGrxS15 NQD-------- 169
SynGrx3 S---------- 107
HsGrx5 HSALLDEKKDQDSK 157
EcGrx4 KYKSEEPDAE---- 115
ScGrx5 LVPEEEEETKDR-- 150

CHAPTER 4

CONCLUSIONS AND FUTURE WORK

The objectives of this research program were to investigate the role of NfuA proteins and monothiol/dithiol glutaredoxins in Fe-S cluster biogenesis using a combination of both *in vivo* and *in vitro* approaches. NfuA proteins constitute a new class of bacterial Nfu-type proteins that comprise of an N-terminal domain with homology to A-type scaffold proteins, but lacking the three conserved cysteine residues, and a C-terminal domain with homology to other Nfu proteins or domains. *A. vinelandii* NfuA was shown to assemble one subunit-bridging $[4Fe\text{-}4S]^{2+}$ cluster per homodimer that is ligated by the cysteine residues in the rigorously conserved thioredoxin-like CXXC motif of the Nfu domain, which can be rapidly and stoichiometrically transferred intact to activate apo aconitase (AcnA). Poplar dithiol and monothiol glutaredoxins, with CGYC and CGFS active sites, respectively, were shown to be able to assemble one subunit-bridging $[2Fe\text{-}2S]^{2+}$ cluster per homodimer using the first active-site cysteines of two glutaredoxins and two glutathiones. However, only the clusters assembled on monothiol glutaredoxins were able to be transferred intact to apo ferredoxin and this cluster transfer occurred at physiologically relevant rates in a stoichiometric reaction. The instability of the cluster assembled on dithiol glutaredoxins in the presence of oxidized glutathione, coupled with inability to transfer these clusters to acceptor apo proteins, argues against a role for dithiol glutaredoxins in Fe-S cluster biogenesis and in favor of a role in regulation of glutaredoxin disulfide reductase activity in response to oxidative stress (1;2) (see Appendix) However, the *in vitro* results clearly implicate roles for NfuA proteins and monothiol glutaredoxins as scaffold proteins for *de novo* synthesis or

storage/delivery of $[4Fe\text{-}4S]^{2+}$ and $[2Fe\text{-}2S]^{2+}$ clusters, respectively. As discussed below, *in vivo* data suggest that *de novo* assembly and storage/delivery of Fe-S clusters are not necessarily mutually exclusive roles for Nfu proteins and monothiol glutaredoxins. Rather the specific role may depend on the cellular location or environment.

In bacteria and mitochondria, which use the ISC machinery for general Fe-S cluster biogenesis, gene inactivation studies indicate that Nfu-type proteins have an important but non-essential role in Fe-S cluster biogenesis. For example, a strain of *A. vinelandii* inactivated for *nfuA* exhibits a substantially lower level of activity for AcnA and also results in a null growth phenotype when cultivated under elevated oxygen concentrations (see Chapter 2). Likewise, gene disruption studies of the *nfu1* gene in *S. cerevisiae* indicate impaired mitochondrial Fe-S cluster biosynthesis as evidenced by significant decreases in the activity of Fe-S cluster-containing respiratory enzymes, including AcnA (3). In contrast, gene deletions of the U-type scaffold proteins in *A. vinelandii* and *S. cerevisiae* are lethal (3;4) and depletion of IscU in *A. vinelandii* causes deficiency in the maturation of Fe-S proteins like aconitase (5), indicating an essential role for U-type scaffold proteins in Fe-S cluster biogenesis mediated by the ISC machinery. Hence U-type scaffold proteins rather than Nfu proteins are likely to function as the primary scaffold for *de novo* synthesis of Fe-S clusters by the ISC machinery. Although this work (Chapter 2) and studies of the human mitochondrial Nfu protein indicate that bacterial and mitochondrial Nfu proteins assemble $[4Fe\text{-}4S]^{2+}$ clusters, the *in vivo* results suggest that Nfu proteins function as intermediate cluster carriers for transferring $[4Fe\text{-}4S]^{2+}$ clusters assembled on U-type scaffolds by the ISC machinery to the apo forms of acceptor Fe-S proteins, see Figure 4-1.

The proposal that NfuA functions as an intermediate carrier of $[4Fe\text{-}4S]^{2+}$ clusters assembled on IscU is supported by *in vitro* cluster transfer experiments involving $[4Fe\text{-}4S]^{2+}$ cluster-bound forms of *A. vinelandii* NfuA and IscU and apo *A. vinelandii* AcnA (6) (see Chapter 2). $[4Fe\text{-}4S]^{2+}$ clusters assembled on IscU are capable of activating apo-AcnA, but the process is not stoichiometric and too slow to represent a true physiological process (6). Initial experiments on the effects of molecular chaperones HscA and HscB on the rate of cluster transfer from [4Fe-4S] IscU to apo-AcnA failed to demonstrate any significant rate enhancement (6;7), indicating that the molecular chaperones do not assist in the transfer of [4Fe-4S] clusters from IscU to apo AcnA. In contrast, $[4Fe\text{-}4S]^{2+}$ clusters preassembled on NfuA are much more effective in activating AcnA. The cluster transfer occurs with a 1:1 stoichiometry and at a rate 10x faster than that established with $[4Fe\text{-}4S]^{2+}$ clusters preassembled on IscU (see Chapter 2). In addition, preliminary experiments have demonstrated unidirectional $[4Fe\text{-}4S]^{2+}$ cluster transfer from IscU to NfuA (S. Bandyopadhyay and M. K Johnson, unpublished results). These *in vitro* results provide additional support for the role of NfuA as an intermediate Fe-S cluster carrier in ISC-mediated Fe-S cluster biogenesis, designed for rapid transfer of [4Fe-4S] cluster from the IscU scaffold protein to apo Fe-S proteins, and permit rationalization of the phenotype associated with *nfuA* gene inactivation, see Figure 4-1.

Cyanobacteria and plant chloroplasts do not have U-type scaffold proteins and the available *in vivo* and *in vitro* evidence indicates that they both use Nfu-type proteins as primary scaffold proteins for the *de novo* synthesis of $[2Fe\text{-}2S]^{2+}$ clusters (8-14). The $[2Fe\text{-}2S]^{2+}$ clusters are ligated by both cysteines of the CXXC motif at the subunit interface of the homodimer. The assembly of more O_2-tolerant $[2Fe\text{-}2S]^{2+}$ clusters rather than $[4Fe\text{-}4S]^{2+}$ clusters is likely to be a consequence of the higher O_2 levels in cyanobacterial cells and plant chloroplasts and is likely to

be related to lack of the N-terminal domain that is present only in bacterial and mitochondrial Nfu proteins and/or the presence of a C-terminal domain that is present only in plant chloroplast Nfu proteins, see Figure 4-2. While more *in vitro* and *in vivo* studies are clearly required, the available evidence indicates that bacterial and mitochondrial Nfu proteins are part of the ISC machinery and function in mediating transfer of $[4Fe\text{-}4S]^{2+}$ clusters from U-type scaffolds to acceptor Fe-S proteins (see Figure 4-1), whereas cyanobacterial and chloroplastic Nfu proteins function as scaffolds for the *de novo* synthesis of $[2Fe\text{-}2S]^{2+}$ clusters most likely as part of the SUF machinery.

Monothiol glutaredoxins (CGFS active sites) are widespread in prokaryotic and eukaryotic organisms and the research described in Chapter 3 provides the first experimental evidence for their ability to bind Fe-S clusters. Plant chloroplast monothiol glutaredoxins were shown to assemble glutathione-ligated and subunit bridging $[2Fe\text{-}2S]^{2+}$ clusters, and this result has provided new insight into the role of a specific yeast monothiol glutaredoxin, Grx5, in mitochondrial Fe-S cluster biogenesis. A role for Grx5 in mitochondrial Fe-S cluster assembly was first indicated by the observation that *Δgrx5* deletion mutants were more sensitive to oxidative stress, accumulate free iron, and have impaired mitochondrial Fe-S cluster biogenesis and respiratory growth (15;16). Moreover, this phenotype was reversed by over expression of established Fe-S cluster assembly proteins (16). Subsequently, immunoprecipitation studies of *Δgrx5* deletion mutants using radiolabeled ^{55}Fe indicated build up of Fe on the U-type scaffold proteins, suggesting Grx5 facilitates transfer of clusters from U-type scaffold proteins to apo Fe-S proteins (17). In view of the established role of glutaredoxins in mediating disulfide reduction, these results were initially interpreted in terms of Grx5 playing a role in preventing disulfide formation between cluster-ligating cysteine residues on apo Fe-S proteins. However, the ability

of two plant monothiol glutaredoxins, GrxS14 and GrxS16, which can each accommodate a $[2Fe\text{-}2S]^{2+}$ cluster, to rescue the defects associated with *grx5* gene deletion in yeast, raises the possibility of an alternative function as an intermediate cluster carrier or storage protein associated with the ISC machinery that accepts preformed $[2Fe\text{-}2S]^{2+}$ clusters from U-type scaffold proteins and delivers them to apo Fe-S proteins, see Figure 4-1. Support for this proposal comes from the observation of rapid and quantitative $[2Fe\text{-}2S]^{2+}$ cluster transfer from GrxS14 to apo *Synechocystis* ferredoxin, a physiologically relevant acceptor protein. Moreover, kinetic studies indicate that the rate of $[2Fe\text{-}2S]^{2+}$ cluster transfer from poplar GrxS14 to apo *Synechocystis* ferredoxin is 25x faster than that observed for HscA/HscB/MgATP-mediated IscU to apo Isc ferredoxin. Hence the results presented in this dissertation lead to a proposal whereby Nfu-type proteins and monothiol glutaredoxins are intermediate cluster carriers associated with the ISC machinery that mediate transfer of $[4Fe\text{-}4S]^{2+}$ and $[2Fe\text{-}2S]^{2+}$ clusters, respectively, from U-type scaffold proteins to apo Fe-S proteins, see Figure 4-1.

It is also possible that monothiol glutaredoxins can function as primary scaffolds for the *de novo* synthesis of $[2Fe\text{-}2S]^{2+}$ clusters in cyanobacteria and plant chloroplasts that lack U-type scaffold proteins. Support for this proposal comes from the ability to reconstitute the $[2Fe\text{-}2S]^{2+}$ cluster in GrxS14 in the presence of glutathione in a cysteine desulfurase-mediated reaction, see Chapter 3. Further support comes from *in vivo* gene disruption studies. Gene-disruption of primary scaffold proteins and other components of the chloroplastic Fe-S cluster assembly machinery in plants are usually associated with a dwarf phenotype or abnormal development (10;11;18;19). Hence the observation of a weak phenotype for GrxS14 involving defects in early seedling growth under oxidative stress conditions, appears to argue against a role as primary scaffold for Fe-S cluster biogenesis (20). However, recent studies by our collaborators have

established a dwarf phenotype for GrxS16, the other $[2Fe\text{-}2S]^{2+}$ cluster-containing chloroplastic monothiol glutaredoxin (N. Rouhier and J.-P. Jacquot, unpublished results). This raises the possibility that GrxS16 can complement the function of GrxS14 in deletion mutants. Alternatively, GrxS14 may be a primary scaffold that plays a role in maturation of specific proteins whose functions are not essential for the plant.

Future work should focus on testing the proposed roles for NfuA and monothiol glutaredoxins as cluster delivery or storage proteins associated with the ISC machinery in *A. vinelandii*, see Figure 4-1. *A. vinelandii* has two monothiol glutaredoxins with CGFS active sites and plasmids for over-expression of these proteins in *E. coli* are now available in Dr. Dennis Dean's laboratory at Virginia Tech. The kinetics of cluster transfer reactions from $[4Fe\text{-}4S]^{2+}$ and $[2Fe\text{-}2S]^{2+}$ cluster-loaded forms of IscU to NfuA and both monothiol glutaredoxins will be investigated in the absence and presence of the HscA/HscB/MgATP molecular chaperone system. In addition the effects of catalytic amounts of NfuA and monothiol glutaredoxins on the kinetics of cluster transfer from cluster-loaded forms of IscU to a range of appropriate acceptor proteins needs to be investigated. It will also be interesting to characterize the cluster binding and transfer properties of yeast Grx5 and the mitochondrial and cytoplasmic monothiol glutaredoxins from poplar, GrxS15 and GrxS17, respectively. Plasmids of each of these proteins for over-expression in *E. coli* have recently been supplied by our collaborator Dr. Nicolas Rouhier in Nancy, France. There is also a pressing need for crystallographic characterization of the cluster-bound forms for NfuA and monothiol glutaredoxins. The cluster coordination sphere for the [2Fe-2S] cluster in monothiol glutaredoxins is likely to be similar to that established by crystallography for dithiol glutaredoxins (21), but molecular-level understanding of the differences in spectroscopic properties and the ability to transfer cluster to acceptor proteins will

require structural characterization. The proposed role of chloroplast Nfu proteins and monothiol glutaredoxins as scaffolds for *de novo* Fe-S cluster biosynthesis also needs to be addressed by investigating their competency individually and together for maturation of a range of chloroplast [2Fe-2S] cluster-containing proteins (e.g. ferredoxin, Reiske protein, ferrochelatase). In addition the role of SufA and the mechanism of assembly of [4Fe-4S] clusters in chloroplasts are unknown and need to be addressed by a combination of *in vivo* and *in vitro* studies.

References

1. Lillig, C. H., Berndt, C., Vergnolle, O., Lönn, M. E., Hudemann, C., Bill, E., and Holmgren, A. (2005) Characterization of human glutaredoxin 2 as an iron-sulfur protein: A possible role as a redox sensor, *Proc. Natl. Acad. Sci. USA 102*, 8168-8173.

2. Johansson, C., Kavanagh, K. L., Gileadi, O., and Oppermann U. (2007) Reversible sequestration of active site cysteines in a 2Fe-2S-bridged dimer provides a mechanism for glutaredoxin 2 regulation in human mitochondria, *J. Biol. Chem. 282*, 3077-3082.

3. Schilke, B., Voisine, C., Beinert, H., and Craig, E. (1999) Evidence for a conserved system for iron metabolism in the mitochondria of *Saccharomyces cerevisiae*, *Proc. Natl. Acad. Sci. USA 96*, 10206-10211.

4. Zheng, L., Cash, V. L., Flint, D. H., and Dean, D. R. (1998) Assembly of iron-sulfur clusters. Identification of an *iscSUA-hscBA-fdx* gene cluster from *Azotobacter vinelandii*, *J. Biol. Chem. 273*, 13264-13272.

5. Johnson, D. C., Unciuleac, M.-C., and Dean, D. R. (2006) Controlled expression and functional analysis of iron-sulfur cluster biosynthetic components within *Azotobacter vinelandii*, *J. Bacteriol. 188*, 7551-7561.

6. Unciuleac, M.-C., Chandramouli, K., Naik, S., Mayer, S., Huynh, B. H., Johnson, M. K., and Dean, D. R. (2007) *In vitro* activation of apo-aconitase using a [4Fe-4S] cluster-loaded form of the IscU [Fe-S] cluster scaffolding protein, *Biochemistry 46*, 6812-6821.

7. Chandramouli, K. and Johnson, M. K. (2006) HscA and HscB stimulate [2Fe-2S] cluster transfer from IscU to apoferredoxin in an ATP-dependent reaction, iochemistry *Biochemistry 45*, 11087-11095.

8. Nishio, K. and Nakai, M. (2000) Transfer of iron-sulfur cluster from NifU to apoferredoxin, *J. Biol. Chem. 275*, 22615-22618.

9. Léon, S., Touraine, B., Ribot, C., Briat, J.-F., and Lobréaux, S. (2003) Iron-sulfur cluster assembly in plants: Distinct NFU proteins in mitochondria and plastids from *Arabidopsis thaliana*, *Biochem. J. 371*, 823-830.

10. Yabe, T., Morimoto, K., Kikuchi, S., Nishio, K., Terashima, I., and Nakai, M. (2004) The arabidopsis chloroplast NifU-like protein CnfU, which can act as an iron-sulfur cluster scaffold protein, is required for the biogenesis of ferredoxin and photosystem I, *Plant Cell 16*, 993-1007.

11. Touraine, B., Boutin, J. P., Marion-Poll, A., Briat, J. F., Peltier, G., and Lobréaux, S. (2004) Nfu2: a scaffold protein required for [4Fe-4S] and ferredoxin iron-sulfur cluster assembly in *Arabidopsis* chloroplasts, *Plant J. 40*, 101-111.

12. Yabe, T. and Nakai, M. (2006) *Arabidopsis* AtIscA-I is affected by deficiency of the Fe-S cluster biosynthetic scaffold AtCnfU-V, *Biochem. Biophys. Res. Commun. 340*, 1047-1052.

13. Saio, T., Kumeta, H., Ogura, K., Yokochi, M., Asayama, M., Katoh, S., Katoh, E., Teshima, K., and Inagaki, F. (2007) The cooperative role of OsCnfU-1A domain I and domain II in the iron-sulphur cluster transfer process as revealed by NMR, *J. Biochem. 142*, 113-121.

14. Balasubramanian, R., Shen, G., Bryant, D. A., and Golbeck, J. H. (2006) Regulatory roles for IscA and SufA in iron homeostasis and redox stress responses in the cyanobacterium *Synechococcus* sp. strain PCC 7002, *J. Bacteriol. 188*, 3182-3191.

15. Rodríguez-Manzaneque, M. T., Ros, J., Cabrito, I., Sorribas, A., and Herrero, E. (1999) Grx5 glutaredoxin plays a central role in protection against protein oxidative damage in *Saccharomyces cerevisiae*, *Mol. Cell. Biol. 19*, 8180-8190.

16. Rodríguez-Manzaneque, M. T., Tamarit, J., Bellí, G., Ros, J., and Herrero, E. (2002) Grx5 is a mitochondrial glutaredoxin required for the activity of iron/sulfur enzymes, *Mol. Biol. Cell 13*, 1109-1121.

17. Mühlenhoff, U., Gerber, J., Richhardt, N., and Lill, R. (2003) Components involved in assembly and dislocation of iron-sulfur clusters on the scaffold protein Iscu1p, *EMBO J. 22*, 4815-4825.

18. Van Hoewyk, D., Abdel-Ghany, S. E., Cohu, C. M., Herbert, S. K., Kugrens, P., Pilon, M., and Pilon-Smits, E. A. (2007) Chloroplast iron-sulfur cluster protein maturation requires the essential cysteine desulfurase CpNifS, *Proc. Natl. Acad. Sci. USA 104*, 5686-5691.

19. Xu, X. M. and Moller, S. G. (2006) AtSufE is an essential activator of plastidic and mitochondrial desulfurases in *Arabidopsis*, *EMBO J. 25*, 900-909.

20. Cheng, N. H., Liu, J. Z., Brock, A., Nelson, R. S., and Hirschi, K. D. (2006) AtGRXcp, an *Arabidopsis* chloroplastic glutaredoxin, is critical for protection against protein oxidative damage, *J. Biol. Chem. 281*, 26280-26288.

21. Rouhier, N., Unno, H., Bandyopadhyay, S., Masip, L., Kim, S. K., Hirasawa, M., Gualberto, J. M., Lattard, V., Kusunoki, M., Knaff, D. B., Georgiou, G., Hase, T., Johnson, M. K., and Jacquot, J. P. (2007) Functional, structural, and spectroscopic characterization of a glutathione-ligated [2Fe-2S] cluster in poplar glutaredoxin C1, *Proc. Natl. Acad. Sci. USA 104*, 7379-7384.

Figure 4-1: Proposed model for the roles of monothiol glutaredoxins and NfuA proteins in ISC-mediated Fe-S cluster biogenesis.

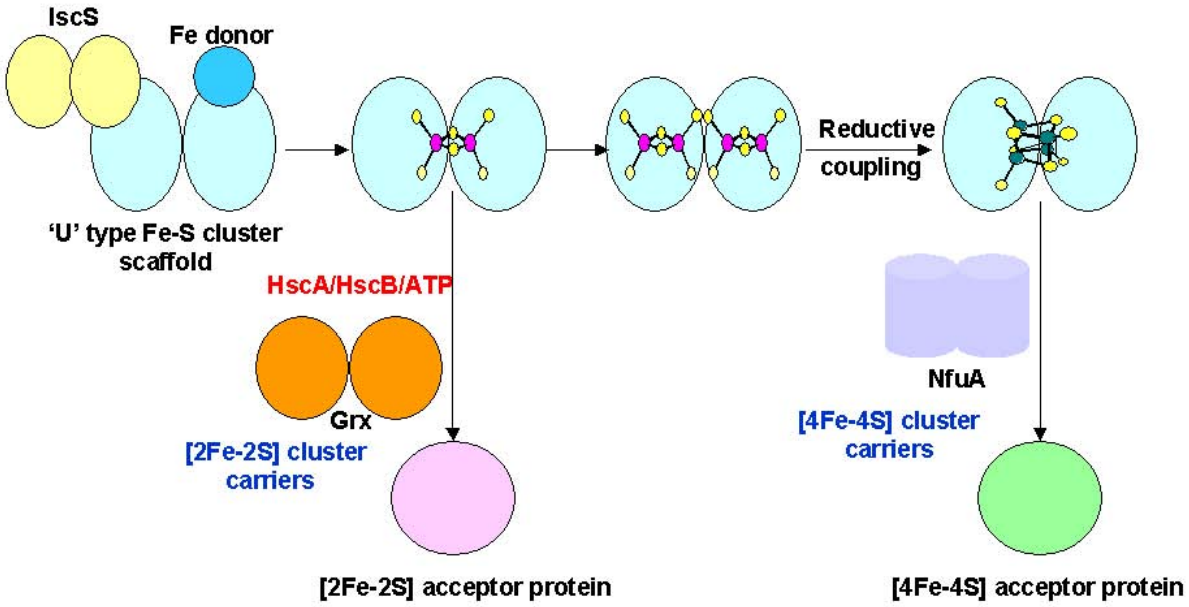
IscS
Fe donor
'U' type Fe-S cluster scaffold
Reductive coupling
HscA/HscB/ATP
Grx
[2Fe-2S] cluster carriers
[2Fe-2S] acceptor protein
NfuA
[4Fe-4S] cluster carriers
[4Fe-4S] acceptor protein

Figure 4-2: Schematic representation of domain structures of IscU/NifU/Nfu proteins from bacteria (*A. vinelandii* *Av*IscU, *Av*NifU, *Av*NfuA and *Haemophilus influenzae* *Hi*IscU), mitochondria (human *Hs*IscU, *Hs*Nfu1 and *A. thaliana* *At*Nfu-I/III), plant chloroplast (*A. thaliana* *At*CnfU-IVa/-IVb/-V) and *Oryza sativa* *Os*Cnfu-1A) and cyanobacteria (*Synechocystis* sp. *Sy*CnfU). The pink boxes represent U-type domains and the brown box represents a Fdx-like domain. Nfu-type domains with a CXXC motif are colored deep blue and those without CXXC motif are colored light blue. The white box represents the N-terminal A-type domain (without the conserved cysteine residues) that is present in bacterial Nfu-type proteins. The yellow boxes represent the N-terminal domain of mitochondrial Nfu-type proteins. The red and grey sticks represent mitochondrial and plastid targeting sequences respectively (adapted from (*13*)).

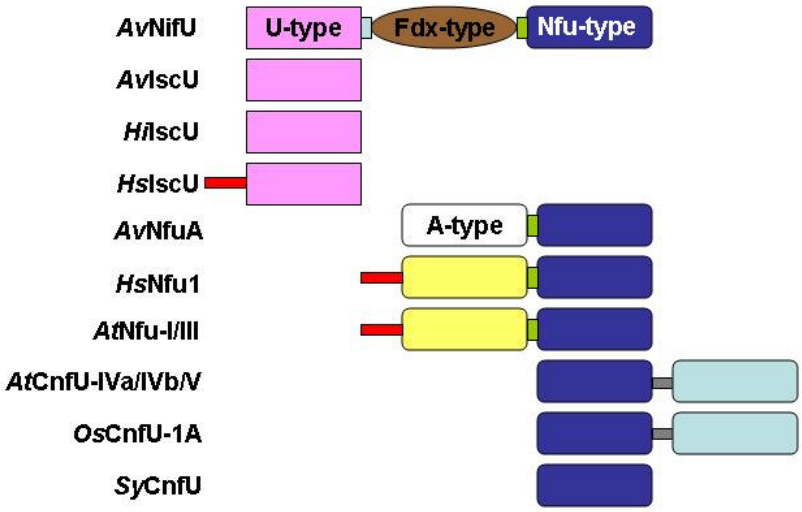
AvNifU
U-type
Fdx-type
Nfu-type
AvIscU
HiIscU
HsIscU
AvNfuA
A-type
HsNfu1
AtNfu-I/III
AtCnfU-IVa/IVb/V
OsCnfU-1A
SyCnfU

APPENDIX

Functional, structural, and spectroscopic characterization of a glutathione-ligated [2Fe-2S] cluster in poplar glutaredoxin C1

When expressed in Escherichia coli, cytosolic poplar glutaredoxin C1 (CGYC active site) exists as a dimeric iron-sulfur-containing holoprotein or as a monomeric apoprotein in solution. Analytical and spectroscopic studies of wild-type protein and site-directed variants and structural characterization of the holoprotein by using x-ray crystallography indicate that the holoprotein contains a subunit-bridging [2Fe-2S] cluster that is ligated by the catalytic cysteines of two glutaredoxins and the cysteines of two glutathiones. Mutagenesis data on a variety of poplar glutaredoxins suggest that the incorporation of an iron-sulfur cluster could be a general feature of plant glutaredoxins possessing a glycine adjacent to the catalytic cysteine. In light of these results, the possible involvement of plant glutaredoxins in oxidative stress sensing or iron-sulfur biosynthesis is discussed with respect to their intracellular localization

Glutaredoxins (Grxs) are small ubiquitous oxidoreductases that belong to the thioredoxin (Trx) superfamily and generally contain a CxxC/S active-site motif. By using a NADPH-dependent glutathione reductase (GR) and reduced glutathione (GSH) as reductants, Grxs are able to reduce disulfide bridges or glutathionylated proteins (1). In higher plants, nearly 30 different Grx isoforms can be classified into three distinct subgroups (2). The first class, which contains Grxs with C[P/G/S][Y/F][C/S] motifs, is homologous to the classical dithiol Grxs such as *Escherichia coli* Grx1 and -3, yeast Grx1 and -2, and mammalian Grx1 and -2. The second

class has a strictly conserved CGFS active-site sequence and includes Grxs homologous to yeast Grx3, -4, and -5 or *E. coli* Grx4. The third class, which is specific to higher plants and involves a CC[M/L][C/S] active site, has yet to be characterized.

In addition to Grxs and Trxs, two groups of proteins that function in reducing disulfide bonds, the thiol/disulfide oxidoreductase family also contains proteins able to form or isomerize disulfide bonds. These proteins are called protein disulfide isomerases (PDI) in eukaryotes and Dsb proteins in prokaryotes. DsbA and DsbB are involved in disulfide bond formation, and DsbC, DsbG (CPYC active site) and DsbD are involved in disulfide isomerization (3). In addition, it was recently shown that the *E. coli* TrxA or some of its active site mutants, which incorporate a [2Fe–2S] into a homodimer, can act as weak oxidants into the *E. coli* periplasm and thus substitute for the naturally occurring DsbA/DsbB pathway (4, 5).

Grxs have also been shown to be involved in iron–sulfur cluster biosynthesis in *Saccharomyces cerevisiae* and *E. coli* (6–9), and human Grx2 was recently shown to bind a subunit-bridging [2Fe–2S] cluster that was reported to be ligated by two non-active-site cysteines based on mutagenesis studies (10). The cluster-containing dimeric form of human Grx2 was shown to be present *in vivo* and to be inactive in classical Grx assays. The Fe–S cluster was proposed to function as a redox sensor for the activation of Grx2 during conditions of oxidative stress. We report here structural and spectroscopic characterization of an Fe–S cluster-bound form of poplar glutaredoxin C1 containing a subunit-bridging [2Fe–2S] cluster that is ligated by the catalytic cysteines of two glutaredoxins and the cysteines of two glutathiones. Furthermore, mutagenesis studies suggest that incorporation of an iron–sulfur cluster is likely to be a general feature of plant Grxs possessing a glycine adjacent to the catalytic cysteine. The functional significance of the ability of Grxs to bind Fe–S clusters is discussed in light of these results.

Materials and Methods: NADPH was obtained from Roche Molecular Biochemicals (Mannheim, Germany), and GR and GSH were obtained from Sigma. DTT, IPTG, kanamycin, and ampicillin were from Euromedex (Souffel Weyersheim, France).

Chemical Analysis: Protein concentrations were determined by using BSA as a standard with the Bio-Rad D_c protein assay in conjunction with the microscale modified procedure of Brown *et al.* (37). Iron concentrations were determined colorimetrically by using bathophenanthroline under reducing conditions after digestion of the protein in 0.8% $KMnO_4$/0.2 M HCl (38).

Cloning, Expression, and Purification of the Recombinant Proteins: The ORFs of poplar Grx C1, C2, C3, and S12 and of A thaliana Grx C1 were amplified by PCR using a leaf cDNA library of Populus tremula x tremuloides as a template or an A. thaliana leaf RT-PCR product and cloned into the expression plasmid pET-3d between NcoI and BamHI restriction sites by using the primers PtGrx C1, PtGrx C2, PtGrx C3, and PtGrx S12 forward and reverse (Table 2). The 10, 22, or 72 first amino acids respectively of Grx C1, Grx C3, and Grx S12 that putatively encode extensions with a signal sequence were excluded. In the case of Grx C1, we also cloned the full-length sequence. In addition, for improved expression, an alanine was added just behind the initiator methionine and the N-terminal sequence of the shorter form of Grx C1 is thus MASKQEL.

The single mutation C31S, G32P, C34S, and C88S and the double mutation Y33F and C34S were introduced in poplar Grx C1 by site-directed mutagenesis using two complementary primers (Table 2) and the strategy described in Jacquot et al. (40) PtGrxC1C31S, PtGrxC1G32P, PtGrxC1C34S, PtGrxC1C88S, and PtGrxC1Y33F C34S for and rev. Site-directed mutagenesis

was also used to change into CGYC, the CPFC active site of Grx C2 (Grx C2 P24G/F25Y) and the CPYC active sites of Grx C3 and C4 (Grx C3 P38G; Grx C4 P28G).

The *E. coli* expression strain BL21(DE3), containing the helper plasmid pSBET, was transformed with each recombinant plasmid. LB cultures of 2.6 liters were grown at 37°C and induced in exponential phase by adding 100 μM IPTG (isopropyl-β-D-thiogalactopyranoside). The bacteria were pelleted by centrifugation for 15 min at 5,000 × g and resuspended in buffer A (30 mM Tris·HCl (pH 8.0)/1 mM EDTA/200 mM NaCl). Bacteria were lysed by sonication and centrifuged for 1 hour at 16,000 × g to eliminate the insoluble part. The proteins of interest were predominantly in the soluble fraction. The soluble fraction was then separated into two fractions by precipitating it with ammonium sulfate successively up to 40% and 80% of the saturation. Grx C1 WT and mutants, Grx C2 WT and P24G F25Y, Grx C3 WT and P38G, Grx C4 P28G and Grx S12 WT and mutant precipitated between 40% and 80% of the saturation. These fractions were first loaded onto an ACA 44 gel filtration column (5 × 75 cm) (BioSepra) equilibrated with buffer A. The fractions containing the protein were pooled and dialyzed against buffer B (buffer A without NaCl). In the case of Grx C1 WT or mutants (except Grx C1 C31S), the apo and holoenzymes were pooled separately. The fractions were loaded onto a DEAE Sephacel column equilibrated with buffer B. Grx C1 WT and mutants, Grx C2 WT and P24G F25Y and Grx S12 WT and S30G passed through the column, whereas Grx C3 WT and P38G, Grx C4 P28G were retained and eluted by using a linear 0-0.4 M NaCl gradient. A final step of carboxymethyl cellulose chromatography was also used for the holoenzyme of Grx C1 because it allowed the obtention of protein preparations with higher A430/A278 ratio. In this latter step, the protein was first dialyzed against excess phosphate buffer 50 mM pH 6.0 and then applied to a carboxymethyl cellulose column equilibrated with the same buffer. As for the DEAE step, the

holoprotein passed through this matrix. Finally, the fractions were concentrated and stored at high concentrations (generally ≈30 mg/ml) at -70°C until further use. SDS-PAGE was used to check the homogeneity of the various proteins.

Complementation of E. coli Strains: The strains used in this study are MC1000 (genotype: F^- araD139 Δ(araA-leu)7679 (codB-lac)X74 galE15 galK16 rpsL150 relA1 thi) and LM108 (MC1000 dsbB::kan5 dsbA::cm). Strains were constructed by P1 transduction. The mutant alleles used for this study are: dsbB::kan5, dsbA::cm (lab collection). All allele substitutions were confirmed by PCR. For cloning steps, pET3d containing Grx plasmids described previously were used as templates to amplify by PCR Grx C1, C1 G32P, and C4 with the following primers Grx C1 pTrc99a forward and reverse (for Grx C1 and C1 G32P) and Grx C4 pTrc99a forward and reverse (for Grx C4) (Table 2). These primers introduce SalI and HindIII restriction sites used to clone the corresponding PCR fragments in pTrc99a-TorAss and pTrc99a-PhoAss (5) to obtain pTrc99a-TorAss-Grx C1, pTrc99a-TorAss-Grx C1 G32P, pTrc99a-TorAss-Grx C4, and pTrc99a- PhoAss-Grx C1.

Motility Assay: Cells from single colonies were grown overnight in $M9_{casein}$ media (1× M9 minimal salts (M6030; Sigma), 0.4% (wt/vol) glucose, 0.1% (wt/vol) casein enzymatic hydrolyzate (C0626; Sigma), 2 mM $MgSO_4$, 0.05 mg/ml thiamine) with the appropriate antibiotic at 37°C with shaking. The overnight culture was diluted to an OD_{600} of 1.0 and then 1.5 μl was spotted into the center of a $M9_{casein}$ motility plate ($M9_{casein}$ media as above with 0.3% (wt/vol) agar). Cells were grown at 37°C for 28 h, at which point the motility halos were determined.

Alkaline Phosphatase Activity Assays: Cells harboring the pTrc99a plasmids containing the coding DNA sequence of the different glutaredoxins with either the Tat specific TorA signal

sequence or the Sec-specific PhoA signal sequence fused to the N terminus were grown in Mops minimal media with a total concentration of inorganic phosphate of 0.1 mM to induce the synthesis of alkaline phosphatase (AP) from the chromosomal copy of the alkaline phosphatase gene (PhoA). Cells were inoculated into 5.5 ml of fresh media and grown for ≈14 h at 37°C with shaking. Then cell OD_{600} was adjusted to 1.0 and 20 μl of cell culture were transferred to a 96-well plate and mixed with 30 μl of lysis buffer (a 2:1 mixture of B-PER Bacterial Protein Extraction Reagent (78248; Pierce Biotechnology, Inc.) and a 0.4 M iodoacetamide solution), lysis took place for 30 min with shaking; then 200 μl of 250 μg/ml p-nitrophenyl phosphate in 0.2 M Tris·HCl (pH 8) was added to each well. Hydrolysis of p-nitrophenyl phosphate was followed at A_{405} on a plate reader (Beckman).

Spectroscopic Methods: Samples for spectroscopic studies were prepared under Ar in a glove box (Vacuum Atmospheres, Hawthorne, CA) at oxygen levels <2 ppm. UV-visible absorption and CD spectra were recorded at room temperature by using a UV-3101PC spectrophotometer (Shimadzu) and J-715 spectropolarimeter (Jasco, Easton, MD), respectively. Resonance Raman spectra were recorded as described (22), by using a Ramanor U1000 spectrometer (Instruments SA, Edison, NJ) coupled with a Sabre argon ion laser (Coherent, Santa Clara, CA), with 20 μl of frozen droplets of sample mounted on the cold finger of a Displex Model CSA-202E closed cycle refrigerator (Air Products, Allentown, PA). X-band EPR spectra were recorded by using a ESP 300D spectrometer (Bruker, Billerica, MA) equipped with an ESR 900 flow cryostat (Oxford Instruments, Concord, MA).

Crystallization, X-Ray Data Collection, Structure Determination, and Refinement: Holoform crystals were obtained by the hanging-drop vapor-diffusion method. X-ray diffraction data for Fe MAD (multiple-wavelength anomalous dispersion) with three wavelengths were

collected at 100 K up to 2.2-Å resolution. X-ray diffraction data for structural refinement was collected to 2.1 Å at 100 K with wavelength of 1.000 Å. The crystals belonged to space group $P6_1$, with unit cell dimensions $a = b = 97.8$ Å, and $c = 91.5$ Å. There are four peptide chains A, B, C, and D of Grx in the asymmetric unit. The polypeptide chain models have been built for residues 2–108 in chain A, for residues 3–113 in chain B, for residues 2–116 in chain C, and for residues 7–107 in chain D, respectively. The structure has been refined for four polypeptide chains, one [2Fe–2S] cluster, four GSH molecules, and 293 water molecules to *R* and *R*-free factors of 18.4% and 22.0%, respectively.

Redox Potential Determination: Oxidation–reduction titrations, using the fluorescence of the adduct formed between the protein and mBBr to monitor the thiol content of the protein, were carried out at ambient temperature as described (39). The reaction mixtures contained 100 µg of protein in 100 mM Hepes buffer (pH 7.0) and a total GSH plus GSSG concentration of 2 mM. The ambient potential (Eh) was set by varying the ratio of GSSG to GSH as described (39). The redox equilibration time was 2 h.

Intracellular Localization via GFP Fusion: For *in vivo* intracellular localization, the full-length poplar Grx C1 ORF was cloned in frame into NcoI and BamHI sites (underlined) of pCK-GFP S65C, under the control of a double 35S promoter, by using the two primers Grx C1 pCK forward and reverse and fused to GFP at the BamHI site (Table 2). *Nicotiana benthamiana* cells were transfected by bombardment of leaves with tungsten particles coated with plasmid DNA, and images were obtained with a LSM510 confocal microscope (Zeiss, Thornwood, NY).

Results and Discussion: To gain insight into the function and structure of plant Grxs, poplar Grxs of subgroup I (Grx C1, C2, C3, and S12) were produced as recombinant proteins in *E. coli*, purified to homogeneity and compared with the previously characterized Grx C4 (2, 12).

Among the various Grx characterized in all kingdoms, GrxC1 is unique to plants having a YCGYC active site, whereas poplar Grx C2 contains a YCPFC active site, Grx C3 and C4 a "classical" YCPYC active site, and Grx S12 a WCSYS active site similar to the one found in human Grx 2 (CSYC) (Figure 5). Unexpectedly, among the five Grxs of subgroup I, recombinant Grx C1 (12,514 Da) eluted in exclusion size chromatography as two successive peaks, one with a higher oligomerization state and a brown coloration characteristic of the presence of an Fe–S center, and a colorless peak of smaller size. Gel filtration compared with proteins of known molecular mass, indicated molecular masses of 34 and 17 kDa for the brown holoprotein and colorless apoprotein fractions, respectively (data not shown). The data are best interpreted in terms of a dimeric holoprotein (predicted M_r = 25 kDa) and a monomeric apoprotein (predicted M_r = 12.5 kDa). Moreover, NMR studies of the holo- and apo- forms of Grx C1 indicate that these proteins are present as a dimer and monomer, respectively (11).

To ensure that the Fe–S center incorporation in Grx C1 is not caused by the removal of the 10 first amino acids (see *Materials and Methods*) and determine whether Fe–S center incorporation is unique to poplar Grx C1 or is a property of all plant Grx containing a CGYC active site, we have also produced the full-length Grx C1 and the Grx C1 homolog from *Arabidopsis thaliana* (At5g63030, AtGrx C1). Both recombinant holoproteins display the same visible absorption characteristics and have not been characterized further (data not shown).

Nature of the Fe–S Center in Grx C1: The nature of the Fe–S center in holoGrx C1 was initially assessed by using a combination of analytical and spectroscopic techniques. Samples purified to homogeneity contained 1.1 ± 0.1 mol of Fe per mol of protein, a result that is consistent with the presence of one $[2Fe–2S]^{2+}$ center per dimer or one $[4Fe–4S]^{2+}$ center per tetramer. However, the UV-visible absorption and CD spectra are uniquely characteristic of a

$[2Fe–2S]^{2+}$ cluster (Figure 1*A*) and are very similar to those recently reported for human Grx2 (10). There are, however, some significant differences compared with other structurally characterized biological $[2Fe–2S]^{2+}$ centers. For example, the absorption spectrum of Grx C1 is dominated in the 400- to 480-nm region by a single band centered at 430 nm, whereas other biological $[2Fe–2S]^{2+}$ centers generally exhibit two resolved bands centered near 420 and 460 nm (12–17). On the basis of the theoretical and experimental ε_{280} values for the apoprotein (9.6 $mM^{-1}cm^{-1}$), ε_{280} and ε_{430} values for the $[2Fe–2S]^{2+}$ center are estimated to be 2.6 $mM^{-1}cm^{-1}$ and 5.0 $mM^{-1}cm^{-1}$, respectively (A_{430}/A_{280} ratio = 0.41 ± 0.02). These extinction coefficients are indicative of ≈0.5 $[2Fe–2S]^{2+}$ clusters per monomer based on published extinction coefficients for biological $[2Fe–2S]^{2+}$ centers (18). Hence the UV-visible absorption and Fe analytical data are consistent in estimating one $[2Fe–2S]^{2+}$ cluster per Grx C1 dimer for homogeneous samples with A_{430}/A_{280} ratios = 0.41 ± 0.02.

In agreement with the anticipated diamagnetic $S = 0$ ground state that results from antiferromagnetic coupling of two high-spin ($S = 5/2$) Fe(III) centers, purified samples of holoGrx C1 do not exhibit an observable EPR signal. Attempts to reduce the $[2Fe–2S]^{2+}$ cluster under anaerobic conditions to yield a stable $[2Fe–2S]^{+}$ cluster by using excess dithionite, electrochemical reduction in the presence of redox mediators or deazariboflavin-mediated photoreduction have not been successful. Absorption studies indicate a gradual and irreversible bleaching of the visible absorption and parallel EPR studies revealed a very weak $S = 1/2$ EPR signal, $g_{\parallel} = 2.04$ and $g_{\perp} = 1.93$, invariably accounting for <0.02 spins per [2Fe–2S] cluster (Figure 1*C*). Hence the cluster appears to be reductively labile, with reductive degradation proceeding via an unstable $S = 1/2$ $[2Fe–2S]^{+}$ intermediate. The inability to reduce the cluster to a stable $[2Fe–2S]^{+}$ state argues against an electron transfer function for the cluster in Grx C1.

The vibrational properties of the Fe–S cluster in holoGrx C1 were characterized by resonance Raman studies (19). The resonance Raman spectrum of Grx C1 in the Fe–S stretching region (240–450 cm^{-1}), obtained with 457.9-nm excitation, is shown in Figure 1*D*. The Fe–S stretching frequencies are most similar to those of $[2Fe–2S]^{2+}$ clusters with complete cysteinyl ligation (14, 20), and distinct from $[2Fe–2S]^{2+}$ centers with two histidine ligands at a unique Fe site (21) or with a single serine or arginine ligands in place of one of the cysteine ligands (22–25). The Fe–S stretching modes for the $[2Fe–2S]^{2+}$ centers in Grx C1 are readily assigned by direct analogy with the assignments established via isotope shifts and normal mode calculations for representatives of the all-cysteine-ligated $[2Fe–2S]^{2+}$ clusters from each of the major classes of ferredoxins, i.e., plant-type (typified by *Spinacia oleracea* ferredoxin), hydroxylase- or Isc-type (typified by adrenodoxin) and thioredoxin-type (typified by *Clostridium pasteurianum* ferredoxin) (Table 1) (14, 20). Hence, taken together, the analytical and spectroscopic properties of the holoform of Grx C1 are consistent with a dimeric protein containing one $[2Fe–2S]^{2+}$ center coordinated exclusively by cysteinyl ligands.

Identification of the Fe–S Cluster Ligands by Site-Directed Mutagenesis: Mutagenesis studies involving each of the three conserved cysteine residues of Grx C1 were used to investigate the cysteine residues involved in $[2Fe–2S]^{2+}$ cluster ligation. No cluster was observed in the Grx C1 C31S variant, indicating that the catalytic cysteine (Cys-31) is likely to be a cluster ligand. However, both the Grx C1 C34S and C88S variants were able to assemble $[2Fe–2S]^{2+}$ clusters with visible absorption and CD characteristics identical to that of the $[2Fe–2S]^{2+}$ center in holoGrx C1 (data not shown) and resonance Raman spectra very similar to those of holoGrx C1 (Figure 1*D*). On the basis of iron-determinations (0.38 ± 0.04 and 0.19 ± 0.04 Fe/monomer for C88S and C34S, respectively) and A_{430}/A_{280} ratios (0.16 ± 0.02 and 0.06 ± 0.02 for C88S and

C34S, respectively), aerobically purified samples of Grx C1 C88S and C34S variants were found to contain ≈0.4 and ≈0.2 $[2Fe–2S]^{2+}$ clusters per dimer, respectively. As discussed below, the substoichiometric cluster content of the C88S and C34S variants appears to be a consequence of enhanced O_2 sensitivity, suggesting that both Cys-34 and Cys-88 may play a role in stabilizing the $[2Fe–2S]^{2+}$ cluster against oxygen degradation. In light of the resonance Raman evidence for a $[2Fe–2S]^{2+}$ cluster with complete cysteinyl ligation, the mutagenesis results were initially very puzzling but were subsequently rationalized by the crystallographic results.

The stability of the Fe–S cluster in wild-type and mutant forms of Grx C1 was monitored aerobically by measuring the absorption at 430 nm in the presence of various reductants and oxidants as a function of time (Figure 2). The results are quite similar to those observed for human Grx2 (10), i.e., reduced glutathione stabilizes the cluster in Grx C1 and in the Grx C1 C34S and C88S variants, whereas oxidized glutathione slightly destabilizes the cluster. DTT also stabilizes the cluster but to a lesser extent than reduced glutathione. We took advantage of the stabilizing ability of reduced glutathione to purify holoforms of AtGrx C1, which was less stable than poplar Grx C1 and poplar Grx C1 C34S and C88S in the presence of GSH.

The sequence required for assembling a [2Fe–2S] cluster in Grxs was investigated by expressing proteins with altered active sites. The active sites sequences of Grx C2, C3 and C4 were thus mutated into CGYC and the one of Grx C1 into CPYC. UV-visible absorption studies of samples purified in the presence of GSH showed that Grx C1 G32P was no longer able to incorporate a $[2Fe–2S]^{2+}$ cluster, whereas Grx C2 P24G/F25Y, Grx C3 P38G, and Grx C4 P28G, all assembled a $[2Fe–2S]^{2+}$ cluster with absorption properties very similar to those of Grx C1. Grx C4 P28G was unique in being the only Grx protein investigated in this work that was purified exclusively in the Fe–S cluster-bound form. Analytical and quantitative UV-visible

absorption/CD studies of Grx C4 P28G indicated 1.1 ± 0.1 $[2Fe–2S]^{2+}$ cluster per dimer and the absorption, CD, and resonance Raman spectra are very similar to Grx C1, indicating analogous electronic, vibrational, and structural properties for the $[2Fe–2S]^{2+}$ centers (Figure 1*B* and *D*). Taken together, these mutagenesis data indicate that the presence of a glycine rather than proline after the first catalytic cysteine is an essential determinant for the ability of Grxs to assemble a $[2Fe–2S]^{2+}$ cluster.

The importance of the glycine residue after the first catalytic cysteine, coupled with lack of role for the second active-site cysteine in cluster assembly, raised the possibility that the class of monothiol Grxs with CGFS active sites may also be able to incorporate Fe–S clusters. This possibility is particularly intriguing because the yeast Grx5 protein, which has been shown to be involved in Fe–S assembly (7, 8), has a CGFS active site. The Grx C1 Y33F/C34S with a CGFS active site was found to incorporate a Fe–S center with UV-visible absorption properties similar to those of Grx C1. Although the presence of an Fe–S cluster has not been reported to date for any purified samples of yeast Grxs with a CGFS active site, this may be a consequence of instability under aerobic conditions or a requirement for other as yet unidentified amino acids needed for the Fe–S assembly.

The recent discovery of a $[2Fe–2S]^{2+}$ cluster in human Grx2 (10), which has a CSYC active site, prompted investigation of Grx S12, which contains a similar CSYS active site. The aerobically purified WT protein and the S30G mutant, which contains a CGYS active site similar to Grx C1 C34S, did not incorporate a cluster, suggesting that either serine is not able to play a role identical to the glycine residue or that other determinants not present in the Grx S12 sequence, but in human Grx2, are important for Fe–S cluster incorporation. Human Grx2 has two active-site cysteines (Cys-37 and Cys-40) and two extra cysteines (Cys-28 and Cys-113), not

conserved in either Grx S12 or in plant sequences but which can form a disulfide bridge (26). Mutagenesis and spectroscopic results lead to the proposal for a subunit-bridging cluster ligated by Cys-28 and Cys-113 (10). However, the great similarity in the UV-visible absorption and CD properties of the $[2Fe–2S]^{2+}$ cluster between human Grx2 and poplar Grx C1, combined with the absence of any mutagenesis results for Cys-37 in human Grx2, suggests that this proposal needs to be reevaluated in light of the results presented herein. In fact, a very recent paper by Johansson *et al.* (26) describing the x-ray crystallographic structure of human Grx2 fully supports the proposal made here, the human Grx2 is actually organized in a very similar way to poplar Grx C1 (26). The Cys-28 and Cys-113 in human Grx2 may only have a structural role that facilitates Fe–S cluster assembly rather than providing cluster ligands. An important feature that may explain the absence of Fe–S cluster incorporation in Grx S12 is the presence of a tryptophan residue before the catalytic cysteine. All of the plant Grx proteins that have thus far been shown to incorporate an Fe–S cluster have, instead, a tyrosine residue. This possibility is supported by recent structural evidence on poplar Grx C4, which was shown to be in equilibrium between monomeric and dimeric states (27). In the dimeric state, the two active-site tyrosine residues (YCPYC) are involved in the formation of a new interface, which delimits a pocket in which some small cofactors like Fe–S clusters could be incorporated. We hypothesize that the presence of a proline residue prevents cluster incorporation.

Structure of the Holoprotein: The x-ray structure of Grx C1, solved to 2.1-Å resolution, indicates that the holoprotein organizes as a tetramer containing one [2Fe–2S] cluster in the crystalline state. This result is surprising because gel filtration, NMR, analytical and UV-visible absorption studies of cluster-replete holoprotein all indicate a dimeric structure containing one [2Fe–2S] cluster in solution (11). However, as the holoprotein gradually loses its cluster under

air, it seems likely that the tetrameric organization detailed below results from cocrystallization of holo and apo forms. In the x-ray structure, the four molecules of Grx in the asymmetric unit exhibit a unique "dimer of dimer structure" shown in Figure 3*A*. Each polypeptide has a typical Trx fold with an averaged pair-wise rms Cα discrepancy of 0.54 Å. One pair of chains A and B and another pair of chains C and D are related by noncrystallographic quasi 2-fold axes (171.1° and 175.4° rotation, respectively), which are roughly parallel to each other (7.3°) and have a distance of ≈10 Å between them. Dimer A/B and dimer C/D are related by third quasi 2-fold symmetry of 176.9° and 179.4° rotations respectively roughly perpendicular to the first two 2-fold axes.

Multiwavelength anomalous diffraction (MAD) analysis revealed the position of Fe atoms at the center of an electron density island, which connects chains A and C. A model of a [2Fe–2S] cluster fits well with the electron density of the metal center. The two Fe atoms of the [2Fe–2S] cluster are linked to the Cys-31 Sγ atom of chains A and C and a compound not assigned to any of the polypeptide side-chains in the electron density map, suggesting the existence of nonprotein ligands. As a consequence, the A–C structure is likely to provide a good representation of the holodimer in solution. The nonprotein ligand was separated from the polypeptide chains by HPLC after an acid treatment of Grx and chemically identified by MALDI-TOF and NMR as GSH, even though the preparation used for crystallography was made in absence of glutathione. In fact, a GSH model fits well into the electron density map, revealing that the two Fe atoms are coordinated by two inorganic sulfur atoms of the cluster, two Cys-31 Sγ atoms, and two Cys Sγ atoms of GSH. In the overall structure, chains A and C, one [2Fe–2S] cluster, and two glutathione molecules are arranged obeying a noncrystallographic 2-fold symmetry, the axis of which passes through the two inorganic sulfur atoms of the [2Fe–2S]

cluster. Tyr 30, Tyr 33, and GSH molecules in chains A and C surround the [2Fe–2S] cluster, sequestering it from the solvent. Hence, both tyrosines in the YCGYC active-site sequence of Grx C1 play a role in stabilizing the cluster (see details of the Fe–S cluster environment in Figure 3*B*). The structure is consistent with the mutagenesis and spectroscopic properties of holoGrx C1.

In an earlier work by Feng *et al.*, we have determined the 3D structure of the reduced apo form of Grx C1 by NMR spectroscopy (11). In addition, by comparing the resonances of the holodimeric form to those of the apo form, we have proposed a model in which the iron sulfur center is coordinated by two cysteines and two external glutathione molecules. In general, the crystallographic data presented here match well those of the Feng paper, and, in particular, the organization of the subunit is similar to that described by NMR (11). The crystallographic structure, however, provides near atomic resolution of the iron–sulfur center and indicates that the model was only partly correct. We had earlier hypothesized that the two Cys residues as well as the two GSH ligands were located in cis with respect to the plane created by the two iron atoms. The data presented here reveal that they are actually placed in trans in the real structure.

In our crystal, Grx chains A–D are each bound to one of four GSH molecules through hydrogen bonds, salt bridges, and hydrophobic interactions except that two of the GSH molecules are covalently linked to the [2Fe–2S] cluster. The four GSH molecules share similar conformations and have essentially the same relative position with respect to their associated Grx molecules. Two GSH molecules in complex with chains B and D face the Cys Sγ atoms of the catalytic cysteine residues at a distance of $\approx$3 Å, without forming covalent bonds. Chains B and D do not directly interact with the [2Fe–2S] cluster but serve to stabilize the tetramer structure.

Among the poplar subgroup I Grxs, only Grx C1 forms an iron–sulfur cluster. Inspection of the structure indicates that the presence of a proline residue adjacent to the catalytic cysteine,

as in Grx C2, C3, or C4, would likely interfere with the cluster formation because of steric constraints involving the side chain. In light of the role played by the two tyrosine residues, the presence of a small residue, and especially a glycine, is likely to be essential for Fe–S cluster incorporation.

Oxidant Properties of Grx C1: In the bacterial periplasm, the formation of disulfide bonds is catalyzed by the soluble enzyme DsbA, which is recycled by the membrane protein DsbB that, in turn, transfers electrons to quinones and the respiratory chain (3). Mutational inactivation of the *dsbB* gene results in several phenotypes including complete loss of motility (28). Following up on recent studies on a mutated Trx with a CACA active site that incorporates a $[2Fe–2S]^{2+}$ cluster (5), we fused Grx C1 to the TorA leader peptide that directs export across the cytoplasmic membrane via the twin arginine transporter (TAT). The TAT pathway allows the membrane translocation of proteins that have acquired metal cofactors and/or disulfide bonds in the cytoplasm (3, 29). The TorA-Grx C1 fusion was exported into the periplasm and restored motility to a significant extent (Figure 4*A*). To further examine the ability of exported Grx C1 to mediate the formation of disulfide bond formation in the periplasm, we monitored the activity of alkaline phosphatase (PhoA), an enzyme that contains two disulfide bonds that are essential for folding into the active native conformation (30). PhoA activity is completely abolished in *dsbB*/*dsbA*-deleted cells (a decrease of >100-fold over the WT parental strain) (Figure 4*B*). However, expression of TorA-Grx C1 restored the level of PhoA activity to that of WT MC1000 strain. Secretion of Grx C1 via the PhoA signal sequence is targeted to the general secretory pathway, (SEC), whereby proteins are exported in an essentially unfolded conformation also restored PhoA activity in *E. coli* LM108. In contrast to the TAT pathway, the SEC pathway is unable to export proteins with cofactors such as iron sulfur clusters. All of the Grxs tested (poplar

Grx C1 or Grx C1 G32P, Grx C4, and *E. coli* Grx1 and -3) were able to promote disulfide bond formation in AP (Figure 4*B* and data not shown), indicating that the apo form of Grx C1 and probably more generally all dithiol Grxs are able to promote disulfide bond formation *in vivo*. Concerning the holo Grx C1, the restoration of AP activity could arise from apoprotein generation because of the instability of the cluster. These results were surprising because the cells lack DsbB, and there is no known periplasmic oxidant for the recycling of reduced Grx C1 after it transfers a disulfide bond to a substrate protein. The best explanation is linked to the postulated presence of GSSG in *E. coli* periplasm (31).

One way to understand this oxidant property is to measure the redox potential of the protein. Both the Grx C1 holo- and apoproteins exhibit redox-active, two-electron processes when titrated by using the thiol-specific reagent monobromobimane (mBBr) to monitor the oxidation state of the proteins. Oxidation–reduction midpoint potential (E_m) values of –160 ± 10 mV and –180 ± 10 mV were measured at pH 7.0 for the holoprotein and apoprotein, respectively. Given the two-electron nature of these redox couples and the fact that mBBr detection was used to monitor the redox process, it seems highly likely that these E_m values, which are slightly more positive than the E_m values previously reported for Grx1 (–233 mV) and Grx3 (–198 mV) of *E. coli* (32), arise from disulfide/dithiol couples. These more positive values for plant Grxs may be a general feature, because the redox potential of Grx C4 also lies in the same range with an E_m value of –170 mV ± 10 mV. The redox process detected with the holoprotein certainly does not reflect redox cycling of the Fe–S center, which is essentially inert under the conditions of these redox titrations. It rather results from the disulfide/dithiol redox activity of apo form generated after interaction with mBBr during the 2-h period required for protein equilibration in the redox buffer. Indeed, monitoring the Fe–S center spectrum in the presence of mBBr indicates that it is

almost completely degraded in this time (data not shown). Assuming this rather oxidant redox potential for Grx C1, we also have measured the reductase activity of apo Grx C1 using classical Grx substrates, hydroxyethyl disulfide and dehydroascorbate. The catalytic parameters are similar to those found with other poplar Grxs (data not shown).

Localization and Physiological Role of Grx C1: The function of Grx C1 in plants is clearly of considerable interest because of its ability to bind an Fe–S cluster. A redox function seems very unlikely in light of the inability of the $[2Fe–2S]^{2+}$ cluster to undergo reversible redox cycling. To address the function of Grx C1, we first determined the localization of the protein, by cloning in-frame the entire sequence of Grx C1 before the GFP protein, and this construction was used to bombard leaf cells from *Nicotiana benthamiana*. As shown in Figure 6, the fluorescence associated with the construction is localized to the cytosol.

Previous studies have implicated some Grxs in the maturation of Fe–S clusters. *In vitro* experiments demonstrated that *E. coli* Grxs in the presence of GSH facilitate assembly of a [4Fe–4S] cluster in the fumarate nitrate reductase regulatory protein by reducing disulfide bridges formed between cluster-ligating cysteines in the apoprotein (6). Yeast Grx5, which has a CGFS active-site sequence that is likely to be able to assemble an Fe–S cluster based on the results reported above, has been shown to play an important role in mitochondrial Fe–S cluster biogenesis (7, 9). Other prokaryotic and eukaryotic monothiol Grxs with CGFS active-site sequences have recently been shown to be effective functional substitutes for yeast Grx5 (8). Although the specific role of yeast Grx5 in Fe–S cluster biogenesis has yet to be elucidated, ^{55}Fe radiolabeling studies of knockout mutants suggest that it is likely to facilitate the transfer of clusters preassembled on the Iscu1p scaffold protein into acceptor proteins (9). The recent discovery that Grx5 is also required for vertebrate heme synthesis (33) is particularly interesting

in this regard, because it raises the possibility that cluster-bound Grx5 plays a direct role in regulating heme biosynthesis in mammals by facilitating assembly of a [4Fe–4S] cluster on iron regulatory protein 1 or activating ferrochelatase by insertion of the catalytically essential [2Fe–2S] cluster (34).

In plants, components of the Fe–S clusters assembly machinery have been described in both mitochondria and plastids, but nothing is known concerning the assembly of cytosolic Fe–S cluster proteins (35). In yeast, where GSH was identified as being important for cytosolic Fe–S cluster maturation, at least six different proteins have been implicated as possibly being involved in cluster assembly (36). As Grx C1 coordinates a [2Fe–2S] cluster by using two external glutathione molecules, an intriguing hypothesis would be that Grx C1 could serve as a scaffold for assembly of cytosolic Fe–S clusters or a chaperone for transfer of Fe–S clusters assembled on scaffold proteins to cytosolic acceptor proteins. *In vitro* experiments to test this hypothesis by using appropriate Fe–S cluster acceptor and donor proteins remain to be completed.

The results presented herein clearly demonstrate that apo Grx C1 is functional in disulfide bond formation. It is currently unclear whether this functionality is maintained in holo Grx C1, but this seems unlikely because the active-site cysteine is a cluster ligand. Moreover, human Grx2, which has a [2Fe–2S] cluster with analogous spectroscopic and stability properties, was shown to be inactive in classical Grx assays. Hence the holo- and apo- forms of Grx C1 can have different functions within the cell, and it is possible that the [2Fe–2S] cluster has dual roles in Fe–S cluster biosynthesis and in sensing the redox status of the cell to activate the disulfide oxidoreductase activity of Grx C1 during conditions of oxidative stress. The latter role was suggested for the [2Fe–2S] cluster in human Grx2, because it appeared to be required only under conditions of oxidative stress (10). Although the presence of a similarly coordinated Fe–S cluster

was shown in mammalian cells for Grx 2, there is still no evidence that this cluster is present in plant cells. *In vivo* studies with plants are planned to address the putative role of the cluster as a sensor of oxidative stress.

References:

1. Fernandes, AP & Holmgren, A. (2004) *Antioxid Redox Signal* **6**, 63–74.
2. Rouhier, N, Gelhaye, E & Jacquot, JP. (2004) *Cell Mol Life Sci* **61**, 1266–1277.
3. Kadokura, H, Katzen, F & Beckwith, J. (2003) *Annu Rev Biochem* **72**, 111–135.
4. Debarbieux, L & Beckwith, J. (1998) *Proc Natl Acad Sci USA* **95**, 10751–10756.
5. Masip, L, Pan, JL, Haldar, S, Penner-Hahn, JE, DeLisa, MP, Georgiou, G, Bardwell, JC & Collet, JF. (2004) *Science* **303**, 1185–1189.
6. Achebach, S, Tran, QH, Vlamis-Gardikas, A, Mullner, M, Holmgren, A & Unden, G. (2004) *FEBS Lett* **565**, 203–206.
7. Rodriguez-Manzaneque, MT, Tamarit, J, Belli, G, Ros, J & Herrero, E. (2002) *Mol Biol Cell* **13**, 1109–1121.
8. Molina-Navarro, MM, Casas, C, Piedrafita, L, Bellí, G & Herrero, E. (2006) *FEBS Lett* **580**, 2273–2280.
9. Muhlenhoff, U, Gerber, J, Richhardt, N & Lill, R. (2003) *EMBO J* **22**, 4815–4825.
10. Lillig, CH, Berndt, C, Vergnolle, O, Lönn, ME, Hudemann, C, Bill, E & Holmgren, A. (2005) *Proc Natl Acad Sci USA* **102**, 8168–8173.
11. Feng, Y, Zhong, N, Rouhier, N, Hase, T, Kusunoki, M, Jacquot, JP & Xia, B. *Biochemistry* **45**, 7998–8008.
12. Rouhier, N, Gelhaye, E & Jacquot, J-P. (2002) *J Biol Chem* **277**, 13609–13614.
13. Stephens, PJ, Thomson, AJ, Dunn, JB-R, Keiderling, TA, Rawlings, J, Rao, KK & Hall, D-O. (1978) *Biochemistry* **17**, 4770–4778.
14. Han, S, Czernuszewicz, RS, Kimura, T, Adams, MW-W & Spiro, TG. (1989) *J Am Chem Soc* **111**, 3505–3511.
15. Link, TA. (1999) *Adv Inorg Chem* **47**, 83–157.

16. Jung, YS, Gao-Sheridan, HS, Christiansen, J, Dean, DR & Burgess, BK. (1999) *J Biol Chem* **274**, 32402–32410.

17. Agar, JN, Krebs, B, Frazzon, J, Huynh, BH, Dean, DR & Johnson, MK. (2000) *Biochemistry* **39**, 7856–7862.

18. Dailey, HA, Finnegan, MG & Johnson, M-K. (1994) *Biochemistry* **33**, 403–407.

19. Spiro, T-G & Czernuszewicz, R-S. (2000) in Physical Methods in Bioinorganic Chemistry. Spectroscopy and Magnetism ed. Que, L Jr. (University Science Books, Sausalito, CA,) pp. 59–119.

20. Fu, W, Drozdzewski, PM, Davies, MD, Sligar, SG & Johnson, MK. (1992) *J Biol Chem* **267**, 15502–15510.

21. Kuila, D, Schoonover, JR, Dyer, RB, Batie, CJ, Ballou, DP, Fee, JA & Woodruff, WH. (1992) *Biochim Biophys Acta* **1140**, 175–183.

22. Cosper, MM, Krebs, B, Hernandez, H, Jameson, G, Eidsness, MK, Huynh, BH & Johnson, MK. (2004) *Biochemistry* **43**, 2007–2021.

23. Crouse, BR, Sellers, VM, Finnegan, MG, Dailey, HA & Johnson, MK. (1996) *Biochemistry* **35**, 16222–16229.

24. Moulis, JM, Davasse, V, Golinelli, MP, Meyer, J & Quinkal, I. (1996) *J Biol Inorg Chem* **1**, 2–14.

25. Meyer, J, Fujinaga, J, Gaillard, J & Lutz, M. (1994) *Biochemistry* **33**, 13642–13650.

26. Johansson, C, Kavanagh, KL, Gileadi, O & Oppermann, U. (2007) *J Biol Chem* **282**, 3077–3082.

27. Noguera, V, Walker, O, Rouhier, N, Jacquot, J-P, Krimm, I & Lancelin, JM. (2005) *J Mol Biol* **353**, 629–641.

28. Dailey, FE & Berg, HC. (1993) *Proc Natl Acad Sci USA* **90**, 1043–1047.

29. Berks, BC, Palmer, T & Sargent, F. (2003) *Adv Microb Physiol* **47**, 187–254.

30. Akiyama, Y & Ito, K. (1993) *J Biol Chem* **268**, 8146–8150.

31. Pittman, MS, Robinson, HC & Poole, RK. (2005) *J Biol Chem* **280**, 32254–32261.

32. Aslund, F, Berndt, KD & Holmgren, A. (1997) *J Biol Chem* **272**, 30780–30786.

33. Wingert, RA, Galloway, JL, Barut, B, Foott, H, Fraenkel, P, Axe, JL, Weber, GJ, Dooley, K, Davidson, AJ & Schmid, B, *et al*. (2005) *Nature* **436**, 1035–1039.

34. Dailey, HA, Finnegan, MG & Johnson, MK. (1994) *Biochemistry* **33**, 403–407.

35. Balk, J & Lobreaux, S. (2005) *Trends Plant Sci* **10**, 324–331.

36. Lill, R & Muhlenhoff, U. (2005) *Trends Biochem Sci* **30**, 133–141.

37. Brown, RE, Jarvis, KL & Hyland, KJ. (1989) *Anal Biochem* **180**, 136–139.

38. Fish, WW. (1988) *Methods Enzymol* **158**, 357–364.

39. Setterdahl, AT, Goldman, BS, Hirasawa, M, Jacquot, P, Smith, AJ, Krantz, RG & Knaff, DB. (2000) *Biochemistry* **39**, 10172–10176.

40. Jacquot JP, Stein M, Suzuki A, Liotett S, Sandoz G Miginiac-Maslow M FEBS Lett 400:293-296.

Table 1: Fe-S stretching frequencies (cm^{-1}) and vibrational assignments for $[2Fe\text{-}2S]^{2+}$ centers in poplar Grxs and ferredoxins

Mode*	Grx C1 WT	Grx C1 C88S	Grx C1 C34S	Grx C4 P28G	*So* Fd†	Ado†	*Cp* Fd†
B_{2u}^{b}	421	420	419	424	427	421	404
A_{g}^{b}	397	391	392	394	395	393	387
B_{3u}^{b}	367	368	370	377	367	349	366
B_{1u}^{t}, B_{2g}^{b}	~360	~356	~358	360	357	341	353
A_{g}^{t}	340	340	346	346	338	329	335
B_{1g}^{b}	324	322	323	324	329	317	313
B_{2u}^{t}	286	286	285	290	283	291	290

*Symmetry labels for Fe-S stretching modes assuming an idealized $Fe_2S_2{}^{b}S_4{}^{t}$ core; *t*, terminal or cysteinyl S; *b*, bridging or inorganic S.

†Assignments are taken from ref. 21; *So*, *Spinacea oleracea*; Ado, adrenodoxin; *Cp*, *Clostridium pasteurianum.*

Table 2: Primers used in the study

Grx C1 forward	5'-CCCCCCATGGCTAGCAAGCAAGAACTTGAT-3'
Grx C1 reverse	5'-CCCCGGATCCTCAAAGCTGGGCAGAGGT-3'
Grx C1 C31S forward	5'-ttcagcaaaacctac**a**gcggctattgcaatagg-3'
Grx C1 C31S reverse	5'-cctattgcaatagccgc**t**gtaggttttgctgaa-3'
Grx C1 G32P forward	5'-AGCAAAACCTACTGC**CC**CTATTGCAATAGGGTG-3'
Grx C1 G32P reverse	5'-CACCCTATTGCAATAG**GG**GCAGTAGGTTTTGCT-3'
Grx C1 Y33F C34S forward	5'-AAAACCTACTGCGGCT**T**T**A**GCAATAGGGTGAAGCAG-3'
Grx C1 Y33F C34S reverse	5'-CTGCTTCACCCTATTGC**T**A**A**AGCCGCAGTAGGTTTT-3'
Grx C1 C34S forward	5'-acctactgcggctat**a**gcaatagggtgaagcag-3'
Grx C1 C34S reverse	5'-ctgcttcaccctattgc**t**atagccgcagtaggt-3'
Grx C1 C88S forward	5'-aaacaaatcggtggt**a**gcgacaccgttgtggag-3'
Grx C1 C88S reverse	5'-ctccacaacggtgtcgc**t**accaccgatttgttt-3'
Grx C1 pCK forward	5'-ccccccatgggttcgctgttaagt-3'
Grx C1 pCK reverse	5'-ccccggatccagctgggcaggGttttTAGC-3'
AtGrx C1 forward	5'-CCCCCCATGGCTAGCAAGGAAGAGATGGAG-3'
AtGrx C1 reverse	5'-CCCCGGATCCTTAAAGTTGAGAAGAGTTATC-3'
Grx C1 pTrc99a forward	5'- CTCTCGTCGACATGGCTAGCAAGCAAGAACTTG-3'
Grx C1 pTrc99a reverse	5'-CTCTCAAGCTTAAAGCTGGGCAGGGTTTTTAGC-3'
Grx C2 forward	5'-CCCCCCATGGCTATGAACAAGGCGAAGGAG-3'
Grx C2 reverse	5'-CCCCGGATCCTTAAGCAGAAGCAGAGAC-3'
Grx C2 P24G, F25Y forward	5'-TTCAGCAAGACATACTGT**GG**AT**A**TTGCGTCAAAGTGAAG-3'
Grx C2 P24G, F25Y reverse	5'-CTTCACTTTGACGCAA**T**AT**CC**ACAGTATGTCTTGCTGAA-3'
Grx C3 forward	5'-CCCCCCATGGCTTTAGCAAATGAATTGAAA-3'
Grx C3 reverse	5'-CCCCGGATCCCTACTCCGTGCCTAGAAG-3'
Grx C3 P38G forward	5'-TCCAAATCTTACTGC**GG**GTATTGTTTGCGTGCC-3'
Grx C3 P38G reverse	5'-GGCACGCAAACAATAC**CC**GCAGTAAGATTTGGA-3'
Grx C4 forward	5'-gggccatggctggcagccctgaagct-3'

Grx C4 reverse	5'-gggggatcctcattctagtttaaagtcatc-3'
Grx C4 P28G forward	5'-TCCAAGTCTTATTGC**GG**GTATTGTAAGAGGGCT-3'
Grx C4 P28G reverse	5'-AGCCCTCTTACAATAC**CC**GCAATAAGACTTGGA-3'
Grx C4 pTrc99a forward	5'-CTCTCGTCGACATGGCTGGCAGCCCTGAAGCT-3'
Grx C4 pTrc99a reverse	5'-CTCTCAAGCTTATTCTAGTTTAAAGTCATCTTTCTGCTCT-3'
Grx S12 forward	5'-ccccccatggcttcctttgggtccaggctc-3'
Grx S12 reverse	5'-ccccggatccttagccctgtgacttttttagc-3'
Grx S12 S30G forward	5'-TCCAAAACTTGGTGT**GG**GTATTCTTTTGAGGTG-3'
Grx S12 S30G forward	5V-CACCTCAAAAGAATAC**CC**ACACCAAGTTTTGGA-3'

Except for At Grx C1 (A. thaliana Grx C1), all the primers allowed to amplify poplar genes. Cloning oligonucleotides in the pET-3d expression vector possessed NcoI or BamHI restriction sites (underlined). Mutated nucleotides are in bold characters in mutagenic oligonucleotides.

Figure 1: Spectroscopic studies. (*A*) UV-visible absorption spectrum (*Upper*) and CD spectrum (*Lower*) of Grx C1. (*B*) UV-visible absorption spectrum (*Upper*) and CD spectrum (*Lower*) of Grx C4 P28G. (*C*) UV/visible absorption spectra of Grx C1 recorded before and after 10, 25, and 60 min of deazariboflavin-mediated photoreduction at 0°C (intensity decreasing with increasing time). (*Inset*) The weak X-band EPR signal corresponding to <0.02 spins/[2Fe–2S] cluster that was observed during reduction. EPR conditions: microwave frequency, 9.60 GHz; microwave power, 10 mW; modulation amplitude, 0.63 mT; temperature, 10 K. (*D*) Resonance Raman spectra of Grx C1, Grx C1 C34S, Grx C1 C88S, and Grx C4 P28G obtained at 17 K by using 457.9-nm laser excitation.

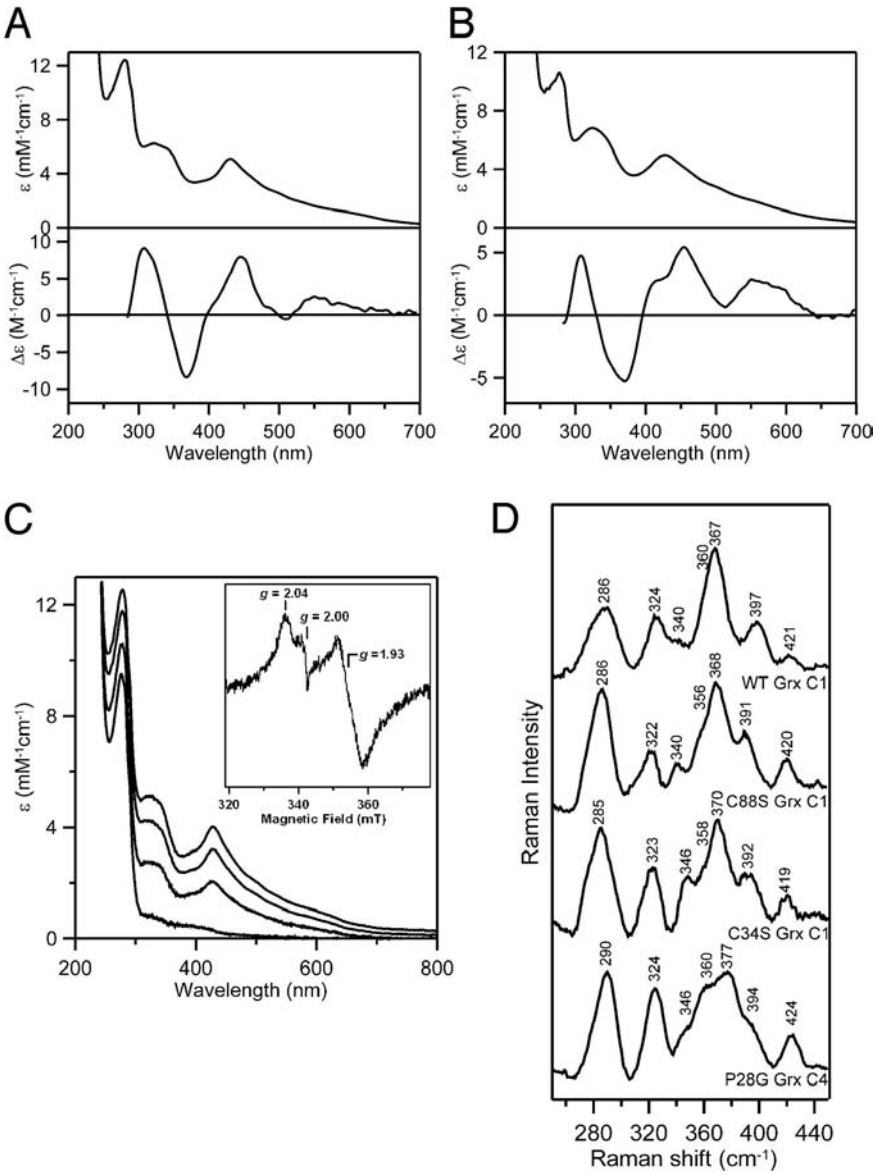
A
B
C
D
ε (mM-1cm-1)
Δε (M-1cm-1)
Wavelength (nm)
g = 2.04
g = 2.00
g =1.93
Magnetic Field (mT)
Raman Intensity
Raman shift (cm-1)
WT Grx C1
C88S Grx C1
C34S Grx C1
P28G Grx C4

Figure 2: Iron–sulfur stability. Stability of the $[2Fe–2S]^{2+}$ clusters in Grx C1, Grx C1 C34S, and Grx C1C88S as monitored by the loss of absorbance at 430 nm as a function of time in aerobic solutions under a variety of different conditions (i.e., 2 mM GSH, DTT, or GSSG).

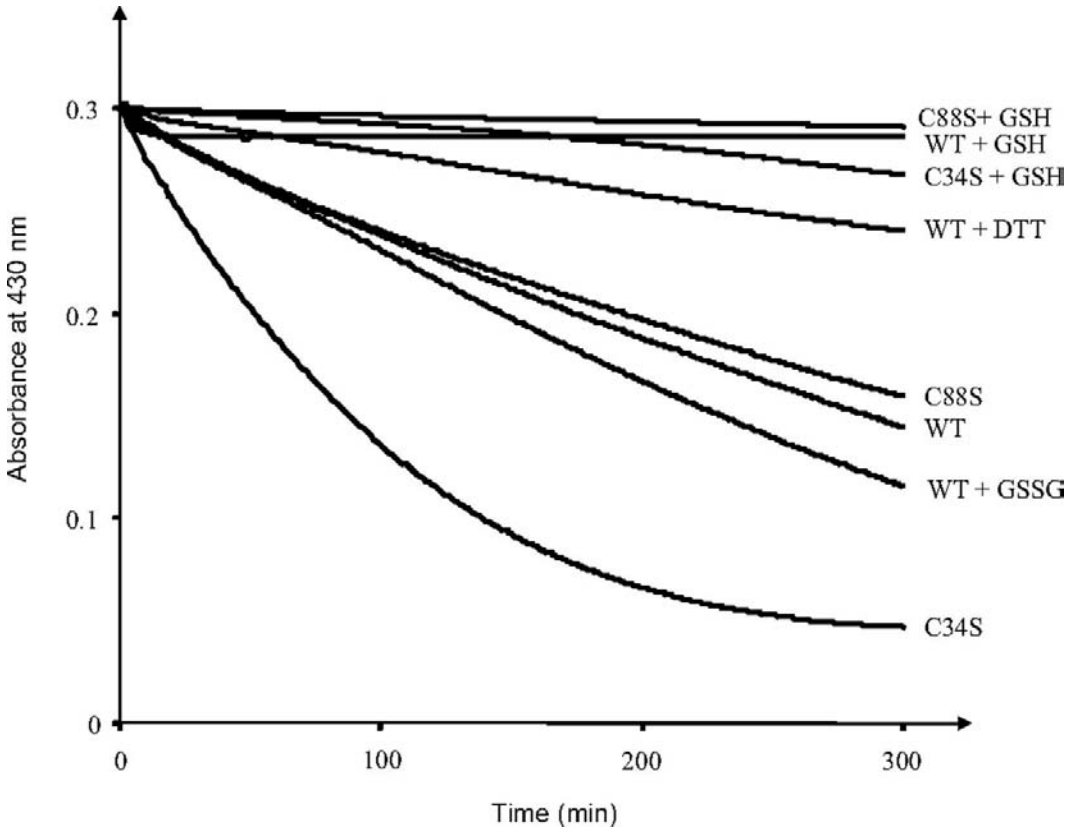
Absorbance at 430 nm
0.3
0.2
0.1
0
0
100
200
300
Time (min)
C88S+ GSH
WT + GSH
C34S + GSH
WT + DTT
C88S
WT
WT + GSSG
C34S

Figure 3: Crystallographic structure of the holoprotein. (*A*) Overall crystallographic structure of the tetramer. Iron atoms are shown in cyan, and sulfur atoms are shown in yellow. Glt indicates an external glutathione molecule (shown in stick). Chains A and D linking the iron–sulfur center are in ribbons and deep blue, and chains B and C are in light blue. (*B*) Blowup of the iron–sulfur center ligands and environment.

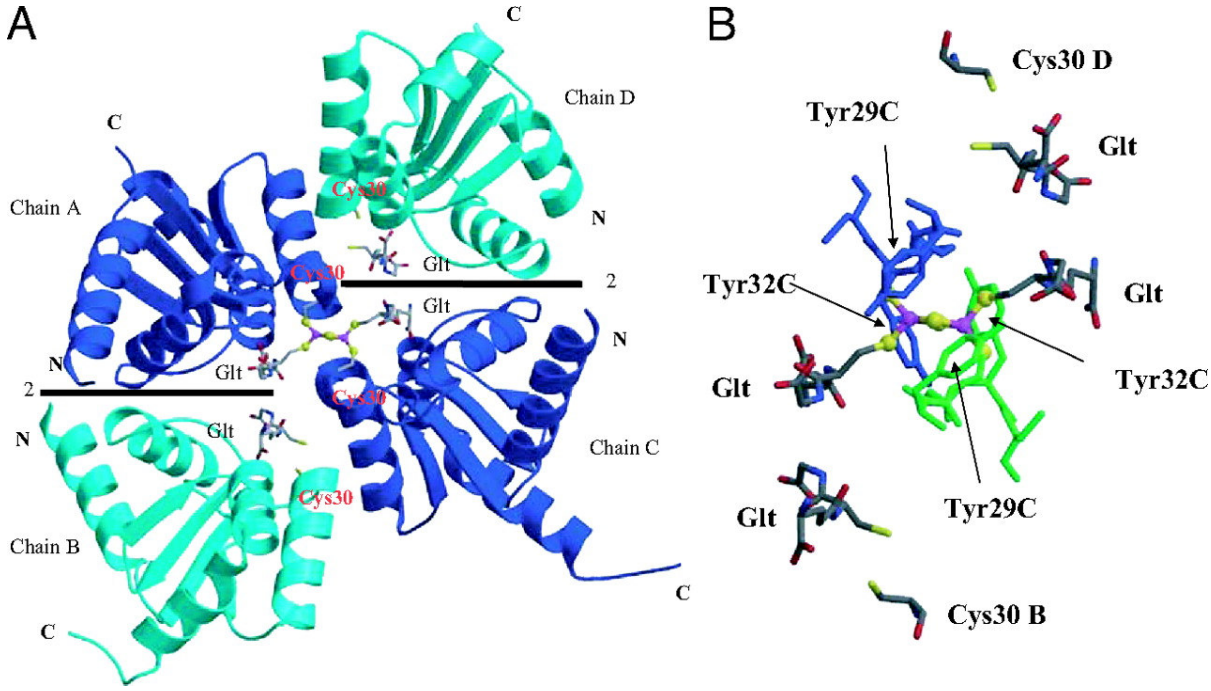
A
C
Chain D
C
Chain A
Cys30
N
Glt
Cys30
2
Glt
N
N
2
Glt
Cys30
N
Glt
Chain C
Cys30
Chain B
C
C
B
Cys30 D
Tyr29C
Glt
Tyr32C
Glt
Glt
Tyr32C
Glt
Tyr29C
Cys30 B

Figure 4: *In vivo* disulfide bond formation by Grx C1. (*A*) Motility assay. *E. coli* LM108 (MC1000 *dsbA dsbB*) negative control (*i*); MC1000, positive control (*ii*); LM108 with GrxC1 fused to the TorA signal sequence and expressed from a pTrc99a plasmid (*iii*). The same number of cells on per OD_{600} basis were spotted on motility plates and grown for 28 h at 37°C. (*B*) Alkaline phosphatase (AP) activity assay of different Grxs exported into the periplasm of MC1000 and LM108 by using different signal sequences. *E. coli* strains were grown in Mops low-phosphate minimal media; the AP activity in cell lysates was determined with *p*-nitrophenyl phosphate. Enzymatic activity was normalized on a per OD_{600} basis and relative to the AP activity of MC1000. Error bars denote standard error.

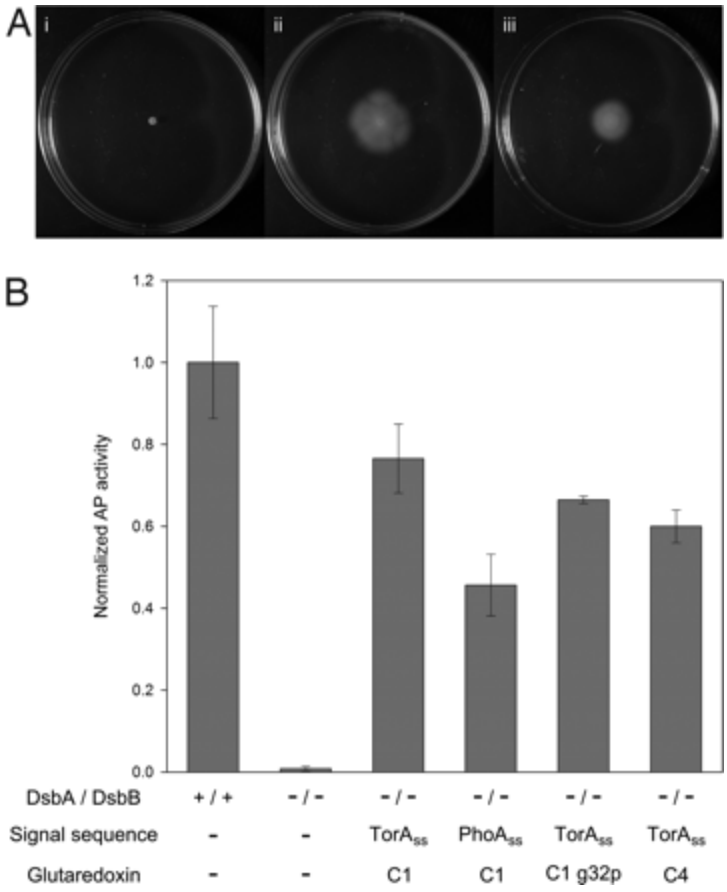
A
i
ii
iii
B
Normalized AP activity
1.2
1.0
0.8
0.6
0.4
0.2
0.0
DsbA / DsbB
+ / +
- / -
- / -
- / -
- / -
- / -
Signal sequence
-
-
TorA$_{ss}$
PhoA$_{ss}$
TorA$_{ss}$
TorA$_{ss}$
Glutaredoxin
-
-
C1
C1
C1 g32p
C4

Figure 5: Amino acid sequence alignment of plant Grx of the subgroup I vs. human Grx2 and yeast Grx 5. Accession numbers are as follows: human Grx2 : NP_932066, yeast Grx 5: NP_015266. Other sequences are translated EST sequences : *Populus trichocarpa:* BU867240 : PtGrx C1, CK095483: PtGrx C2, BU825153: PtGrx C3, CK087968 : PtGrx C4 and CV249364 : PtGrx S12, *Nicotiana benthamiana*: NtGrx C1, CN748724; *Medicago truncatula*: MtGrx C1, BG456561, *Lupinus albus :* LaGrx C1, CA411497; *Vitis vinifera* : VvGrx C1, BM436376, *Solanum tuberosum* : StGrx C1, BI435398; *Lycopersicon esculentum* : LeGrx C1,AI771353.

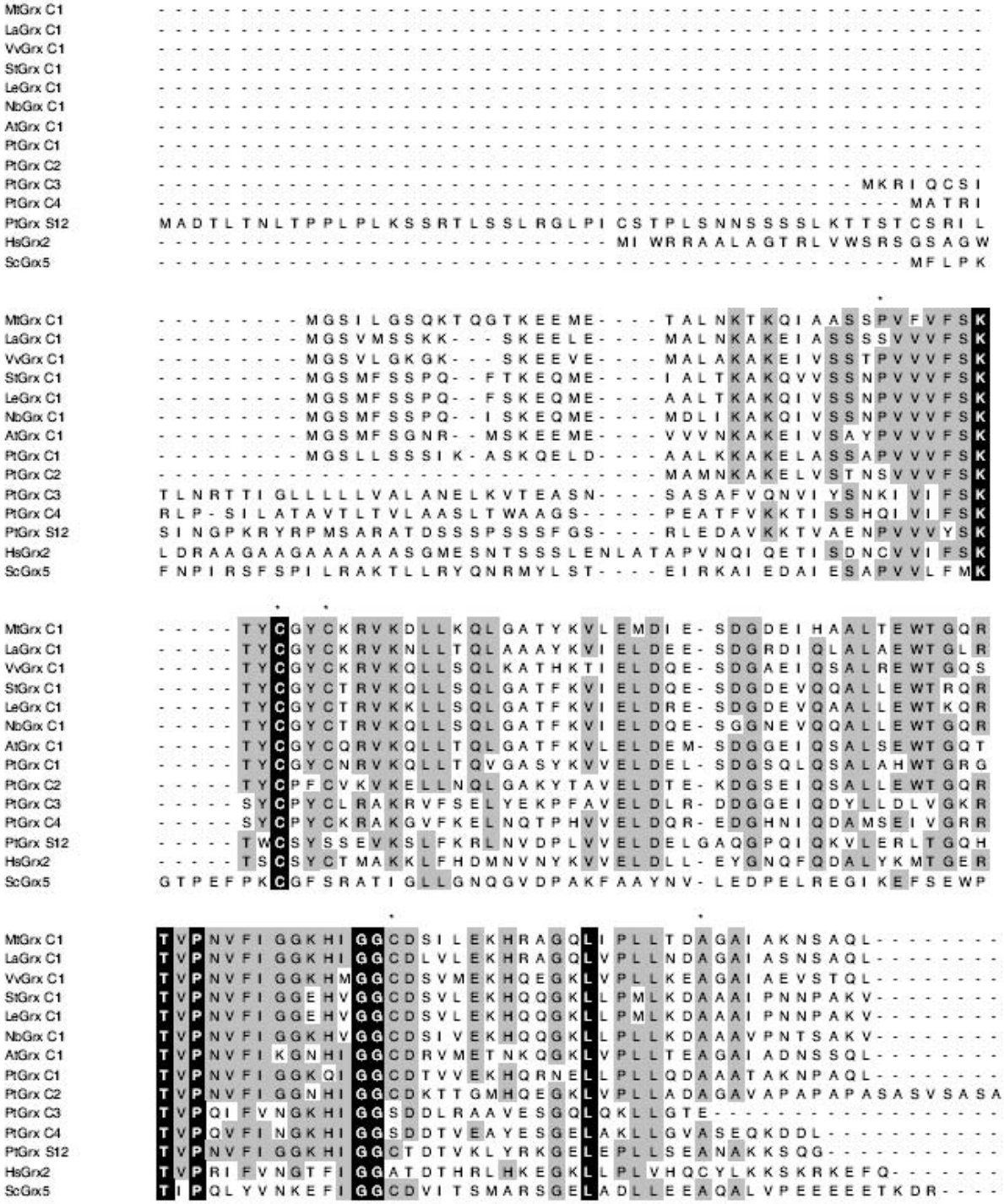
MtGrx C1
LaGrx C1
VvGrx C1
StGrx C1
LeGrx C1
NbGrx C1
AtGrx C1
PtGrx C1
PtGrx C2
PtGrx C3
PtGrx C4
PtGrx S12
HsGrx2
ScGrx5

Figure 6: Subcellular localization of poplar Grx C1. The entire ORF of Grx C1 was fused in 5' of the sequence coding for a GFP. The construction was used to bombard stomatal cells. From top to bottom: visible light, fluorescence of a mitochondrial marker (red) or a chloroplastic marker (blue), fluorescence of the construction, merged images.